ABSTRACT

Title of dissertation: LITHIUM ISOTOPIC SYSTEMATICS OF THE CONTINENTAL CRUST

Fang-Zhen Teng, Ph.D., 2005

Dissertation directed by: Professor William F. McDonough, Geology

In order to fully utilize Li isotopes as a geochemical tracer, it is necessary to characterize the Li isotopic compositions of different geological reservoirs, and quantify the magnitude of isotopic fractionations for various conditions and compositions. However, our knowledge of Li isotope geochemistry is mostly limited to the hydrosphere and mantle. Little is known about either the Li isotopic composition of the continental crust or the mechanisms by which Li isotopes are fractionated.

The primary objective of this thesis is to characterize the Li isotopic composition of the continental crust. Over 50 upper crustal rocks including loess, shale, granite, and upper crustal composites, have been measured and show a limited range of Li isotopic composition (-5 to +5), with an average ($0 \pm 2‰$ at 1σ) that is lighter than the average upper mantle ($+4 \pm 2‰$). More than 70 high-grade metamorphic rocks, including granulite xenoliths and composite samples from high-grade metamorphosed terranes have been analyzed to constrain the Li isotopic composition of the deep crust. Thirty composite samples from eight Archean terranes show mantle-like Li isotopic composition

(+4 ± 1.4‰ (at 1σ)) while 44 granulite xenoliths display a much larger Li isotopic range from –17.9‰ to +15.7 with an average of -1± 7‰ (1σ), isotopically lighter than the mantle.

These data indicate that the continental crust on average has a lighter Li isotopic composition than the upper mantle from which it was derived. Given that Li isotopes do not fractionate during high-T magmatism, juvenile crust and the mantle should have identical Li isotopic compositions. Therefore, the isotopically light continental crust is likely the result of secondary processes, e.g., weathering, metamorphism and low-T intracrustal melting. Previous studies have shown that weathering can strongly fractionate Li isotopes, with heavy Li leaching into the hydrosphere, leaving the rock residue isotopically light. Studies carried out in this thesis indicate that Li isotopes can be fractionated by diffusion, metamorphic dehydration and granite differentiation. Collectively, these processes shift the continental crust to isotopically lighter and the hydrosphere heavier than the mantle with respect to δ^7Li.

LITHIUM ISOTOPIC SYSTEMATICS OF THE CONTINENTAL CRUST

By

Fang-Zhen Teng

Dissertation submitted to the Faculty of the Graduate School of the
University of Maryland, College Park, in partial fulfillment
of the requirements for the degree of
Doctor of Philosophy
2005

Advisory Committee:
Professor William F. McDonough, Chair
Professor Neil V. Blough
Professor Richard W. Carlson
Professor Roberta L. Rudnick
Professor Richard J. Walker

Foreword

The work presented in this thesis was carried out while I was a full-time student at the Department of Geology, University of Maryland, College Park, between August 2001 and October 2005. All samples analyzed are from my co-authors either provided as powders or rock specimens. For the latter, I made the powders. All mineral separates from lower crust granulite xenoliths were done by me. I conducted all Li measurements in all published papers, submitted manuscripts and manuscripts in preparation, and wrote first-drafts of each section. Claude Dalpe, Bill McDonough and Roberta Rudnick taught me to do the instrumental analysis while Roberta Rudnick, Bill McDonough and Paul Tomascak taught me about Li chemical separation techniques. All my co-authors helped me revise the manuscripts.

Acknowledgements

Some people wrote this part with a totally different format from other parts of their dissertation. I decided to keep this part identical to the other parts of my dissertation, that is, always giving evidence before drawing conclusions.

I still remember on my first day to the department, how disappointed I was after spending more than twenty minutes looking for the Geochemistry corridor, only to find that Prof. McDonough ‘s office was locked. Later when I first met Bill in the lab, he told me that I would need five papers to graduate. I worried about this a lot and my friends comforted me: “you can ask him how many papers he published during his Ph.D.!” I finally didn’t negotiate about this with Bill because I found Bill published more than five papers from his Ph.D. work.

Now I am pretty sure that I can dig out at least five papers from my Ph.D. work. Four years ago, I knew nothing about Lithium and very little about crust. Owing to Bill and Roberta’s guidance, now I am familiar with both of them. I am really indebted to Bill and Roberta for letting me start with this great project, helping me with everything from clean lab, instrumental analysis to writing and speaking English, encouraging me whenever I need, and giving me freedom to do my research. This kind of relationship makes me consider them not only as mentors but also as good friends. Whenever I talked about my ideas, Bill always encouraged me and gave me more suggestions while Roberta would say, “hold on, it is good… but you need get papers published. That is very important too.” They helped me understand how to keep things balanced and enjoy my research. Their mentoring has not only been empowering, but also enjoyable. I haven’t

realized time goes by so quickly that I have been here for more than four years. Everything happened just like yesterday!

I'm also grateful to my other advisors, Rich Walker and Rick Carlson, for keeping me on the right track. I could not imagine what I would have gotten if I had insisted on doing some experimental work. I also owe a great deal of gratitude to them for their meticulous comments and suggestions on an early version of the dissertation.

Rich is also thanked for encouraging me to study the Tin Mountain pegmatite and Harney Peak Granite, which formed my third and fourth projects. I remember how excited I was when Rich said, "I am very happy to let you do this."

I would like to thank Boz Wing for so many good conversations and help, from providing me samples to discussing details of my projects. Whenever I wanted to find somebody to talk, Boz was always there.

I thank Claude Dalpe and Richard Ash for help on mass spectrometers and Paul Tomascak for help in the clean lab. Without their efforts I would not have been able to enjoy my research.

I thank Katie Cooney for help, encouragements and friendship. A number of people from our department are thanked for help: James Farquhar, Jay Kaufman, Harry Becker, Bill Minarik, Ji Li, Tracey Centorbi, Kristina Brody, Sandy Romeo, Jeanne Martin and Dorothy Brown.

Shan Gao, Rich Walker, Bruce Chappell, Boz Wing, John Ferry, Mike Brown and Fuyuan Wu provided me samples. I appreciate their generosities.

Finally, I thank my parents and my wife Jianying for their love and support.

Table of Contents

List of Tables

Chapter 2

Chapter 3

Chapter 4

Chapter 5

Chapter 6

List of Figures

Chapter 2

Chapter 3

Chapter 4

Chapter 5

Chapter 6

Chapter 1: Introduction

Lithium, the lightest lithophile element, has an ion radius similar to Mg^{2+}, allowing Li to readily substitute for Mg^{2+} in many rock-forming minerals coupled with charge compensation. Lithium is also moderately incompatible during mantle melting, which results in its enrichment in the crust relative to the mantle (Brenan et al., 1998a; Ryan and Langmuir, 1987). Lithium is fluid-mobile (Berger et al., 1988; Brenan et al., 1998b; Chan and Kastner, 2000; Edmond et al., 1979; Kogiso et al., 1997; Seyfried Jr. et al., 1998) and during weathering, when primary minerals break down, it, together with other alkaline elements, is leached away. Unlike other alkaline elements, however, Li^{+} can substitute for Mg^{2+} in clays in highly weathered rocks. The concentrations of Li in various geological reservoirs differ by up to a factor of > 100 (Teng et al., 2004a).

Lithium has two stable isotopes, ^{6}Li and ^{7}Li, with an average relative abundances of approximately 7.6% and 92.4%, respectively. These two isotopes have many unique chemical characteristics including low cosmic abundance, an extremely high nuclear cross section of ^{6}Li, and ~17% mass difference (Olive and Schramm, 1992). The relatively large mass difference, which results in a large mass-dependent isotopic fractionation, makes Li isotopic studies a potentially powerful tool in studying many geological problems. Lithium isotope ratios have been measured in geological materials to variable degrees of accuracy and precision by a number of mass spectrometric techniques: thermal ionization (TIMS) (Chan, 1987; Datta et al., 1992; Flesch et al., 1973; Green et al., 1988; Hoefs and Sywall, 1997; Hogan and Blum, 2003; James and Palmer, 2000; Klossa et al., 1981; Krankowsky and Muller, 1967; Michiels and Debievre, 1983; Moriguti and Nakamura, 1993; Oi et al., 1997; Qi et al., 1997; Sahoo and Masuda, 1998;

Svec and Anderson, 1965; Tera et al., 1970; Xiao and Beary, 1989; You and Chan, 1996), Secondary Ion Mass Spectrometry (SIMS) or Ion Probe (Chaussidon and Robert, 1998; Decitre et al., 2002; Gurenko et al., 2005; Hervig et al., 2004; Kobayashi et al., 2004; Richter et al., 2003; Williams and Hervig, 2005), quadrupole ICP-MS (Gregoire et al., 1996; Koirtyohann, 1994; Kosler et al., 2001; Sun et al., 1987), and Multi-Collector (MC) ICP-MS (Bryant et al., 2003b; Jeffcoate et al., 2004a; Kasemann et al., 2005; Magna et al., 2004; Nishio and Nakai, 2002; Pistiner and Henderson, 2003; Seitz et al., 2004; Teng et al., 2004a; Tomascak et al., 1999a). Of these techniques, only measurements from the last 15 years demonstrate adequate reproducibility to yield useful results on geological and cosmochemical samples. The MC-ICP-MS techniques have advantages over TIMS techniques with small sample size (40 ug versus 250 ug), fast analysis (10 minutes versus 2.5 hours), for similar accuracy and precision. SIMS analyses allow for in-situ determination of Li isotopes, but suffer from greater uncertainties and significant matrix effects.

Due to analytical advances, our knowledge of Li isotope geochemistry has increased significantly over the last decade. To date, Li isotopic geochemistry has been used to understand a wide range of geological and environmental processes, e.g., river and lake water geochemistry, hydrothermal activity and alteration of the oceanic crust, surface weathering and cycling of material between the mantle and the oceanic crust. Seawater has a homogeneous heavy Li isotopic composition with δ^7Li value ($\delta^7Li = [(^7Li/^6Li)_{sample}/(^7Li/^6Li)_{LSVEC}-1] \times 1000$) at 30‰ (Bryant et al., 2003b; Chan and Edmond, 1988; Hall, 2005; James and Palmer, 2000; Moriguti and Nakamura, 1998b; Tomascak et al., 1999b; You and Chan, 1996), river water and hydrothermal fluid have δ^7Li values

from 6 to 44‰ (Huh et al., 1998; 2001; Tomascak et al., 2003; Zhang et al., 1998) while basalts from both mid-oceanic ridges (MORB) and oceanic islands (OIB) have a homogeneous light Li isotopic composition with δ^7Li value at 4‰. Arc lava displays a similar range of δ^7Li values as oceanic basalts (Bouman et al., 2004; Chan et al., 1992; 2002b; Chan and Frey, 2003; Leeman et al., 2004; Moriguti and Nakamura, 1998a; 2004; Ryan and Kyle, 2004; Tomascak and Langmuir, 1999; Tomascak et al., 1999b; 2000; 2002). While it is well established that the oceanic crust is well known with δ^7Li values, on average, heavier than the mantle and lighter than the hydrosphere (Bouman et al., 2004; Chan et al., 1992; 1993; 1994; James et al., 2003; You et al., 1996), little has been known about the Li isotopic composition of the continental crust and the Li isotopic fractionation that occurs in the crust, both of which are fundamental for using Li as a tracer of processes and of provenance. One objective of this thesis is to characterize the Li isotopic compositions of the upper and lower continental crust, which can be used to better constrain the Li isotopic budget of the silicate Earth. Another objective is to study Li isotopic fractionation that occurs during granite differentiation and metamorphism, which happens widely in the deeper parts of the continents and in subduction zones.

The following five chapters of this thesis are presented as five independent papers. The first two chapters discuss the Li concentration and isotopic composition of the continental crust while the next three late chapters concentrate on Li isotopic fractionation during different geological processes. A summary of this dissertation is given in the last chapter.

Chapter two examines Li in the upper continental crust. In order to characterize the Li concentration and isotopic composition of the upper continental crust, over 50

upper crustal rocks including loess, shale, granite, and upper crustal composites have been measured. These lithologies possess a limited range of Li isotopic compositions (-5‰ to +5‰), with an average (0 ± 2‰ at 1σ) that is representative of the average upper continental crust. Thus, the Li isotopic composition of the upper continental crust is lighter than the average upper mantle (+4 ± 2‰), reflecting the influence of weathering on the upper crustal composition. This work was published in an article entitled "Lithium isotopic composition and concentration of the upper continental crust" in *Geochimica et Cosmochimica Acta*.

Chapter three examines Li concentration and isotopic composition of the deep continental crust by analyses of high-grade metamorphic rocks, including granulite xenoliths and composite samples from high-grade metamorphic terranes. Thirty composite samples from eight Archean terranes in East China, including TTG gneiss, amphibolites and felsic to mafic granulites, have a narrow range of Li isotopic composition from +1.7 to +7.5‰, with an average of +4 ± 1.4‰ (1σ), which is indistinguishable from the upper mantle. In contrast, 44 granulite xenoliths sampled from three different suites in Australia and China display a much larger range of Li isotopic composition from –17.9‰ to +15.7 with an average of -1± 7‰ (1σ). The difference between granulite xenoliths and composite samples may reflect the homogenization of Li isotopes in high-grade terranes by retrograde fluids and large Li isotopic fractionation during metamorphic dehydration for granulite xenoliths. Parts of this work will be submitted to *Geochimica et Cosmochimica Acta*.

Chapter four examines Li isotopic fractionation during granite differentiation. Lithium concentration and isotopic composition have been measured for Harney Peak

granites, the spatially associated Tin Mountain pegmatite and possible metasedimentary source rocks. Lack of correlations between Li isotopic composition and granite differentiation indicates insignificant isotopic fractionation during granite differentiation. The highly differentiated Tin Mountain pegmatite, however, is isotopically heavier than the surrounding metasedimentary rocks and Harney Peak granites, consistent with ^{7}Li enrichment accompanying extensive crystal-liquid fractionation. This work has been submitted as an article entitled "Lithium isotopic systematics of granites and pegmatites from the Black Hills, South Dakota" to *American Mineralogist*.

Chapter five examines Li isotopic fractionation during diffusion. Samples from country rocks of the Tin Mountain pegmatite have been measured for Li concentrations and isotopic compositions. Both Li and δ^{7}Li vary greatly within both amphibolites (~10 m traverse) and schist country rocks (~300 m traverse). This large variation (~30‰) can be modeled by Li isotopic fractionation accompanying Li diffusion from the pegmatite into country rocks. Simple two end-member mixing or Li isotopic fractionation during fluid infiltration cannot produce this large range of δ^{7}Li. This work has been submitted as an article entitled "Diffusion-driven extreme lithium isotopic fractionation in country rocks of the Tin Mt. pegmatite" to *Earth and Planetary Science Letters*.

Chapter six examines Li isotopic fractionation during metamorphic dehydration by studying the Onawa contact aureole, Maine. Major and trace element concentrations in all metapelites vary little except for loss on ignition (LOI), which decreases with the increasing metamorphic grade. Both Li concentration and isotopic composition within these metapelites fall within the range observed in schists and typical post Archean shales. Lithium concentrations decrease with progressive metamorphism towards the igneous

pluton, while samples from the retrograde andalusite-cordierite (a-c (r)) and melting (l-v) zones have higher Li concentrations than their prograde count parts, falling off the trend. Compared with the large variation in Li concentration, δ^7Li shows very small variation and slightly decrease with increasing metamorphic grade towards the pluton. These observations show that Li isotopic fractionation at this range of temperature is very small and metamorphic temperature, protolith and mineralogy of metamorphic rocks are three factors controlling Li concentration and isotopic compositions of metamorphic rocks. This work has been submitted as an article entitled "Lack of lithium isotopic fractionation during progressive metamorphic dehydration in metapelite: A case study from the Onawa contact aureole, Maine" to Chemical Geology.

Conclusions and perspectives for future research are the subject of Chapter 7.

Chapter 2: Lithium concentration and isotopic composition of the upper continental crust

Abstract

The Li isotopic composition of the upper continental crust is estimated from the analyses of well-characterized shales, loess, granites and upper crustal composites (51 samples in total) from North America, China, Europe, Australia and New Zealand. Correlations between Li, δ^7Li, and chemical weathering (as measured by the Chemical Index of Alteration (CIA), and δ^7Li and the clay content of shales (as measured by Al_2O_3/SiO_2), reflect uptake of heavy lithium from the hydrosphere into clays. S-type granites from the Lachlan fold belt (-1.1 to –1.4‰) have δ^7Li indistinguishable from their associated sedimentary rocks (-0.7 to 1.2‰), and show no variation in δ^7Li throughout the differentiation sequence, suggesting that isotopic fractionation during crustal anatexis and subsequent differentiation is less than analytical uncertainty (±1‰, 2σ). The isotopically light compositions for both I- and S-type granites from the Lachlan fold belt (-2.5 to +2.7 ‰) and loess from around the world (-3.1 to +4.5‰) reflect the influence of weathering in their source regions. Collectively, these lithologies possess a limited range of Li isotopic compositions (δ^7Li of -5‰ to +5‰), with an average (δ^7Li of 0 ± 2‰ at 1σ) that is representative of the average upper continental crust. Thus, the Li isotopic composition of the upper continental crust is lighter than the average upper mantle (δ^7Li of +4 ± 2‰), reflecting the influence of weathering on the upper crustal composition. The concentration of Li in the upper continental crust is estimated to be 35 ± 11 ppm (2σ), based on the average loess composition and correlations between insoluble

elements (Ti, Nb, Ta, Ga and Al_2O_3, Th and HREE) and Li in shales. This value is somewhat higher than previous estimates (~20 ppm), but is probably indistinguishable when uncertainties in the latter are accounted for.

1. Introduction

Assessing the Li isotopic compositions of crustal rocks and minerals is important for tracing weathering processes in the crust and documenting interaction between the crust and mantle. Our knowledge of Li isotopic geochemistry, however, is mostly limited to the hydrosphere and mantle. Little is known about its general characteristics in the continental crust, which is of fundamental importance for using Li as a geochemical tracer of crustal recycling. The published data that existed prior to this study suggest the continental crust is isotopically lighter than seawater (~30‰), but heavier than mantle-derived magma (~4 ± 1 ‰ for MORB) and the mantle itself (Chan et al., 1994; Huh et al., 1998; Huh et al., 2001; James et al., 1999; James and Palmer, 2000; You et al., 1995). If so, it raises the dilemma that all major reservoirs in the silicate Earth appear to have heavier Li isotopic compositions than the upper mantle, which is generally considered to reflect the isotopic composition of the bulk Earth.

In order to better constrain the Li isotopic composition of the upper continental crust, we have undertaken a systematic study of granite, upper crustal composites and sedimentary rocks. These data place constraints on the average Li concentration and Li isotopic composition of the continental crust, particularly the upper continental crust, and thus yield further insights into the Li budget of the silicate Earth.

2. Samples

Two approaches have generally been used to determine the composition of the upper continental crust (for details, see Rudnick and Gao, 2003). One is to establish weighted averages of the compositions of rocks exposed at the surface. This is the method used to derive estimates of the concentrations of major element and a number of soluble trace element in the upper continental crust. The other approach is to determine the average concentrations of insoluble elements in fine-grained clastic sedimentary rocks or glacial deposits and use these to infer the average composition of their source regions.

Here we use both methods to evaluate the Li concentration and isotopic composition of the upper continental crust. Samples investigated here include all major upper crustal silicate rock types i.e., both I (igneous)- and S (sedimentary)-type granites from the southeastern Australia type localities (Chappell and White, 1974), upper crustal composites from China that include graywackes, shales and granites (Gao et al., 1991; 1992; 1998), loess from around the world (Taylor et al., 1983) and the suite of Post Archaean Australian Shales (PAAS), ranging in age from Proterozoic to Triassic, which S.R. Taylor and co-workers used to constrain the rare earth element (REE) content of the upper crust (Nance and Taylor, 1976). All of the samples we measured have been extensively characterized in previous investigations and previously published chemical data are supplied as an electronic annex.

2.1. Granites

Granite is a significant component of the upper continental crust, so the Li isotopic composition of granite can be used to place constraints on the δ^7Li value of the upper crust. Moreover, given their origin as infracrustal melts, and assuming that Li does

not fractionate significantly at magmatic temperatures (Tomascak et al., 1999b), granites may provide insight into the isotopic composition of their source regions in the middle and lower crust. To date, only a few δ^7Li data have been published for felsic igneous rocks (2 granite and 1 diorite standards), and these vary from –1.2 to +2.3 (James and Palmer, 2000).

We have analyzed eight I-type granites from the Bega Batholith and two S-type granites from the Wagga Batholith, Southeastern Australia, which is the type locality for defining I- and S-type granites (Chappell and White, 1974). The Bega Batholith is subdivided into eight supersuites, within which the rocks share similar compositional features (Chappell, 1984; Chappell and White, 1992; Chappell et al., 2000). I-type granites from seven of these supersuites were chosen for this study. The two S-type granites represent the two end members of the S-type granite spectrum from the Koetong suite: (1) the most mafic rock (VB30), a mafic biotite-cordierite granodiorite, and (2) the most felsic rock (VB98), a strongly fractionated two-mica granite. The temperature of formation of this suite is estimated to range from ~ 800 to 720°C, using the zircon saturation thermometrer of Watson and Harrison (1983). We have also analyzed two sedimentary rocks that are interpreted to be similar to the source for the S-type granites, although less feldspathic (Chappell et al., 2000). They cover most of the observed compositional range for Ordovician sedimentary rocks from the Lachlan Fold Belt, ranging from clay-rich (OS35) to quartz-rich (OS37) bulk compositions (for mineralogical description of these samples, see Wyborn and Chappell, 1983). All samples are fresh, having been sampled far from weathering surfaces, and, in the case of

the sedimentary rocks, deep underground during construction of water tunnels through the Snowy Mountains.

2.2. Loess and shales

Loess is wind-blown sediment derived from glacial outwash and desert regions. It has been used to study the average composition of the upper continental crust (e.g., Barth et al., 2000 ; Gallet et al., 1998; Peucker-Ehrenbrink and Jahn, 2001; Taylor et al., 1983) because it samples large geographical areas and is produced by the mechanical abrasion of glaciers, thus limiting the chemical effects of weathering (Flint, 1947; Smalley and Cabrera, 1970). Quartz, feldspar and muscovite (or illite) are the most important minerals in the loess investigated here, along with small amount of clay minerals (generally < 10%) (Taylor et al., 1983) . In addition, some samples (e.g., those from Kaiserstuhl) contain calcite and dolomite. The major element compositions of loess deposits demonstrate that their source lithologies have experienced at least one cycle of aqueous sedimentary processing (Gallet et al., 1998). To date, there are no published Li isotopic compositions for loess, although a δ^7Li value of ~ +15‰ is plotted for one loess sample from Mississippi in a diagram in Huh et al. (1998).

Loess from a number of different geological provinces have been investigated here (e.g., New Zealand, China, North America, Europe). Most of these samples were previously studied by Taylor et al. (1983) and Barth et al. (2000) in order to define the composition of the upper continental crust. The provenance of these samples is diverse. Loess from Banks Peninsula, New Zealand, derive from Mesozoic graywackes in the Southern Alps. Loess from the Kaiserstuhl, Germany, derive from glacial erosion of the Alps. Chinese loess derives from non-glacial alluvium in the Gobi desert, and the loess

from the Midwestern USA are probably derived from river outwash from the Rocky Mountains (Taylor et al., 1983). The loess studied here typically show a restricted range of weathering, as reflected by their relatively low chemical index of alteration (CIA) values between 50 and 75, with an average of 60 (CIA = molar $Al_2O_3/(Al_2O_3+CaO^*+Na_2O+K_2O)$, where CaO* refers only to Ca that is not in carbonate and phosphate, Nesbitt and Young, 1982; McLennan, 1993). Unweathered igneous rocks typically have CIA around 50±5 (Nesbitt and Young, 1982). The relatively restricted range and low values of CIA in loess suggests a similar degree of moderate weathering for loess source regions (Gallet et al., 1998).

Shales are fine-grained sedimentary rocks, composed primarily of clays and silt-sized quartz that provide another means of accessing the insoluble element composition of the upper continental crust. In contrast with loess, shales form by more complex processes (e.g., chemical and physical erosion, transportation, deposition and lithification, including diagenesis and metamorphism) and generally reflect higher degrees of weathering. Nevertheless, insoluble element ratios vary little in shales (e.g., La/Yb, La/Th, McLennan, 2001; Taylor and McLennan, 1985), thus allowing one to use the composition of shales to derive an estimate of the average composition of their upper crustal source regions. Previously, only three Li isotopic values have been reported for shales: two from an accretionary prism in Japan at -1.5‰ and –2.7‰ (Moriguti and Nakamura, 1998a) and one international shale standard SCO-1, with a δ^7Li value of 5.2‰ (James and Palmer, 2000).

The shales measured here were originally studied by Nance and Taylor (1976) to determine the average REE composition of the upper continental crust (the PAAS

samples, which are further described in Taylor and McLennan, 1985). They were deposited in four separate basins in Australia (Perth Basin, Canning Basin (both in western Australia), Amadeus Basin, Central Australia and State Circle, Australian Capitol Territory). The age of deposition of these samples ranges from upper Proterozoic (850 Ma) to Triassic. All samples were obtained as well cores in order to avoid problems of surface weathering and leaching. CIA values of the samples measured here range from 58 to 80, with an average value of 70 (cf. 60 in loess).

2.3. Crustal composites

The composite samples were previously used to study the chemical composition of the upper continental crust in eastern China (Gao et al., 1991; 1992; 1998) and comprise all major upper continental crust rock types including graywackes, pelites, granites, granodiorites and one diorite. Each composite was produced from between 10 to 100 individual rock samples of the same age and lithology. The samples range in age from Precambrian to Phanerozoic and derive from three tectonic units in China: the North Qinling Belt, the South Qinling Belt and the Yangtze craton, each of which is further divided into different sub-units. Samples from the North Qinling Belt and the South Qinling Belt are slightly metamorphosed (up to greenschist-facies and one graywacke (D059) that is amphibolite-facies), while those from the Yangtze craton are unmetamorphosed. Care was taken during sampling to avoid any weathered material by sampling road cuts and fresh stream cuts.

3. Analytical methods

Samples used in this study were dissolved in a 3:1 mixture of concentrated HF-HNO_3 in Savillex® screw-top beakers on the hotplate ($T<120^oC$), followed by

replenishment of the dried residua with HCl until solutions were clear. After drying, the samples were re-dissolved in 5 ml 1M HNO_3 and mixed with 3 ml of 100% methanol (CH_3OH); these solutions were added to the cation exchange column (12 ml columns of BioRad AG50W-x8). Lithium is eluted completely with 100 ml 1.0 M HNO_3 in 80% methanol elution solution (Tomascak et al., 1999a; 1999b). The total Li procedural blank during this study was ~200 pg, having a δ^7Li value of ~ -20‰. Compared with samples used in this study (≥ 100 ng Li with δ^7Li values within 0 ± 5‰), the Li procedural blank is negligible at present levels of precision (e.g., ± 1‰, 2 σ).

Prior to analyses, the Na/Li voltage ratio of each solution is evaluated semi-quantitatively on the mass spectrometer. Solutions with a high Na/Li voltage ratio (≥ 5) are reprocessed through a 2nd clean-up column (similar to the 3rd column procedure of Moriguti and Nakamura 1998b), with 11 ml of 0.5 M HCl in 30% ethanol (CH_3CH_2OH) solution eluted through 1 ml of cation exchange resin (BioRad AG50W-x12). The procedural blank for this step is <10 pg. Samples with Na/Li voltage ratios <5 consistently give accurate and precise δ^7Li values.

Purified Li solutions (~100 ppb Li in 2% (*v/v*) HNO_3 solutions) are introduced to the Ar plasma using an auto-sampler (ASX-100® Cetac Technologies) through a desolvating nebulizer (Aridus® Cetac Technologies) fitted with a PFA spray chamber and micro-nebulizer (Elemental Scientific Inc.). Samples are analyzed using a Multi-Collector-Inductively Coupled Plasma-Mass Spectrometer (MC-ICP-MS) from Nu-Plasma (Belshaw et al., 1998), with ^{7}Li and ^{6}Li measured simultaneously in two opposing Faraday cups (^{7}Li in the high mass Faraday cup (H6) and ^{6}Li in the low mass faraday cup (L5)). Each sample analysis is bracketed before and after by measurement of the L-

SVEC standard (Flesch et al., 1973) having similar solution concentration (within ~50%). At least two other Li standards (e.g., the in-house Li-UMD-1 [a purified Li solution from Alfa Aesar®] and IRMM-016 (Qi et al., 1997)) were routinely analyzed during the course of an analytical session. For a solution with ~100 ppb Li and solution uptake rate of 30 μL/min, we typically measure a $^{7}Li^{+}$ ion current of 50 pA (10^{11} ohm resistor) or 5 V, thus the ion yield for Li is ~ 0.007%. In comparison, the procedural blank is ~10 mV on mass 7. The in-run precision on $^{7}Li/^{6}Li$ measurements is ≤ ± 0.2‰ for two blocks of 20 ratios each, with no apparent instrumental fractionation. The external precision, based on 2 σ of repeat runs of pure Li standard solutions, is ≤ ± 1.0‰. For example, IRMM-016 gives $\delta^{7}Li$ = -0.1 ± 0.2‰ (2 σ, n > 100 runs); and in-house standard Li-UMD-1 gives $\delta^{7}Li$ = 54.7 ± 1‰ (2 σ, n > 100 runs).

The Li concentrations of shales and loess samples were determined by isotope dilution using a ^{6}Li-enriched spike (^{ID}Li), following the same preparation procedure for isotopic analysis. We have also measured the Li concentration in unspiked samples by voltage comparisons (^{V}Li) with that obtained for L-SVEC standard of known concentration and then adjusting for sample weight. Both methods yield results to within 5% of one another (Table 2). The precision obtained by isotope dilution is better than ± 2%.

4. Results

Lithium concentrations and isotopic compositions are reported in Table 1 for granite samples, Table 2 for loess and shale samples, and Table 3 for Chinese composite samples. All samples show a limited spread in $\delta^{7}Li$ values (Fig. 1), with a distinct mode in $\delta^{7}Li$ values at about 0‰ and a comparable dispersion ± 3‰ (1σ). This figure also

shows the data for suspended load from the Orinoco River, which is mainly supplied by the three largest tributaries of the Andes and less so from the Guayana shield (Huh et al., 2001). The similar and relatively restricted range of Li isotopic compositions observed for all of the crustal samples provide a coherent picture of the δ^7Li value of the upper continental crust.

4.1. Granites

The southeastern Australian I- and S-type granites and the associated Ordovician sedimentary rocks show a relatively restricted range in Li isotopic compositions (-2.5 to +2.7) regardless of their diverse lithologic origins, bulk compositions and markedly different Li concentrations. The mafic S-type granite end member has a lithium concentration within the range observed for the Ordovician sedimentary source rocks, and is on the high side of concentrations observed for the I-type granites. In contrast, the most evolved S-type granite has the highest Li concentration observed in the suite (187 ppm). Both S-type granites have lithium isotopic compositions within uncertainty of those of the Ordovician sedimentary rocks. Li concentration in the I-type granites ranges from 16 to 62 ppm and δ^7Li ranges between –2.5 to +2.7 ‰.

4.2. Loess and shales

Shales have δ^7Li values that range from –3.2 to +3.9 and show a factor of 3 spread in Li concentrations (28 to 109 ppm). Loess have a comparable spread of δ^7Li values (-3.1 to +4.8). However, in contrast to shales, loess have a relatively constant Li content at 29 ± 16 ppm (2 σ), matching their restricted range of CIA values (57-64). A comparison of these features for shales and loess are shown in Figure 2.

Table 2-1. Lithium concentration and isotopic composition of granites (I- and S- types) and sedimentary rocks from Southeastern Australia and previously published felsic international rock standards.

Sample	Unit	Rock type	δ^7Li [1]	^{V}Li (ppm)[2]	CIA[3]
Ordovician Sedimentary Rocks					
OS35		Shale	1.2	49	72
OS38		Graywacke	-0.7	31	65
Lachlan Fold Belt Granites					
VB30	Ganmain	S-type, mafic	-1.4	44	57
VB98	Mt Flakney	S-type, felsic	-1.1	187	58
MG14	Moruya	I-type	0.3	22	50
MG20	Bodalla	I-type	0.8	30	52
AB40	Kameruka	I-type	-2.5	21	51
AB105	Bemboka	I-type	-2.1	34	50
AB128	Cobargo	I-type	0.1	26	48
AB249	Yalgatta	I-type	2.7	18	49
AB289	Cann Mtn	I-type	1.8	62	51
AB293	Braidwood	I-type	-0.1	16	48
Felsic Rock Standards					
G-2	Inter. Rock Std.[4]	Granite	-1.2	34	
JG-2	Inter. Rock Std.[4]	Granite	-0.3	43	
DR-N	Inter. Rock Std.[4]	Diorite	2.3	40	

1. The Li isotopic compositions are average values from at least 2 repeat measurements that agree within 1‰ for the same solution. $\delta^7Li = [(^7Li/^6Li)_{Sample}/(^7Li/^6Li)_{LSVEC}-1]x1000$. Analytical uncertainty is ± 1 ‰(2σ), based on analyses of pure lithium solutions (see text).
2. ^{V}Li = lithium measured by voltage comparison with standard of known concentration. See text for details.
3. CIA refers to the chemical index of alteration and is the molar ratio of $Al_2O_3/(Al_2O_3+CaO^*+Na_2O+K_2O)$ as defined by Nesbitt and Young (1982), where CaO^* represents Ca in the silicate fraction only. Higher CIA values are characteristic of more altered samples. McLennan's (1993) correction to the measured CaO content for the presence of Ca in carbonates and phosphates is used here. Major element data for CIA calculations are from Chappell (1984), Chappell and White (1992) and Chappell et al., (2000).
4. Data from James and Palmer (2000).

Table 2-2. Lithium concentration and isotopic composition of loess and shales

Location	Sample ID	δ^7Li [1]	^{ID}Li (ppm)[1]	^{V}Li[2] (ppm)	CIA[3]
		Loess			
Banks Penn., New Zealand	BP-1	-2.6	37	40	59
	BP-2	-1.7	37	38	59
	BP-3	-3.1	30	28	61
	BP-4	1.4	40	39	57
	BP-5	-0.7	41	41	57
Kaiserstuhl, Germany	1	-0.9	26	26	65
	2	-0.7	23	25	65
Hungary	H	-0.6	29		
	H replicate[1]	-1.1			
Kansas	CY-4a-A	4.5	17	18	59
Kansas	CY-4a-B	4.8	18	18	59
Kansas	CY-4a-C	4.2	17	16	58
Iowa	I	-0.3	26	37	64
Long Island	LI	-1.0	34	32	
China	CH	0.7	34		
		Shales			
Perth Basin	PW-5	2.0	109	104	80
Canning Basin	PL-1	-0.3	96	92	78
	PL-1 replicate[1]	-1.4			
State Circle	SC-7	-0.7	30	30	77
State Circle	SC-8	-0.2	28	29	75
Amadeus Basin	AO-6	-2.9	67	65	58
	AO-6 replicate[1]	-3.2			
Amadeus Basin	AO-7	-2.3	51	46	64
Amadeus Basin	AO-9	-2.6	71	77	70
Amadeus Basin	AO-10	-0.7	61	59	72
Amadeus Basin	AO-12	2.9	80	71	66
	AO-12 replicate[1]	3.9			
	AO-12 replicate[1]	3.4			
Japan[4]	S-605	-2.7	57		72
Japan[4]	S-606	-1.5	40		65
North America[4]	SCO-1	5.2	45		

1. ID = Isotope dilution; replicate = repeat dissolution and chemical separation of individual samples.
2. ^{V}Li = lithium measured by voltage comparison with standard of known concentration. See text for details.
3. The major element data for CIA calculations are from Nance and Taylor (1976) for PAAS and Taylor et al., (1983) for loess (see electronic data annex). The three loess samples (LI, H, CH) are from Diane McDaniel for which major elements are not available. The major

element compositions of the Japanese shales are from E. Nakamura (pers. comm., 2002) (see data annex for full chemical analyses).

4. Japanese shales are from Shimanto accretionary prism. Li isotopic data and concentrations reported in Moriguti & Nakamura (1998a). The international Rock Standard data (SCO-1) is from James and Palmer (2000).

Analytical uncertainty is ± 1 ‰ (2σ), based on analyses of pure lithium solutions (see text).

Table 2-3. Lithium concentration and isotopic composition of composites from China

Sample	Unit[1]	n[2]	Age	Rock type	δ^7Li	^{V}Li[3] (ppm)	CIA[4]
D059	II	82	Paleoproterozoic	Graywacke	-1.1	49	54
D060	II	36	Mesoproterozoic	Graywacke	0.4	31	62
D062	II	5	Paleoproterozoic	Graywacke	0.6	65	55
D075	IV	16	Neoproterozoic	Graywacke	-0.1	21	54
D100	III	16	Devonian	Pelite	0.9	51	57
D104	III	2	Carboniferous	Pelite	-5.2	77	80
D111	III	24	Silurian	Pelite	-0.1	46	68
D119	IV	15	Neoproterozoic	Pelite	1.2	41	66
D122	IV	25	Silurian	Pelite	-2.1	48	71
D124	IV	7	Jurassic	Pelite	0.1	49	76
D355	III	172	Devonian	Pelite	-2.6	42	67
D276	II	23	Cretaceous	Granodiorite	1.3	18	51
D284	III	21	Neoproterozoic	Diorite	-3.4	22	50
D308	IV	12	Neoproterozoic	Granodiorite	0.2	18	48
D312	IV	12	Neoproterozoic	Granite	-0.5	22	52
D314	IV	15	Neoproterozoic	Granite	3.0	8	51

1. Unit. II = The North Qinling Belt; III = The South Qinling Belt; IV = The Yangtze craton. For details, see: Gao et al., (1998)
2. n = Number of individual samples comprising the composite.
3. ^{V}Li = lithium measured by voltage comparison with standard of known concentration. See text for details.
4. The major element data for CIA calculations are from Gao et al., (1998) and are provided in the data annex.

Analytical uncertainty is ± 1 ‰(2σ), based on analyses of pure lithium solutions (see text).

The relatively low CIA values in loess are consistent with these sediments having experienced limited weathering. In contrast, shales, which show a greater spread in Li concentrations and CIA values, are more strongly weathered (i.e., higher clay component). Shales show a positive, albeit weak, correlation of CIA values with Li concentrations and δ^7Li values, whereas loess show no trend (Figure 2). It has been recognized that Li and Al_2O_3 contents correlate positively for most sediments (Holland, 1984) and the Australian shales follow the global correlation, although PAAS cover a narrower range of Al_2O_3 contents (Figure 3f). In addition, these shales also define weak positive correlations between Li and insoluble elements (e.g., Ti, Ga, Nb, Ta, HREE and Th concentrations; Figure 3).

4.3. Crustal composites

The Chinese composites have similar Li isotopic compositions to one another, comparable to those seen in the other upper crustal samples. Four composite graywackes have very uniform δ^7Li values from –1.1 to +0.6, whereas the seven composite pelites show a larger spread in δ^7Li values from –5.2 to +1.2 (average = -1.1‰). The –3.4 to +3.0 range of δ^7Li values in Chinese granite composites is only slightly greater than that observed for the southeastern Australian granites. The Li concentrations of the composite samples vary considerably (from 8 to 77 ppm Li); the pelites have the highest concentrations and the granites the lowest.

5. Discussion

The similar average δ^7Li composition for each group of upper crustal samples we investigated here is surprising considering the diversity of processes that gave rise to

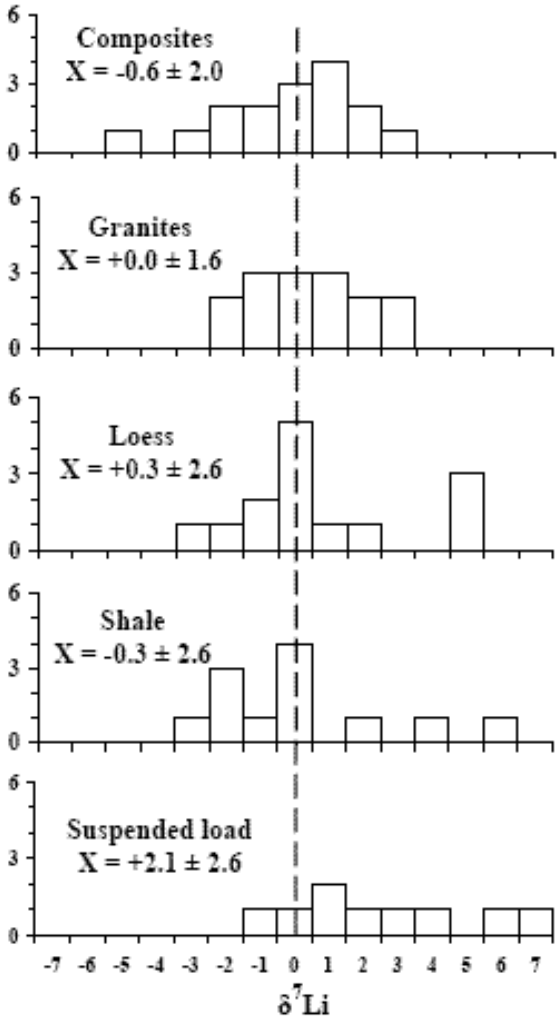

Figure 2-1. Lithium isotopic compositions of different crustal rocks.

Data are from Tables 2-1, 2-2 and 2-3. Suspended load data are from Huh et al. (2001). The vertical dashed line is drawn at δ^7Li of 0 for reference. See text for explanation.

these samples (e.g., weathering, sedimentation, mechanical erosion, partial melting, crystal fractionation, vapor-melt equilibrium), and the fact that Li is a fluid-mobile (soluble) element that experiences large fractionation between minerals and fluids at low temperatures. In this section we evaluate how these processes may have affected the Li content and isotopic composition of the samples and then use our data to derive estimates for the Li abundance and isotopic composition of the upper continental crust. We finally use our upper crustal estimate to model Li mass balance in the silicate Earth.

5.1. Behavior of Li during weathering and mineral-fluid exchange

Shales arise through chemical and physical weathering of pre-exiting rocks (igneous, metamorphic and sedimentary), which produces clays and detrital minerals that are transported through water, deposited and lithified. There are thus multiple opportunities for fluid-mineral interaction and element exchange during the formation of shales, and this might be expected to be reflected in their lithium isotopic compositions. On the other hand, loess, with its lower clay content, is primarily a mechanically-generated sediment that experienced limited fluid-rock interaction during its formation. The Li isotopic composition of loess should therefore reliably reflect its source lithologies, which may also include pre-existing sedimentary rocks (e.g., Peucker-Ehrenbrink and Jahn, 2001).

During shale formation, there are two main opportunities for Li isotope fractionation: during weathering of the protolith and fluid-rock exchange during transport and deposition. During weathering, ^{7}Li is preferentially leached into ground waters, as witnessed by the very light isotopic composition of saprolites compared to their protoliths (Njo et al., 2003) and the slightly lighter Li compositions in a weathering

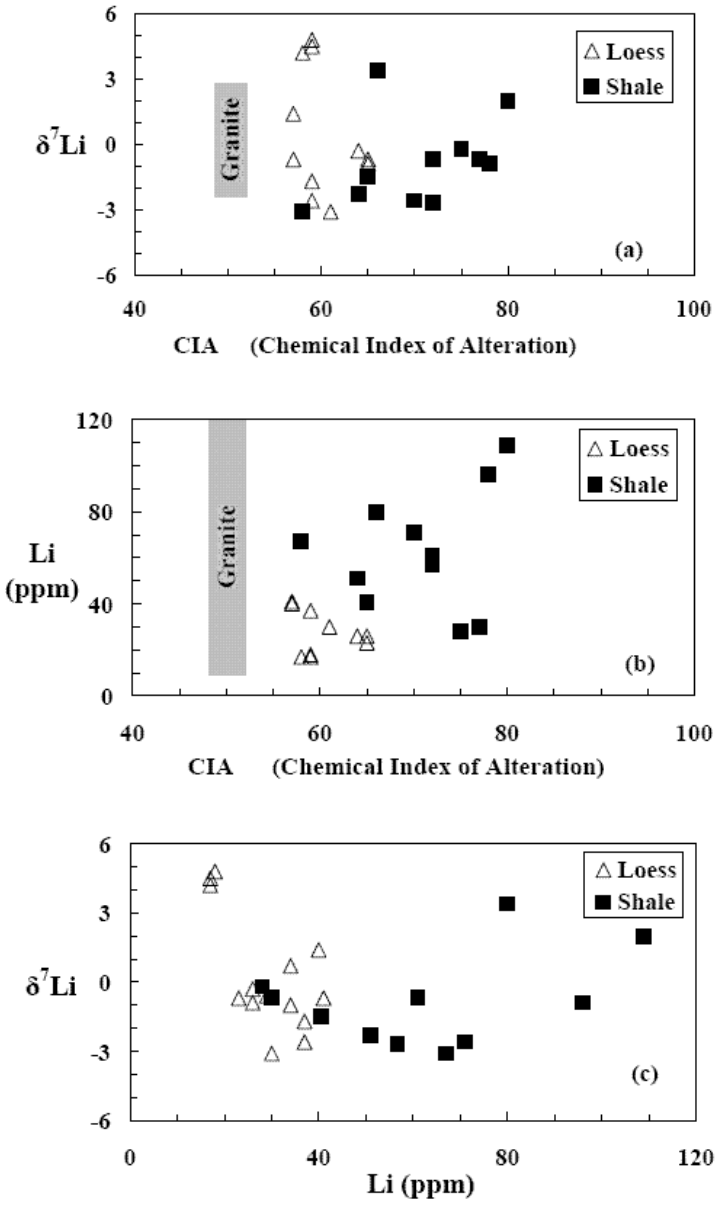

Figure 2-2. (a) δ^7Li versus CIA (b) Li versus CIA (c) δ^7Li versus Li

CIA ranges for granite are from Nesbitt and Young (1982). Data from Tables 2-1 and 2-2. See text or Table 2-2 for definition of CIA.

profile on an Icelandic basalt compared to that of unweathered basalt (Pistiner and Henderson, 2003). Water-mineral exchange experiments also document preferential sorption of ^{6}Li onto some weathering products (e.g., gibbsite and ferrihydrite), although sorption onto smectite did not result in isotopic fractionation (Pistiner and Henderson, 2003).

From the above discussion, one can conclude that both weathering and mineral-fluid exchange should result in isotopically light weathered products and heavy waters. However, our results reveal that shales, which represent the most weathered of the upper crustal samples we investigated, have, on average, $\delta^{7}Li$ values that are within uncertainty of those of the less weathered samples (loess, greywacke composites, granites). The reasons for this unexpected result may lie in the uptake of heavy lithium from the hydrosphere into the clays of shales and the presence of weathered materials in the source regions of the granites and loess.

Lithium is concentrated in the clay fraction of shales and this Li is isotopically heavy. Support for this idea comes from the correlations observed in shales between Li concentration and $\delta^{7}Li$, CIA (Fig. 2), and Al_2O_3 (Fig. 3), and $\delta^{7}Li$ and Al_2O_3/SiO_2 (Fig. 4). The trend on the latter diagram reflects mixing between clays (illite and smectite with Al_2O_3/SiO_2 between 0.3 to 0.9) and quartz ($Al_2O_3/SiO_2 = 0$), and shows that the clay-rich shales have heavier Li isotopic compositions. This mixing is similar to that observed in low-T alteration of mid-ocean ridge basalts, which results in the uptake of heavy seawater lithium by clays (Chan et al., 1992). Such reactions have also been documented experimentally (James et al., 2003; Seyfried Jr. et al., 1998).

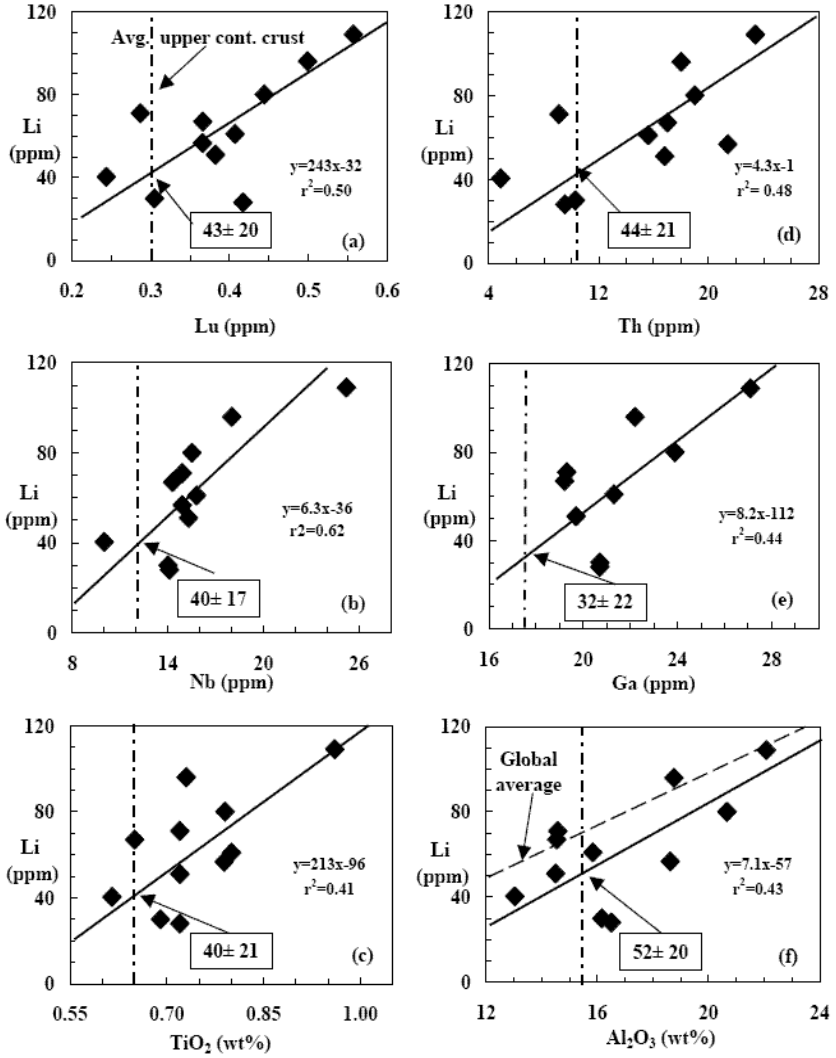

Figure 2-3. Li ppm verses concentrations of insoluble elements in shales
Data are from Table 2-2 and Barth et al. (2000) (all data are available in the electronic data annex). Nb and Al_2O_3 data for the two Japanese shales are from E. Nakamura (pers. comm., 2002). Ta (not shown) produces a similar correlation to Nb, and yields a lithium concentration of 27 ± 17. The dot-dashed line represents the element concentration in the upper continental crust from Rudnick and Gao (2003). The global average correlation for Li versus Al_2O_3 (f) is from Holland (1984). The lithium concentration of the upper continental crust and associated uncertainty (1 σ) is shown in each panel, as well as the linear regression (calculated in Isoplot (Ludwig, 1999), using analytical uncertainties as errors for individual data points). The least squares method of Isoplot minimizes distance from the regression line (as opposed to minimizing y-axis deviations from the line, as in other software such as Excel). The weighted mean Li content from these regressions is 39 ± 14 ppm (2 σ), derived from the following expression (Bevington and Robinson, 2003):

$$weighted\ \ mean = \frac{\sum \frac{\bar{x}}{\sigma^2}}{\sum \frac{1}{\sigma^2}} \quad \text{var}\,iation\ \ on\ \ mean = \sqrt{\frac{1}{\sum \frac{1}{\sigma^2}}}$$

where $\bar{x}$ = mean from linear regression, σ is one standard deviation from regression.

If this explanation is correct, sorption of Li onto clays results in increased lithium concentrations, with the isotopic composition of the added lithium being a function of the composition of the waters from which it is derived and the amount of isotopic fractionation that occurs during sorption. Assuming Pistiner and Henderson's (2003) results for smectite are generally applicable to clays (i.e., no isotopic fractionation during sorption), the added lithium reflects the isotopic composition of the water. We expect lithium in continental waters to be relatively heavy, as heavy lithium is preferentially leached during weathering (Njo et al., 2003; Pistiner and Henderson, 2003). Indeed, heavy lithium is observed in groundwaters (7 to 31 ‰, with 3-14 ppb Li, see: Hogan and Blum, 2003; Tomascak et al., 2003) and the dissolved loads of rivers (7 to 36‰, with 0.2 to 5 ppm Li; Huh et al., 2001). Moreover, seawater, in which shales are deposited, has very heavy lithium (~30‰, 0.2 ppm Li; see Figure 6 for references). Thus, the final Li isotopic composition of shales reflects the balance between light lithium generated during weathering and heavy lithium added by sorption during transport and deposition of the clays.

5.2. Behavior of Li during granite genesis

Granites are derived from melting of the middle and lower crust followed by crystal fractionation and/or restite unmixing during magma ascent, assimilation of upper crustal rocks and finally, fluid exsolution at relatively shallow levels. It has previously been demonstrated that lithium isotopes do not fractionate during differentiation of basaltic magmas at temperatures >1050^{o}C (Tomascak et al., 1999), however, the temperature dependence of the fractionation factor (α) for lithium isotopes is not well constrained. In principle, lithium isotopes could fractionate during any of the above

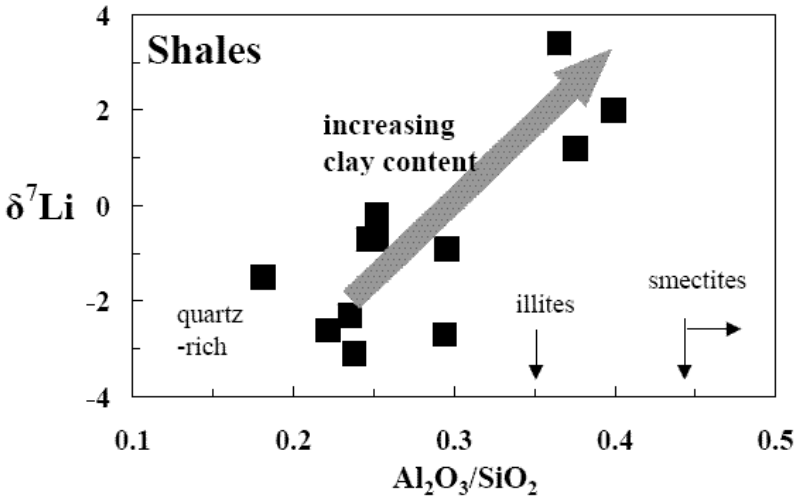

Figure 2-4. δ^7Li versus Al_2O_3/SiO_2 for shales

granite-forming steps. The data reported here allow us to evaluate the influence of some of these processes.

The two S-type granites have δ^7Li values similar to the Ordovician sedimentary rocks, suggesting that lithium is not significantly fractionated at the temperatures of their formation (~ 800°C). Moreover, although the lithium concentration increased four-fold during differentiation within the S-type suite, δ^7Li value remains unchanged, again suggesting no fractionation at temperatures as low as 720°C. Finally, it is possible that exsolution of a vapor phase may cause lithium isotope fractionation. Although we cannot evaluate this possibility with the data we have here, the remarkable similarity of δ^7Li in the granites we measured suggests either that these granites did not exsolve a magmatic vapor phase, or if they did, this exsolution did not significantly fractionate lithium isotopes within the granites. We thus conclude the δ^7Li values of the granites faithfully record the isotopic composition of their middle- to lower-crustal sources and these sources are isotopically lighter than the mantle, as sampled by MORB.

Previous work (O'Neil and Chappell, 1977) showed that I- and S-type granite plutons of the Berridale Batholith (Southeastern Australia) are distinct in δ^{18}O, with I-types having δ^{18}O values between +7.9‰ to +10‰ (well above mantle values) and S-types having δ^{18}O values > +10‰. More significantly, unpublished data (J. O'Neil, pers. comm.) for the I-type Bega Batholith (samples from this study) also show that the most isotopically primitive suites on the eastern side of the batholith (average ^{87}Sr/^{86}Sr ~ 0.704 and ε_{Nd} ~ +2.2) have an average δ^{18}O value of +8.2‰. In at least these cases, I-type granites with Sr and Nd isotopic compositions closest to mantle values have oxygen isotopic compositions significantly higher than values typical of the mantle ~ +5.4‰

(Eiler, 2001). Elevated values of $\delta^{18}O$ require that at least some of the source materials for these I-type granites experienced a low temperature weathering cycle. The significance for this study is that such weathering is expected to fractionate Li isotopes to lower $\delta^{7}Li$ values, which may account for the observed displacement of Li isotopic compositions of the granites relative to mantle values. In this context it is noteworthy that I-type granites from the New England Batholith (NEB), Australia, which are believed to represent an accreted intraoceanic arc that formed far from the continent, range to heavier lithium isotopic compositions ($\delta^{7}Li$ = 2 to 8‰), whereas NEB S-type granites are light (-0.1 to +2.1‰), with compositions that overlap those observed here (Bryant et al., 2003a).

Since the lithium concentration in shales is significantly greater than that of unaltered mafic igneous rocks (e.g., ~60 vs. 4 ppm, average of data in Table 2 and value from Tomascak, 2004), relatively small amounts of shales in the I-type source region will have a dominating influence on lithium, but little influence on oxygen. For example, a mixture of 20% shale (having $\delta^{7}Li$ = 0‰ and 60 ppm Li and $\delta^{18}O$ = 20‰) and 80% mantle-derived gabbro (having $\delta^{7}Li$ = 4‰ and 4 ppm Li and $\delta^{18}O$ = 5‰), would have $\delta^{7}Li$ = 0.8‰ and $\delta^{18}O$ = 8.0‰ (assuming oxygen contents of shale and gabbro are equal). This explains why the oxygen signature of I- and S-type granites are distinct, whereas the lithium signatures are similar.

5.3. Lithium in the upper continental crust

Collectively, our data suggest that the isotopically light lithium observed in all of the upper crustal samples investigated here results from weathering of the continents and

release of heavy lithium to the oceans. In this section we use our data to derive the lithium concentration and isotopic composition of the upper continental crust.

5.3.1 Lithium concentration in the upper continental crust

Estimates of the Li content of the upper continental crust date back to the pioneering work of F. W. Clarke (Clarke, 1889; Clarke and Washington, 1924), who suggested that there is ~50 ppm Li in the crust, based on an average of hundreds of analyses of exposed rocks. More recent studies have converged on a lower Li content, ca. 20 ppm, for the upper continental crust (Table 4).

The loess samples investigated here show a relatively restricted range of Li concentrations, from 17 ppm to 41 ppm, which is the result of physical mixing of glacially eroded sediments derived from a large variety of upper crustal rock types (igneous, metamorphic and sedimentary). The population shows a distribution with an average value of 29 ± 16 ppm (2 σ); this number provides a first-order estimate of the Li concentration of the upper continental crust.

Due to the weathering and sorption processes discussed above, the Li contents of shales vary considerably from 28 to 109 ppm, depending on their proportion of clays to quartz. To compensate for these effects, we examined the positive correlation between Li and elements considered to be immobile during weathering (see Fig. 4 of Rudnick and Gao, 2003). Lithium correlates positively ($R^2 \geq 0.4$) with the following elements: Ti, Nb, Ta, Ga, Al_2O_3, Th and HREE (Fig. 3). Using these correlations and average upper crustal concentrations of these insoluble elements (Rudnick and Gao, 2003), we determined a Li concentration of the upper crust from each correlation (Fig. 3). The weighted mean of these results is 39 ± 14 ppm (2 σ) (see figure caption for details of

Table 2-4. Estimates of the Li concentration in the upper continental crust

Li (ppm)	References
50[a]	Clarke (1889)*, Clarke and Washington (1924)
20[b]	Taylor (1964)*, Wedepohl (1969), Taylor and McLennan (1985; 1995), McLennan (2001)
22[c]	Shaw et al. (1967; 1976; 1986); Wedepohl (1995)
21[d]	Gao S. et al. (1998)
35 ± 11[e]	**This study**

*Original estimate; later papers shown used this same estimate.
a: Based on an average of hundreds of analyses of exposed rocks.
b: Assuming the upper crust consists of a 1:1 mixture of granites (30 ppm) and basalts (10 ppm), and using Li data compiled by Heier and Adams (1964).
c: Based on averages of surface samples from Canadian Precambrian shield.
d: Based on composite samples from China.
e: Based on Li-immobile element trends in shales and average concentration of loess (see text and Fig. 3 for derivation). Uncertainty is 2 sigma.

calculations). Combining these estimates from loess and shales, we obtain a weighted mean upper crustal Li concentration of 35 ± 11 ppm (2 σ). This value is somewhat higher than the more recent estimates of the lithium concentration of the upper continental crust (Table 4), however, no uncertainties are provided for these previous estimates and it is likely that they would agree, within uncertainty, of the value obtained here.

5.3.2 Lithium isotopic composition in the upper continental crust

The average δ^7Li of the samples studied here is –0.2 ± 2.1‰ (1 σ). This result is in agreement with the scant published data for other rocks from the upper continental crust (i.e. granites, diorite, shales and suspended load sediments from the Orinoco River; Fig. 2 and Tables 1-3 and references therein). Based on all of these data, the Li isotopic composition of the upper continental crust is estimated at δ^7Li = 0 ± 2‰ (Figure 5). This light isotopic value relative to the mantle (i.e., MORB-source region) reflects the influence of weathering on the composition of the upper crust, a conclusion supported by the higher CIA of the average upper continental crust (53) compared to that of the middle and lower crust (49 for both, data from Rudnick and Gao, 2003).

5.4. Lithium budget of the silicate Earth

The continental crust comprises ~0.6% of the mass of the silicate Earth, and contains <10% of its Li budget (Taylor and McLennan, 1985). Various studies of Li show that it is incompatible during mantle melting, with a bulk partition coefficient comparable to Dy, a HREE (Ryan and Langmuir, 1987). The upper crust has 1 to 3 times as much Li as the deeper crust (Rudnick and Gao, 2003) and both the upper and deeper

Table 2-5. Mass balance model for Li in the silicate Earth and its reservoirs

Reservoirs	Mass (10^{22} kg)	Mass (%)	Li (ppm)	Li (%)	δ^7Li
Hydrosphere	0.2	0.049	0.2	0.006	30
Upper Cont. Crust	1.0	0.25	30	4.8	0
Lower Cont. Crust	1.0	0.25	13	1.9	0 ± 50
Oceanic crust	0.6	0.15	10	0.92	5
Mantle	404.3	99.3	1.5	92.4	4
Silicate Earth	407.1	100	1.6	100	4

Mass of reservoirs from Yoder (1995); Li data in hydrosphere is based on seawater values; Li data of upper continental crust (this study); Li concentration of the lower continental crust (Rudnick and Gao, 2003) and its δ^7Li value is calculated assuming all the other reservoirs known; Li data in oceanic crust is average value of altered and fresh basalts (Chan et al., 1992; 2002a); Li concentration in the mantle (Jagoutz et al., 1979) and its δ^7Li value from Figure 2-6. Li concentration in the silicate Earth is from McDonough and Sun (McDonough and Sun, 1995); its δ^7Li value is taken as that for fresh basalts.

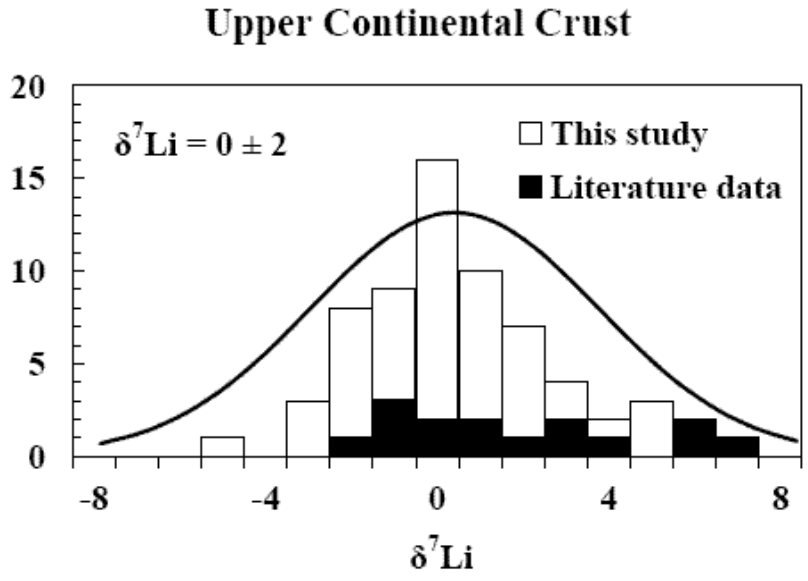

Figure 2-5. Lithium isotopic composition of the upper continental crust
Literature data are from Tables 2-1, 2-2 and Figure 2-2. All these data form a gaussian distribution with an average δ^7Li value at 0 and standard deviation at 2. Solid line is the fitted gaussian curve.

crust are important for understanding Li isotopic composition of the whole crust, and consequently the Li isotopic balance of the silicate Earth.

The range of Li isotopic compositions in various terrestrial rocks and seawater is illustrated in Figure 6. The mantle, as represented by fresh basalts (i.e., MORB, and Hawaiian basalts, the later being representative of the ocean island basalts), appears to have an average δ^7Li value of about +4‰. Likewise, modern seawater has a homogeneous δ^7Li value of ~+30‰. Altered basalts and most marine sediments have δ^7Li values that are generally intermediate between that of the mantle and seawater, due to the uptake of heavier seawater Li. The upper continental crust, in contrast, is isotopically lighter (~ 0‰) than all of these other reservoirs. Only orogenic eclogites have δ^7Li values substantially lighter than the upper crust, and reflect loss of heavy lithium during metamorphic dehydration in the upper portions of a subducting slab (Zack et al., 2003). Thus, it is yet unclear how recycling of altered oceanic basalts into the mantle at subduction zones influences the δ^7Li of various mantle reservoirs.

A first-order model for the distribution of Li in the silicate Earth is presented in Table 5. Most of the Earth's Li is in the mantle (>90%), with the remainder concentrated mostly in the continental crust and lesser amounts in the oceanic crust and hydrosphere. The composition of the lower continental crust is the independent variable and was calculated in this model from mass balance.

While offering a perspective on various reservoirs in the silicate Earth, this Table highlights where there are still significant uncertainties in our understanding of lithium (i.e., mantle reservoirs and the lower continental crust). A minor change in the δ^7Li value

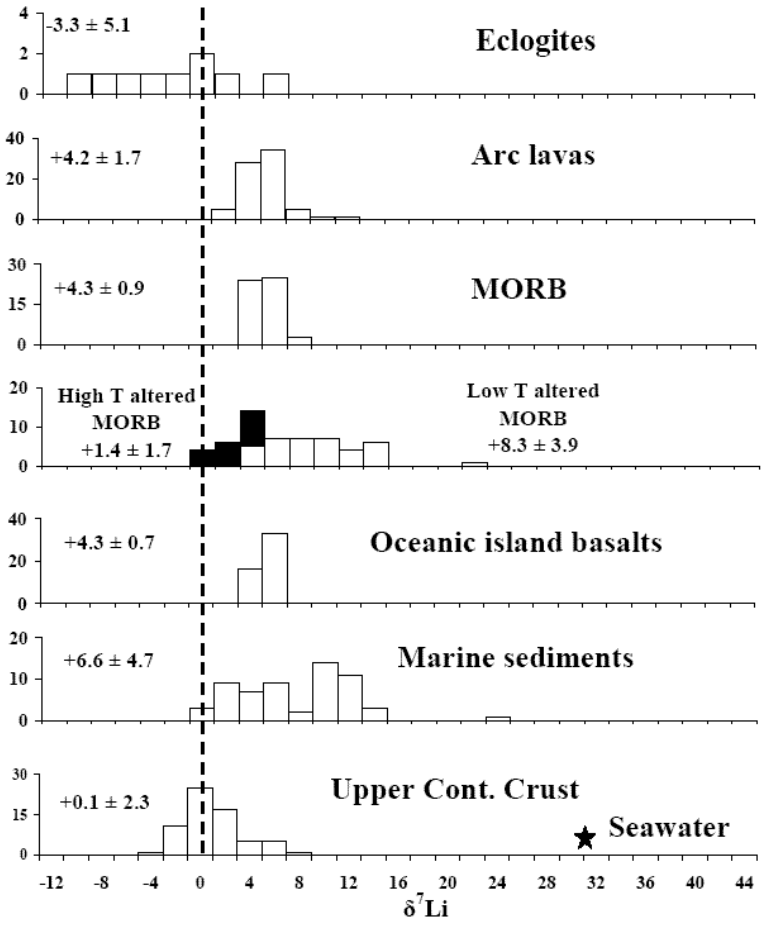

Figure 2-6. Histograms of δ^7Li values for a variety of terrestrial rock types
The vertical dashed line is drawn at 0 for reference. Eclogite data (Zack et al., 2003); Arc lava data (Chan et al., 2002b; Moriguti and Nakamura, 1998a; Tomascak et al., 2000; Tomascak et al., 2002). Fresh basalt data (Chan et al., 1992; Chan et al., 2002b; Moriguti and Nakamura, 1998a; Tomascak and Langmuir, 1999). Altered basalt data (Chan et al., 1992; 2002a). Oceanic island basalt (OIB) data (Chan and Frey, 2003; Tomascak et al., 1999b). Marine sediment data (Chan et al., 1994; Chan and Kastner, 2000; James et al., 1999; Zhang et al., 1998). Seawater (Bryant et al., 2003b; Chan and Edmond, 1988; James and Palmer, 2000; Moriguti and Nakamura, 1998b; Tomascak et al., 1999b; You and Chan, 1996).

for the mantle (e.g., measurement uncertainty, ±1‰) will shift the calculated Li isotopic composition of the lower continental crust reservoir greatly (>±50‰). Therefore, to make more precise models for the Li isotopic budget of the Earth we need to gain insights into the size and composition of the mantle reservoir that supplies ocean island basalts, as well as insights into the lithium composition of the lower continental crust.

The only region in the Earth where Li isotopes are significantly fractionated is in the outermost layer (hydrosphere, continental and oceanic crust). Considering that continental growth occurs mainly either at convergent margins or intra-plate settings, both of which produced lavas with δ^7Li values greater than that of the upper continental crust, there must be processes that shift the Li isotopic compositions of these new continental additions towards lighter values. Two major processes involving fluid-rock interactions might accomplish this Li isotopic fractionation: weathering (on or near the Earth surface, see Njo et al., 2003; Pistiner and Henderson 2003) and metamorphic dehydration (in the deep crust, see Williams and Hervig, 2003; Zack et al., 2003). During both processes, light lithium is preferentially partitioned into minerals relative to fluids, which ultimately drives Li in the continental crust to lighter compositions and Li in the hydrosphere to heavier compositions relative to the mantle.

6. Conclusions

The main conclusions to be drawn from our data are:

1. Loess from North America, China, Europe and New Zealand have a narrow range of Li isotopic compositions (δ^7Li = 0 ± 3‰) and Li concentrations (29 ± 16 ppm,

2 σ) offering important insights into the average composition of Li in the upper continental crust.

2. Shales, which are more weathered than loess, provide less robust estimates for the upper crust, but offer insight into the processes that lead to Li isotope fractionation at the Earth's surface. Correlations between Li and δ^7Li with CIA or Al_2O_3/SiO_2 in shales reflect uptake by clays of isotopically heavy Li from the hydrosphere.
3. The similar Li isotopic composition of shales and loess (δ^7Li = 0 ± 3 ‰), reflect the competing influences of loss of heavy lithium during weathering and its re-introduction during transport and deposition in shales, and the presence of weathered materials in the source regions of loess.
4. The similarity between S-type granite δ^7Li values and that of associated sedimentary rocks interpreted to be similar to their source, coupled with the similar and restricted range of δ^7Li in I-type granites, suggests little lithium isotopic fractionation has occurred during granite genesis (temperatures of 720-800^{o}C). The isotopically light δ^7Li of both types of granites reflects the presence of weathered material in their source regions.
5. Southeastern Australian granites, crustal composites from China, and previously published data for suspended river load sediments all have relatively similar δ^7Li values (0 ± 3 ‰), comparable to those found in loess and shales. Collectively these observations show that the upper continental crust has a relatively homogeneous δ^7Li value (0 ± 2 ‰), which is significantly lighter than that of the

mantle and probably reflects the influence of weathering on upper crustal composition.

6. Based on the average Li concentration of loess and Li-immobile element correlations in shales, we propose that the average upper crustal Li content is 35 ± 11 ppm (2 σ).

Chapter 3: Lithium concentration and isotopic composition of the deep continental crust

Abstract

The Li isotopic composition of the deep continental crust has been studied by analyzing composite samples from Archean high-grade metamorphic terranes in East China and granulite-facies xenoliths from East China (Hannuoba suite) and Queensland, Australia (Chudleigh and McBride suites). The 30 composite samples, including TTG gneiss, amphibolites and felsic to mafic granulites, have a narrow range of δ^7Li values from +1.7 to +7.5‰, with an average of +4 ± 1.4‰ (1σ), which is indistinguishable from the upper mantle (+4.3 ± 0.9‰ (1σ)). In contrast, three granulite xenolith suites display a much larger range in δ^7Li, from –17.9‰ to +15.7 with average values decreasing in the order: Hannuoba (–0.7 ± 4.9‰ (1σ, 18 samples)), Chudleigh (-2.5 ± 5.5‰ (1σ, 14 samples)) and McBride (–3.8 ± 7.6‰ (1σ, 12 samples)). The xenoliths are, on average, lighter than the composites. Lithium concentrations are also variable, with xenoliths having lower Li concentration than composites (5 ± 4 ppm vs. 13 ± 6 ppm, 1σ).

δ^7Li correlates positively with H_2O for 12 granulite composites; mafic samples have the highest H_2O contents and δ^7Li values while felsic ones have the lowest. This, together with an excellent positive correlation between Li concentration and Mg# for 13 TTG gneiss composites, suggests that both metamorphic dehydration and protolith lithology play important roles in controlling Li concentration and isotopic composition of metamorphic rocks. This is further corroborated by the positive correlation of δ^7Li with Al_2O_3/CaO and negative correlations with Li, FeO, MgO, CaO and Co in the Hannuoba

granulite xenoliths. The extreme isotopic variation in granulite xenoliths results from large Li isotopic fractionation during metamorphic dehydration while the small range of δ^7Li in high-grade terranes reflects the homogenization of Li isotopes by retrograde fluids. Overall, the deep continental crust is very heterogeneous, with an average δ^7Li = +1 ± 6‰(1σ) after averaging all data collected here. This value is similar to the upper continental crust and slightly lighter than the mantle, consistent with ^{6}Li enrichment accompanying surface weathering and metamorphic dehydration. After combining granulite xenolith data from this study and literature, the Li concentration of the lower continental crust is estimated to be ~8 ppm, which is similar to previous estimates.

1. Introduction

The composition of the continental crust is important for understanding its formation and evolution as well as the Earth as a whole. Based on studies of shale, loess, granite and upper crustal composites, Teng et al. (2004a) show that the upper continental crust appears to have a lighter Li isotopic composition (0 ± 2‰ (1σ)) than the upper mantle (+4 ± 0.8‰ (1σ)), from which it was derived. This is likely a result of secondary processes, e.g., surface weathering and metamorphic dehydration, which fractionate Li isotopes, with ^{7}Li preferring the hydrosphere to rocks causing a shift in the present upper continental crust towards lighter Li isotopic composition. Compared with the knowledge about Li in the upper continental crust, very little is known about Li in the deep continental crust (middle and lower crust).

In order to better characterize the Li concentration and isotopic composition of the deep continental crust, we have undertaken a systematic study of high-grade terranes and granulite xenoliths including felsic to mafic lithologies of both igneous and sedimentary

origins. This study, following the previous study (Teng et al., 2004a), will further characterize the Li concentration and isotopic composition of the continental crust, help to understand Li isotopic fractionation during regional metamorphism and place constraints on the Li budget of the silicate Earth.

2. Samples and their geological background

Seismological studies indicate that the deep continental crust (below ~10-15 km depth) can be divided into two heterogeneous layers: the middle crust and lower crust. The middle crust is between ~10-15 and 20-25 km depth and is dominated by amphibolite facies to lower granulite facies metamorphic rocks with more evolved compositions. The lower crust is below ~20-25 km depth and mainly consists of granulite facies rocks with more mafic compositions. Two types of samples have been used to characterize the composition of the deep crust: high-grade metamorphic terranes and lower crust xenoliths carried in volcanic pipes. The former is considered representative of the middle to upper lower crust and the latter representative of the deep lower crust (for details, see: Rudnick and Gao, 2003).

In this study, samples from both types of deep crustal samples, including whole rocks and mineral separates, have been studied: composites of high-grade metamorphic rocks from eight different metamorphosed terranes in East China including TTG gneiss, amphibolite and felsic to mafic granulites (Gao et al., 1998); three suites of granulite xenoliths from Damaping, Hannuoba, East China (Liu et al., 2001), McBride and Chudleigh, North Queensland, Australia (Rudnick et al., 1986; Rudnick and Taylor, 1987). All samples are well characterized and have been used to study the composition of the deep continental crust in previous investigations.

2.1. Composites of high-grade metamorphic rocks from East China

The composite samples are from eight different high-grade metamorphic terranes in the two largest Archean cratons in East China. Seven are from the North China craton including the Wutai, Jinning, Wulashan, Fuping, Hengshan, Taihua and Zhongtiao amphibolite and granulite-facies terranes. The other one is the Kongling high-grade terrain, which forms the oldest basement of the Yangtze craton. Most composites were produced with >2 individual rock samples of the same age and lithology. 13 TTG gneiss, five amphibolites, four felsic, four intermediate and four mafic granulite composites are analyzed. The freshness of samples is guaranteed by petrographic examinations.

All these high-grade terranes have been extensively studied and previously used to estimate the composition of the deep crust in East China. More details about these Archean terranes can be found in Gao et al. (1992; 1996; 1998) and Zhao et al. (2001).

2.2. Granulite xenoliths from Damaping, Hannuoba, China

The Cenozoic Hannuoba basalts occur in the north margin of theNorth China craton and are surrounded by the Huai'an granulite terrane (part of Qianxi granulite terrane), which is considered to be an exposed lower crustal section (Zhai, 1996). In Damaping, lower crustal granulite xenoliths are dominated by maficcompositions. Previous studies suggest that these granulites are crystallization products of underplated basaltic magmas, which were contaminated by late-Archean to Proterozoic lower crust (Liu et al., 2001). All granulite xenoliths equilibrated at high temperatures (700-1000 ^{o}C) at depths of 25-40 km (Liu et al., 2001).

Eighteen samples with distinct mineralogical and chemical compositions have been chosen for this study. They are the same as those studied by Liu et al (2001; 2004).

2.3. Granulite xenoliths from McBride, North Queensland, Australia

The late Cenozoic basalts from the McBride volcanic province, North Queensland, erupted through and onto Proterozoic crust of the Georgetown Inlier, which is composed of greenschist to amphibolite facies metamorphic rocks. Lower crustal granulite and upper mantle peridotite xenoliths widely occur. These granulites exhibit diverse compositions ranging from mafic through felsic, with mafic orthogneisses including one possible metasediment compositions dominating. The ages of their protoliths and the granulite facies metamorphism have been determined by U-Pb zircon dating. Most protoliths formed at 300 Ma, a time of extensive calc-alkaline igneous activity in this region, but several protoliths formed during the Proterozoic at about 1570 Ma (Rudnick and Williams, 1987). All xenoliths underwent granulite facies metamorphism at 300 Ma, followed by slow cooling in the lower crust. A wide range of whole-rock $^{143}Nd/^{144}Nd$ and $^{87}Sr/^{86}Sr$ follows a mixing trend at 300 Ma, suggesting most of these xenoliths were formed during large scale mixing between mantle-derived basalts and preexisting crust at this time (Rudnick, 1990).

Twelve granulite xenoliths ranging from felsic to mafic compositions have been measured. These samples were originally studied by Rudnick et al (1987) for constraining the composition and petrogenesis of the lower crust.

2.4. Granulite xenoliths from Chudleigh, North Queensland, Australia

The Chudleigh volcanic province in North Queensland is south of McBride. Granulite xenoliths were carried by recent alkali basalts erupted on the boundary between the Proterozoic Georgetown Inlier and the Paleozoic Tasman fold belt of eastern Australia (Rudnick et al., 1986). These xenoliths have exclusively mafic compositions

(Mg# from 40 to 81) and equilibrated at depths between 20 to 40 km (Rudnick et al., 1986; Rudnick and Taylor, 1991). The chemical and isotopic compositions of these xenoliths (O, Os, Sr, Nd, Pb) indicate they are cogenetic crystal cumulates derived from a mafic magma, which underwent assimilation and crystal fractionation as they intruded and cooled in the lower crust less than 100 m.y. ago (Kempton and Harmon, 1992; Rudnick et al., 1986; Rudnick, 1990; Rudnick and Goldstein, 1990; Saal et al., 1998). Plagioclase-rich xenoliths are the most common variety and show little variation in major element composition over a very wide range in mineralogy

Fourteen granulites, covering the range of Mg#, have been chosen for this study. All these samples are the same as those used in previous studies (Rudnick et al., 1986).

3. Analytical methods

All sample powders are the same as those used in previous studies (Gao et al., 1998; Liu et al., 2001; Rudnick et al., 1986; Rudnick and Taylor, 1987). Mineral separation was carried out by using the Frantz® Magnetic Separator at the Geochemical Laboratory of the University of Maryland, College Park. Plagioclase and pyroxene mineral separates were hand-picked from grain size factions of 180-300 μm or 150-180 μm and cleaned with Milli-Q water for 3 x 10 minutes in the ultrasonic bath.

Samples were dissolved in a ~ 3:1 mixture of concentrated HF-HNO_3 in Savillex screw-top beakers overnight on a hot plate (T< 120 ^{o}C), followed by replenishment of the dried residua with concentrated HNO_3 overnight and dried again, then picked up in concentrated HCl until solutions are clear. The solutions were then dried down and re-dissolved in 4 M HCl, in preparation for chromatographic separation. Around 100 ng Li in 1 ml 4 M HCl is loaded on the first column. Lithium is eluted though three sets of

columns, each containing 1 ml of cation exchange resin (BioRad AG50W-x12) following the first three column procedures described by Moriguti and Nakamura (1998b). Columns were calibrated using samples with different matrix (e.g., peridotite, basalt, granite and pure Li solution). In order to check Li yields, before/after cuts for each sample were collected and analyzed by single collector ICP-MS (Thermo Finnigan Element 2). With ~100 ng sample Li loaded (corresponding to 1 to10 mg of sample), the column procedure separates Li from other matrix elements with >98% yield.

The MC-ICP-MS analysis protocol is similar to that reported in Teng et al. (2004a). In brief, prior to Li isotopic analyses, the Na/Li voltage ratio of each solution is evaluated from voltage ratios using the axial Faraday cup. Solutions with a Na/Li voltage ratio ≥ 5 are reprocessed through the 3rd column. Purified Li solutions (~100 ppb Li in 2% HNO_3 solutions) are introduced to the Ar plasma using an auto-sampler (ASX-100® Cetac Technologies) through a desolvating nebulizer (Aridus® Cetac Technologies) fitted with a PFA spray chamber and micro-nebulizer (Elemental Scientific Inc.). Samples are analyzed using a Nu-Plasma MC-ICP-MS (Belshaw et al., 1998), with ^{7}Li and ^{6}Li measured simultaneously in separate Faraday cups. Each sample analysis is bracketed by measurements of the L-SVEC standard (Flesch et al., 1973) having a similar solution concentration and acid strength (although tests reveal that standard/sample concentration ratios can vary by up to an order of magnitude without detriment to the measurement). Two other Li standards (e.g., the in-house Li-UMD1, a purified Li solution from Alfa Aesar®, and IRMM-016 (Qi et al., 1997)) are routinely analyzed during the course of each analytical session. A rock standard (AO-12, a Post Archean Australian shale (PAAS), Teng et al., 2004a), is also routinely analyzed for quality control purposes.

International rock standard BCR-1 was also measured during the course of this study. The in-run precision on $^{7}Li/^{6}Li$ measurements is $\leq \pm 0.2‰$ for two blocks of 20 ratios each, with no apparent instrumental fractionation. The external precision, based on 2 σ of repeat runs of both pure Li standard solutions and natural rocks, is $< \pm 1.0‰$. For example, pure Li standard solutions (IRMM-016 and UMD-1) always have values falling within previous established ranges (-0.1 ± 0.2‰ and +54.7 ± 1‰, Teng et al., 2004a); AO-12 gives $\delta^{7}Li = +3.5 \pm 0.6$ ‰ (2 σ, n = 36 runs with 4 replicate sample preparations); and BCR-1 gives $\delta^{7}Li = +2.0 \pm 0.7$ ‰ (2 σ, n = 10 runs).

Lithium concentrations were determined by voltage comparison with that measured for the L-SVEC standard of known concentration and then adjusting for sample weight. The precision of this measurement is better than ± 10%.

4. Results

Lithium concentrations and isotopic compositions are reported in Table 1 for composites of high-grade metamorphic rocks from East China, Table 2 for granulite xenoliths from Hannuoba, Table 3 for granulite xenoliths from McBride and Table 4 for granulite xenoliths from Chudleigh.

4.1. Composites of high-grade metamorphic rocks from East China

All samples show similar $\delta^{7}Li$ values with an average of +4 ± 1.4‰ (1σ) (Fig. 1), indistinguishable from oceanic basalts (Chan and Edmond, 1988; Chan et al., 1992; Chan and Frey, 2003; Moriguti and Nakamura, 1998a; Ryan and Kyle, 2004; Tomascak and Langmuir, 1999; Tomascak et al., 1999b). Lithium concentrations in these samples vary from 5 to 33 ppm, with one intermediate granulite having the highest Li concentration and one granite gneiss having the lowest value.

Table 3-1. Lithium concentration and isotopic composition of composites from high-grade metamorphic terranes in East China

Sample	Rock type[2]	Terrane	n[1]	δ^7Li	Li (ppm)[3]	Li (ppm)[4]	Mg#[4]	H_2O (wt%)[4]
D138	Dio gneiss	Dengfeng	1	+2.8	21.3	20.2	54.8	1.35
14R110	TTG gneiss	Wutai	10	+2.6	19.4	20.0	61.4	0.59
D141	Ton gneiss	Taihua	4	+3.2	16.9	15.6	51.2	1.57
14R118	Ton gneiss	Wutai	15	+5.6		14.2	48.2	1.02
14R117	Ton gneiss	Wutai	15	+5.2	11.5	12.0	41.8	1.64
14R116	Tro gneiss	Wutai	15	+7.5		15.3	40.0	0.50
D142	Tro gneiss	Taihua	1	+3.9	9.8	10.7	31.9	0.87
D139	Tro gneiss	Dengfeng	3	+3.7	12.2	12.6	39.0	1.24
D147	Tro gneiss	Kongling	7	+2.9	16.2	15.2	51.5	1.53
14R109	Grd gneiss	Wutai	10	+5.2	22.2	19.3	56.2	0.98
D143	Gra gneiss	Taihua	3	+4.0	6.6	5.2	19.3	1.51
D140	Gra gneiss	Dengfeng	2	+3.8	6.5	6.5	29.1	1.08
D148	Gra gneiss	Kongling	4	+2.7	17.5	16.0	41.9	1.24
D149	Amphibolite	Dengfeng	10	+3.4		10.9	49.9	2.74
D153	Amphibolite	Taihua	12	+6.8	5.8	5.2	45.4	2.10
14R162	Amphibolite	Fuping	2	+3.9	8.7	10.5	58.4	2.36
14R167	Amphibolite	Hengshan	8	+3.7		11.0	46.8	2.09
D171	Amphibolite	Kongling	8	+6.2	8.2	8.1	49.5	2.76
D154	Mafic granulite	Taihua	2	+4.4	8.3	8.3	43.1	1.62
14R161	Mafic granulite	Fuping	8	+4.7	8.9	6.7	40.3	1.88
14R168	Mafic granulite	Hengshan	1	+5.7		8.1	32.0	1.83
D368	Mafic granulite	Jinning	10	+3.4		7.3	46.5	1.09
15R281	Inter granulite	Wulashan	10	+2.3	32.6	30.8	45.1	0.59
15R267	Inter granulite	Wulashan	10	+5.1	12.5	10.3	54.6	1.05
15R278	Inter granulite	Wulashan	10	+3.2		15.9	41.6	0.93
15R266	Inter granulite	Wulashan	10	+2.4		20.9	35.9	0.55
D366	Felsic granulite	Jinning	3	+2.8		8.4	46.2	0.89
15R277	Felsic granulite	Wulashan	10	+1.7		20.8	44.1	0.74
15R268	Felsic granulite	Wulashan	10	+3.1	8.7	8.6	42.6	0.92
15R263	Felsic granulite	Wulashan	10	+2.8	12.8	11.3	33.7	0.62

1. n = Number of individual samples comprising the composite.
2. Dio = diorite; Ton = tonalite; Tro = trondhjemite; Grd = granodiorite; Gra = granite.
3. Lithium measured by voltage comparison with 50 or 100 ppb LSVEC.
4. Data from Gao et al. (1998).

Table 3-2. Lithium concentration and isotopic composition of granulite xenoliths from Hannuoba, East China

Sample	Rock type	δ^7Li	Li (ppm)[1]	Li (ppm)[2]	Mg[#2]	Al_2O_3/CaO[2]
DMP-10	Pyroxenite	-4.2		4.1	76.1	0.453
DMP-11	Two-pyroxene	-1.9	2.4	2.2	77	0.409
DMP-03	Two-pyroxene	+0.5	4.5	5.8	78.9	1.259
DMP-09	Two-pyroxene	-1.9	5.2	4.9	77.9	1.181
DMP-28	Two-pyroxene	-8.0	6.9	7.7	70.2	0.838
DMP-45	Two-pyroxene	-9.6		7.4	74.3	1.347
DMP-66	Two-pyroxene	-2.9	3.7	3.5	77.7	0.997
DMP-68	Two-pyroxene	-3.3	5.4	5.6	77.6	0.833
DMP-08	Garnet bearing	+0.2	2.3	1.9	71.6	1.423
DMP-15	Garnet bearing	+4.3	4.4	4.1	70.2	1.175
DMP-06	Plagioclase-rich	+13.8	2.1	2.7	64.4	3.338
DMP-07	Plagioclase-rich	+2.2	4.2	4.6	61	2.022
DMP-62	Plagioclase-rich	+6.7	2.0	1.9	72.2	3.955
DMP-75	Plagioclase-rich	+1.3	3.3	3.4	55.6	2.13
DMP-01	Intermediate	+12.1	0.6	0.5	71.5	3.948
DMP-27	Intermediate	-5.1	4.6	5.7	47.3	2.373
DMP-61	Intermediate	+3.8	0.9	0.9	69.5	3.101
DMP-70	Intermediate	+7.1	1.4	1.2	65.4	2.98

1. Lithium measured by voltage comparison with 50 or 100 ppb LSVEC.
2. Data from Liu et al. (2001).

Table 3-3. Lithium concentration and isotopic composition of granulite xenoliths from McBride, North Queensland, Australia

Sample	Rock type	δ^7Li	Li (ppm)[2]	Mg#
85-100	Two-pyroxene	-2.4	10.2	66.0
85-100 replicate[1]		-1.9	10.2	
85-106	Garnet-clinopyroxene	+5.8	16.7	62.8
85-106 replicate		+5.0	16.8	
85-114	Garnet-clinopyroxene	-10.4	4.3	48.9
85-114 replicate		-10.6	4.7	
83-159	Garnet-clinopyroxene	-13.5	3.5	46.7
83-159 replicate		-13.1	4.2	
85-108	Two-pyroxene garnet	0	5.3	54.9
85-108 replicate		-0.3	5.7	
85-108 plagioclase	180-300 μm	-5.6	1.6	
83-157	Intermediate	0	6.6	53.0
83-157 replicate		-1.8	7.2	
83-160	Felsic	+2.7	6.8	47.5
83-162	Felsic	-3.1	7.5	41.2
83-162 replicate		-3.8	6.9	
85-101	Intermediate	-3.3	7.5	44.8
83-158	Two-pyroxene garnet	2.8	21.1	61.3
83-158 plagioclase	180-300 μm	+6.0	3.8	
85-107	Garnet-clinopyroxene	+15.7	2.3	21.2
85-107 pyroxene	180-300 μm	+7.5		
85-120	Two-pyroxene	-4.6	9.5	63.4

1. Replicate = two times of column chemistry from the same stock solution.
2. Lithium measured by voltage comparison with 50 or 100 ppb LSVEC.

Table 3-4. Lithium concentration and isotopic composition of granulite xenoliths from Chudleigh, North Queensland, Australia

Sample	Rock type	δ^7Li	Li (ppm)	Mg#
83-112	Plagioclase-rich	+1.2	4.6	41.1
83-117	Plagioclase-rich	-12	4.6	76.4
83-125	Plagioclase-rich	-17.9	2.3	71.9
83-125 plagioclase	180-300 μm	-13.6	2.8	
83-133	Plagioclase-rich	-16.3	2.6	69.3
83-133 plagioclase	180-300 μm	-15.2	0.5	
83-138	Plagioclase-rich	-5.5	4.4	72.7
83-126	Plagioclase-rich	-2.4	0.2	72.0
BC	Plagioclase-rich	-1.3	3.3	80.6
BC replicate[1]		-1.1		
BC pyroxene	180-300 μm	+0.4	3	
BC pyroxene	150-180 μm	-0.3	2.6	
83-107	Plagioclase-rich	+1.1	3.6	66.9
83-107 pyroxene	180-300 μm	0		
83-114	Plagioclase-rich	+4.7	2.1	69.0
83-114 replicate		+3.3	2	
83-114 plagioclase	180-300 μm	+2.0	1.8	
83-131	Plagioclase-rich	-2.7	1.8	71.6
83-131 replicate		-1.3	1.7	
83-131 plagioclase	180-300 μm	-0.7	0.9	
83-127	Plagioclase-rich	+5.1	1.3	72.2
83-127 replicate		+5.9	1.7	
83-140	Plagioclase-rich	-8.7	3.9	62.6
83-140 replicate		-9.1	3.6	
83-110	Pyroxene-rich	+6.1	6.2	73.4
83-110 replicate		+5.7	7.0	
83-115	Pyroxene-rich	-3.9	3.2	77.8
83-115 replicate		-4.4		
83-115 pyroxene	180-300 μm	-6.7	22.9	
83-115 pyroxene	150-180 μm	-7.4	20.3	
83-115 others[2]	180-300 μm	-4.6		

1. Replicate = two times of column chemistry from the same stock solution.
2. Other minerals except pyroxene and plagioclase.

Lithium measured by voltage comparison with 50 or 100 ppb LSVEC.
Analytical uncertainty is < ± 1‰ for δ^7Li and <10% for Li concentration

4.2. Granulite xenoliths

There is good correspondence between the δ^7Li of mineral separates and whole rocks for the Chudleigh suite (Fig. 2). Two whole rock samples from the McBride suite are isotopically heavier than their mineral separates, which may reflect interactions with isotopically heavy retrograde fluids. Compared with granulites from Archean terranes, both mineral separates and whole rock granulite xenoliths define a much larger range in δ^7Li (-17.9 to +15.7‰, Fig. 3), with whole rock granulites having lower Li concentrations (5 ± 4 ppm, 1σ). Since most of the mineral separates (8 out of 10) are similar to whole rocks over a large range in δ^7Li, δ^7Li of whole rock is representative of that of the granulite xenoliths. Therefore, whole rock data, for those granulite xenoliths that have no mineral data available, are considered representative of δ^7Li of the deep crust.

The δ^7Li of 14 granulites from Hannuoba varies from –9.6 to +13.8‰ with an average of –0.7 ± 4.9‰ (1σ). Seven two-pyroxene mafic granulites and one pyroxenite show negative δ^7Li values down to, –9.6‰ while plagioclase-rich and garnet bearing mafic granulites have positive δ^7Li values, up to +13.8‰. δ^7Li values of four intermediate granulites vary from –5.1 to 12.1‰ and fall within the range observed in mafic granulites. Lithium concentrations of mafic granulites have a narrow range compared with intermediate granulites (1.9 to 7.7 ppm vs. 0.5 to 5.7 ppm).

The McBride suite also displays a large range in δ^7Li from –13.3 to +15.7‰ with a lighter average of –3.8 ± 7.6‰ (1σ). The four garnet-clinopyroxene mafic granulites define the δ^7Li range. The other eight samples including two-pyroxene, two-pyroxene

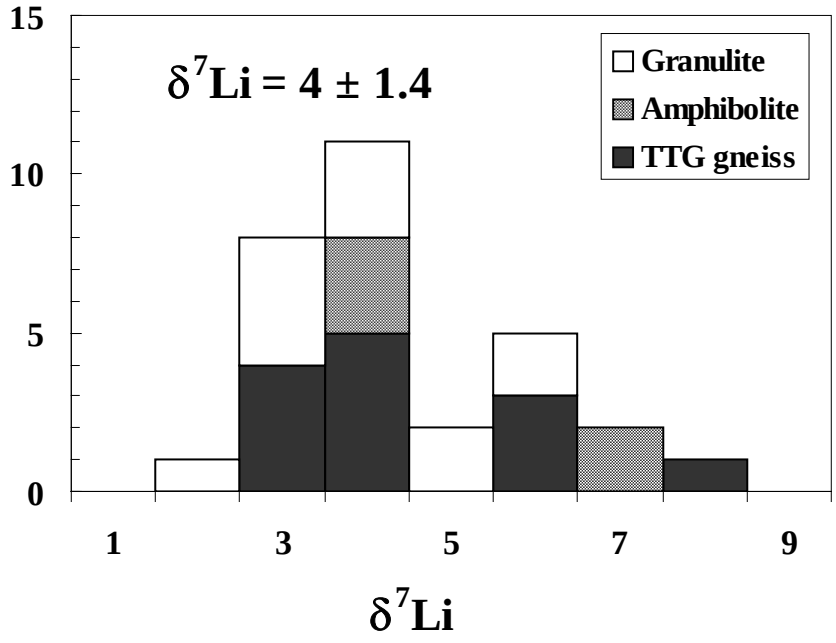

Figure 3-1. Lithium isotopic composition of composites from Archean high-grade metamorphic terranes in East China.

Data are from Table 3-1.

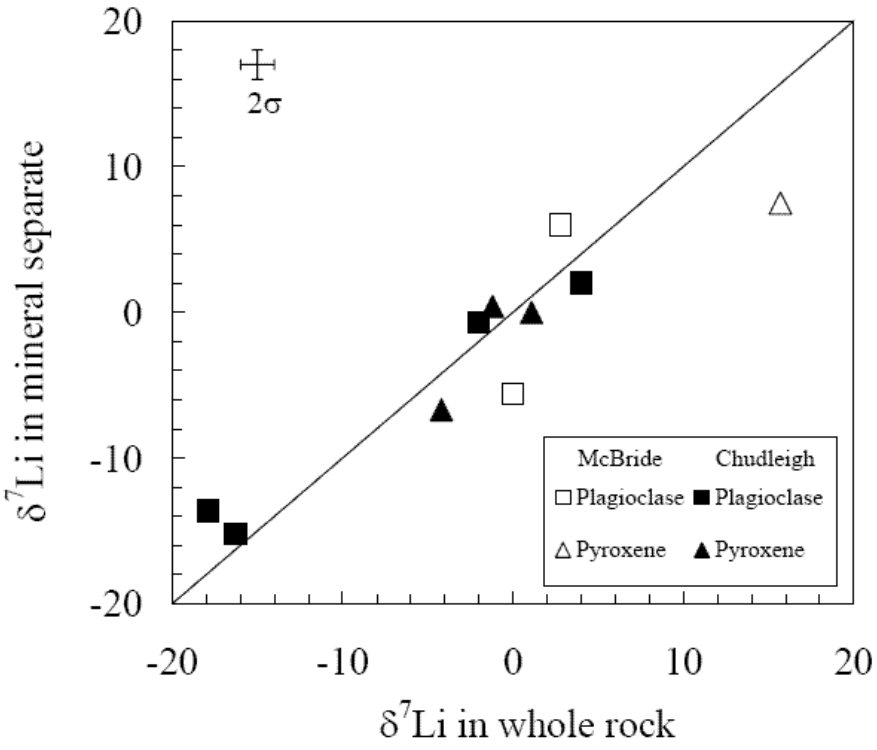

Figure 3-2. Comparison between δ^7Li of whole rock and mineral separates. Diagonal line marks a 1:1 correlation.

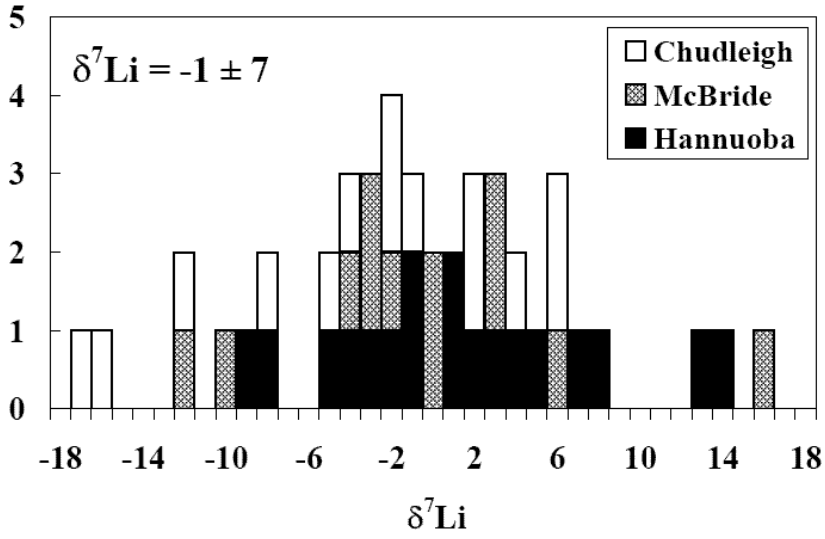

Figure 3-3. Lithium isotopic composition of granulite xenoliths.
Data are from Tables 3-2, 3-3, and 3-4.

garnet, intermediate and felsic granulites show a relatively small range from –4.6 to +5.4‰. Lithium concentrations of these granulites show one order of magnitude change from 2 to 21 ppm.

The 14 mafic granulite xenoliths from Chudleigh have δ^7Li values ranging from –17.9 to +5.9‰ with an average of –2.5 ± 5.5‰ (1σ). The seven mineral separates also show large variations with δ^7Li from –15.2 to 2‰. Two plagioclase-rich granulites define the lowest δ^7Li values known for metamorphic rocks. One pyroxene-rich granulite has the highest δ^7Li values in this suite. Lithium concentrations of these granulites vary from 0.2 to 7.0 ppm.

5. Discussion

Samples studied here are high-grade metamorphic rocks and their Li isotopic compositions may reflect their protolith δ^7Li, processes fractionating Li isotopes during metamorphic processes, or both. The large differences in Li and δ^7Li between composites and granulite xenoliths provide us with a chance to study how protolith and metamorphic processes affect Li concentration and isotopic compositions of metamorphic rocks. Below, we first evaluate Li geochemical behavior during metamorphism, and then use our data to derive estimates for the Li concentration and isotopic composition of the deep continental crust.

5.1. Lithium geochemistry of metamorphic rocks

Lithium is mobile during high temperature hydrothermal processes (Berger et al., 1988; Brenan et al., 1998b; Chan et al., 1993; 1994; Seyfried Jr. et al., 1984; 1998) and metamorphic dehydration (Teng et al., 2005c; Zack et al., 2003). Data from regional

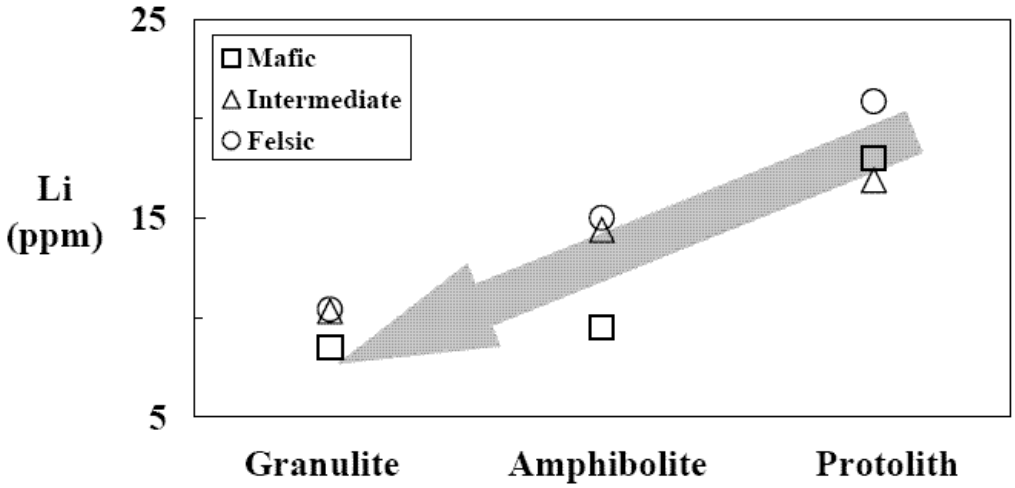

Figure 3-4. Variation of Li concentration verses increasing metamorphic grades. Data from Gao et al. (1998).

metamorphic rocks also show Li depletion with increasing metamorphic grade, regardless of lithology (Fig. 4). This depletion is mainly due to Li loss during metamorphic dehydration. An excellent positive correlation between Li concentration and Mg# has been observed for 13 TTG gneiss composites (Fig. 5). This may reflect the control of lithology on Li concentration in metamorphic rocks.

Lithium isotope fractionation at relatively high temperature has also been documented by studying hydrothermal alteration (Chan et al., 1993; Chan et al., 1994; Seyfried Jr. et al., 1998), contact metamorphism (Teng et al., 2005c) and granite differentiation (Teng et al., 2005a). During all these processes, isotopically heavy Li preferentially fractionates into fluids compared to rocks. Metamorphic rocks are, therefore, expected to evolve towards lower Li and δ^7Li values with increasing metamorphic grade. However, retrograde samples usually have higher Li concentrations and slightly heavier isotopic composition than their prograde counterparts, due to interactions with isotopically heavy fluids (Teng et al., 2005c)

All three suites of granulite xenoliths studied here show extremely large variations in δ^7Li values. Although these granulites have heterogeneous origins (Liu et al., 2001; 2004; Rudnick et al., 1986; Rudnick and Taylor, 1987; Rudnick and Williams, 1987; Rudnick, 1990; Rudnick and Goldstein, 1990), this large range is far beyond that observed in typical upper crustal rocks (granites, shale and loess) and basalts, and therefore it must result from other processes. Previous studies indicate that granulite xenoliths from Chudleigh are cumulates crystallized from underplated basalt, which

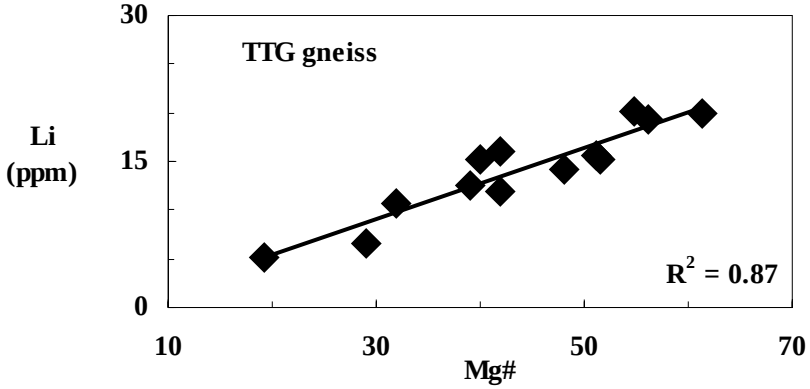

Figure 3-5. Correlation between Li and Mg# for TTG gneiss composites from Archean high-grade metamorphic terranes in East China.

Data are from Table 3-1.

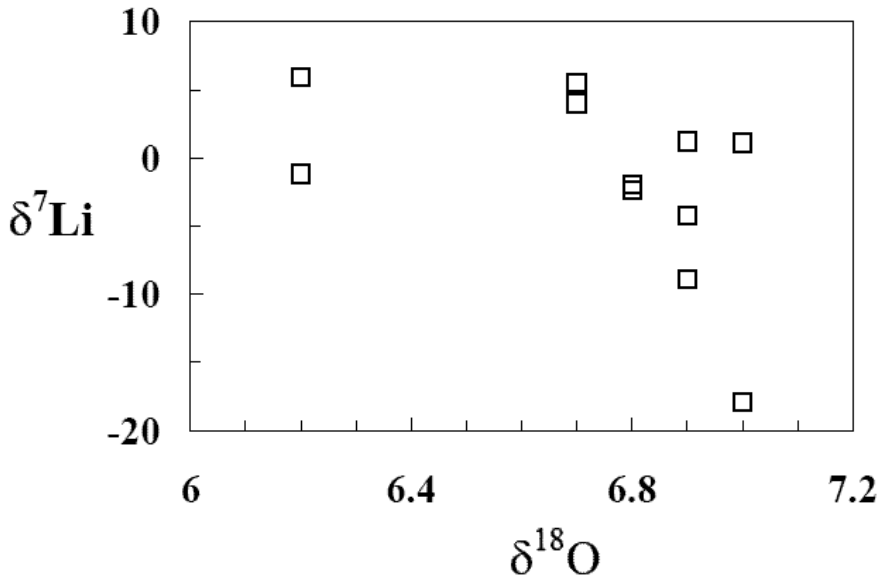

Figure 3-6. Correlation between δ^7Li and δ^{18}O for Chudleigh granulite xenoliths. Data are from Table 3-4.

assimilated pre-existing lower crust (Rudnick et al., 1986; Rudnick, 1990; Rudnick and Goldstein, 1990; Saal et al., 1998). This process can be modeled by assimilation fractionation crystallization (AFC). Plots of δ^7Li with Li, Sr, Nd, and Pb show no correlations. δ^7Li vs. δ^{18}O, however, shows a rough negative correlation (Fig. 6). This can be explained by contamination of underplated basalts with pre-existing isotopically light lower crust. The extremely light δ^7Li values of the lower crustal end member may be produced by large isotopic fractionation during metamorphic dehydration, as indicated by a study of eclogites (Zack et al., 2003) and modeling (Teng et al., 2005c). No systematic variations between δ^7Li and other isotopic systems (Sr, Nd, Pb, and O) are found in the granulite xenoliths from the other two suites. This may be due to their diversity of origins, involving different amounts and types of surface materials with different lithologies. For the Hannuoba xenoliths, δ^7Li correlates positively with Al_2O_3/CaO (Fig. 7) and negatively with Li, FeO, MgO, CaO and Co, indicating that the protolith composition may play some role in controlling the Li isotopic composition of these rocks.

Compared with the granulite xenoliths, composites from Archean high-grade terranes display a narrow range in δ^7Li (+1.7 to +7.5‰) and higher Li concentrations (13 ± 6 ppm vs. 5 ± 4 ppm). This difference indicates that different factors control Li concentration and isotopic compositions in xenoliths compared with high-grade terranes. The 12 granulite composites show a positive correlation between δ^7Li and H_2O, with mafic samples having the highest H_2O contents and heaviest Li isotopic composition (Fig. 8). This agrees with the expectation that metamorphic dehydration shifts metamorphic rocks to isotopically light compositions. The fact that mafic granulites are

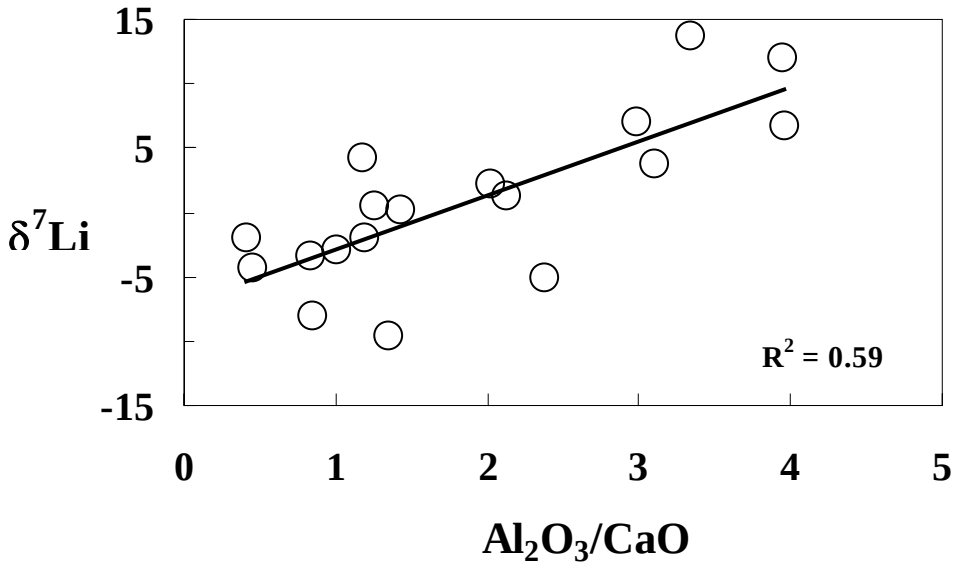

Figure 3-7. Variation of δ^7Li verses Li content and Al_2O_3/CaO ratio for Hannuoba granulite xenoliths.
Data from Table 3-1 and Liu et al. (2001)

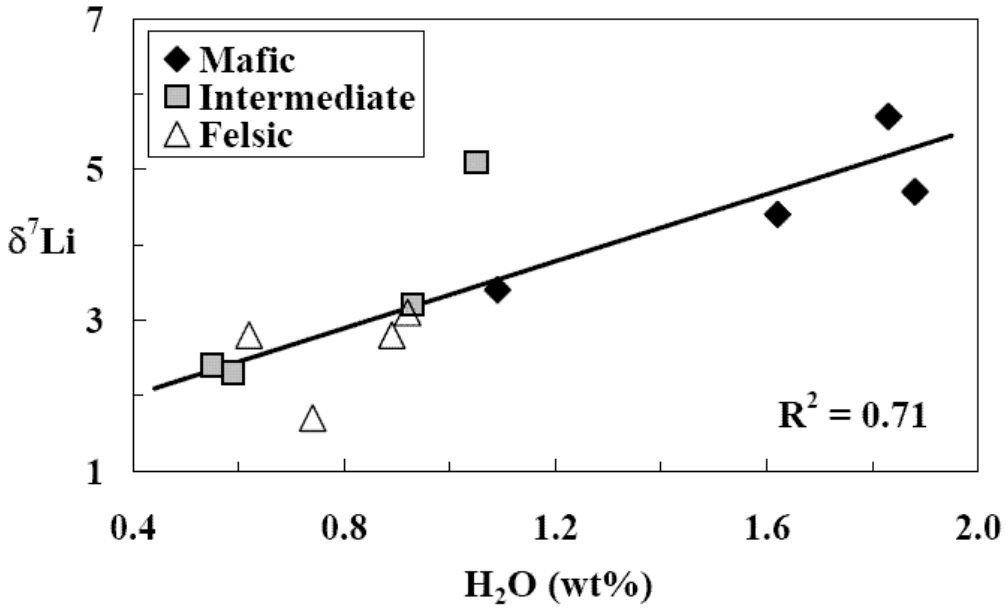

Figure 3-8. Correlation between δ^7Li and H_2O content in granulite composites from Archean high-grade metamorphic terranes in East China.

Data are from Table 3-1.

more enriched in H_2O than felsic ones may result from their different protoliths and mineralogies. However, the overall variation of δ^7Li in terrane granulites is very small compared with that in granulite xenoliths. The granulite xenoliths carried by basaltic lava reach the Earth's surface very quickly, on the order of hours to thousands of years (Spera, 1980). This quick ascent enables minor interactions between xenoliths and basaltic lava, with decompression-induced melting likely. The deep crustal terranes now exposed at the surface, however, often have complex thermal histories and slow exhumation rates on the order of > million years. During the process of exhumation, retrograde reactions occurred widely and may buffer and homogenize any Li heterogeneity produced during granulite-facies metamorphism. Granulite xenoliths, which have not experienced retrograde metamorphism, can preserve the isotopic heterogeneity. This may indicate that during granulite-facies metamorphism in the deep crust, pervasive fluid migration and interaction have not happened or happened at only a small scale, which prevents the homogenization of Li isotopes. This interpretation is consistent with B elemental and O isotopic studies (Kempton and Harmon, 1992; Leeman et al., 1992).

5.2. Lithium concentration of the deep continental crust

Estimates of the Li content of the upper continental crust date back to 1889 (Clarke, 1889; Clarke and Washington, 1924), while the first estimate of Li concentration in the deep crust was made by Heier 1964, who estimated 10 ppm Li in deep crust by studying rocks from middle to high-pressure granulite-facies terranes (Heier and Adams, 1964). Later studies followed the same methods by studying different high-grade metamorphic terranes worldwide, except for Taylor & McLennan (1985), who estimated Li abundance in the deep continental crust based on a theoretical model. All these

estimates give similar low values from 6 ppm to 15 ppm and show that the deep crust is depleted in Li relative to the upper crust (Gao et al., 1998; Rudnick and Fountain, 1995; Shaw et al., 1994; Taylor and McLennan, 1985; Wedepohl, 1995). Due to the lack of Li data FOR granulite xenoliths, all these estimates heavily rely on samples from high-grade metamorphic terranes.

Here we use Li data collected in this study and combine them with data in the literature (after Rudnick, 1992) to place constraints on the average Li concentration of the lower crust. Average Li concentrations of granulite xenoliths from Australia, China, France and Germany vary from 4 ppm to 14 ppm with an average of 8 ppm (Table 5). This value represents the average Li concentration in the lower crust derived from lower crustal granulite xenoliths and is slighter lower than estimates obtained by using samples from granulite terranes. As illustrated in previous sections, this is mainly due to the different roles played by metamorphic fluids.

The Li concentration of the bulk continental crust is estimated at 18 ppm by assuming 35 ppm Li in the upper crust (Teng et al., 2004a), 12 ppm Li in the middle crust (Rudnick and Gao, 2003) and 8 ppm Li in the lower crust (this study) with the weight proportion of the various crustal sections being 0.317:0.295: 0.388 (Rudnick and Gao, 2003). Thus, Li concentrations decrease with depth from upper, middle, lower continental crust to the mantle, with insignificant amounts of Li in the hydrosphere and none in the Earth's core. This reflects the incompatibility of Li during mantle melting and crustal differentiation (Brenan et al., 1998a; Ryan and Langmuir, 1987).

Table 3-5. Lithium concentration in granulite xenoliths and lower crust

Location	N.O.	Ave. Li (ppm)	Reference
Northern Hessian Depression, Germany	32	14	Mengel (1990), Mengel and Hoefs (1990)
Massif Central, France	95	7	Leyreloup et al. (1977), Dostal et al. (1980), Downes et al. (1989)
Hannuoba, China	27	4	Liu et al. (2001)
North Queensland, Australia	26	6	This study
Lithium in the lower crust	**180**	**8**	**Average**

N.O. = total sample numbers

5.3. Lithium isotopic composition of the deep continental crust

Compared with the upper continental crust, which can be averaged by clastic sedimentary rocks (shale and loess), estimating the average composition of the deep continental crust is more difficult. The average composition of the deep continental crust can only be estimated by analyzing a large number of representative deep crustal samples. The average δ^7Li values for high-grade metamorphic composites and xenoliths are 4.0‰ and –1.1‰ separately. The average for both types is +1 ± 6‰(1σ), which is representative of the average deep continental crust.

Previous studies indicate that the Li isotopic composition of granite can reflect the δ^7Li of their source rocks due to the small Li isotopic fractionation during granite petrogenesis (Bryant et al., 2004b; Teng et al., 2004a; 2005a). Since granites crystallized from magmas derived from the deep crust, their Li isotopic composition may provide some constraints on the δ^7Li of the deep continental crust. Moreover, compared with xenoliths, which represent small-scale samples, granite is derived from large-scale melting of deep crustal rocks and can, therefore, be used to constrain the average Li isotopic composition of the deep crust. Granites, including I-, S- and A-types worldwide, yield an average δ^7Li of 1.7 ± 2.2 (1σ) (Fig. 10), which is within uncertainty of the value estimated by using high-grade metamorphic rocks.

Therefore, the deep continental crust, like the upper continental crust (Teng et al., 2004a), is isotopically lighter than the upper mantle, as sampled by oceanic basalts (Chan and Edmond, 1988; Chan et al., 1992; Chan and Frey, 2003; Moriguti and Nakamura, 1998a; Ryan and Kyle, 2004; Tomascak and Langmuir, 1999; Tomascak et al., 1999b).

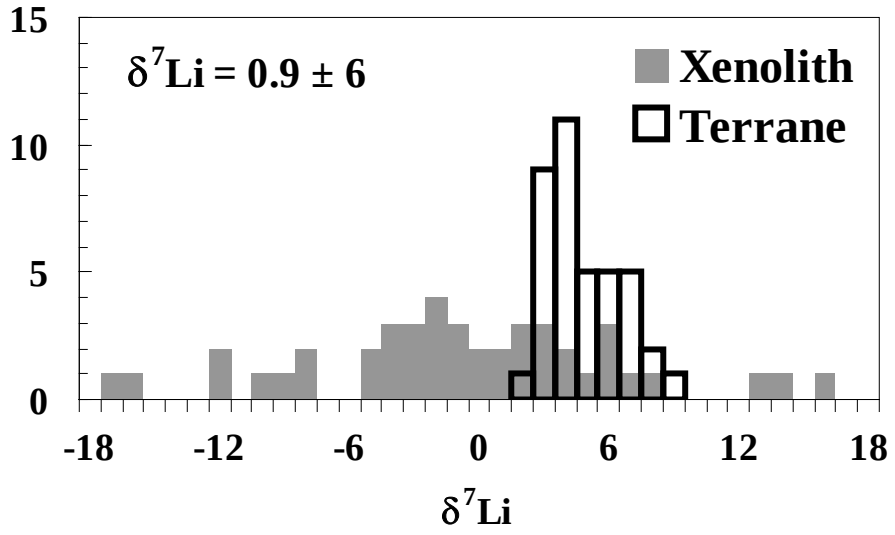

Figure 3-9. Lithium isotopic composition of the deep continental crust. Data are from Tables 3-1, 3-2, 3-3 and 3-4.

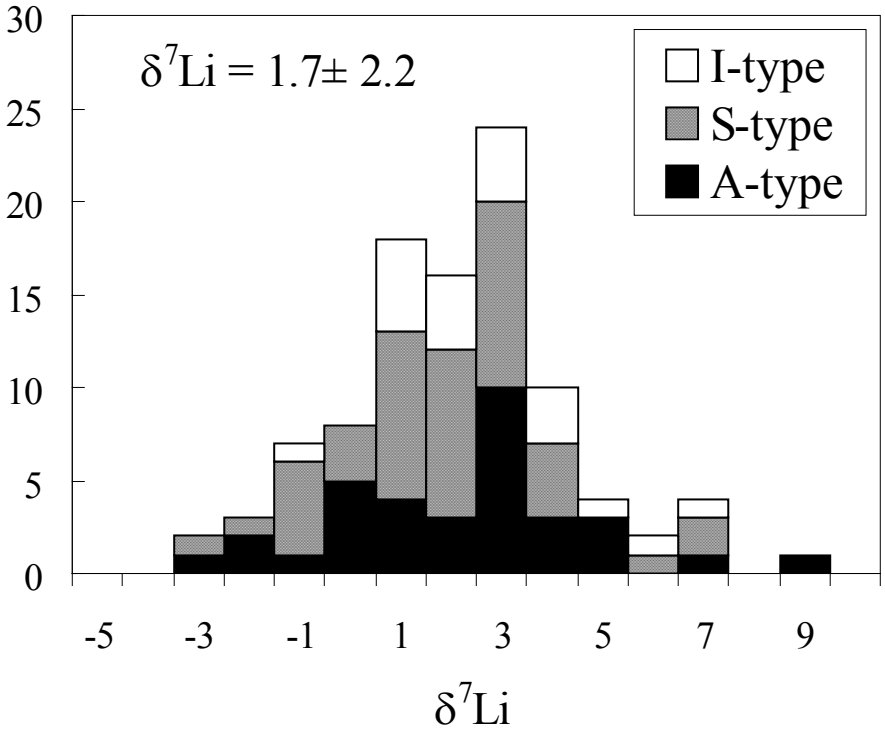

Figure 3-10. Lithium isotopic composition of granites.
Data are from Teng et al. (2004a; 2005a), Rudnick et al. (2004), Bryant et al. (2004a), James and Palmer (2000) and Table A2-1.

Compared with the silicate Earth, the hydrosphere is isotopically the heaviest Li reservoir (Chan et al., 1992; Huh et al., 1998). This heterogeneous Li isotopic distribution in Earth reservoirs mainly results from surface weathering (Huh et al., 2004; Kisakurek et al., 2004; Pistiner and Henderson, 2003; Rudnick et al., 2004), seafloor and hydrothermal alteration (Bouman et al., 2004; Chan et al., 1992; 2002a; Foustoukos et al., 2004; James et al., 2003; Seyfried Jr. et al., 1998) and metamorphic dehydration (Benton et al., 2004; Teng et al., 2004b; Williams and Hervig, 2005; Zack et al., 2003); during all these processes, isotopically heavy Li prefers fluids to rocks, and the shifts the continental crust towards lighter δ^7Li while hydrosphere moves towards heavier δ^7Li values.

6. Conclusions

The main conclusions to be drawn from our data are

1. The 30 composite deep crustal samples, including TTG gneiss, amphibolites and felsic to mafic granulites from Archean high-grade metamorphic terranes in East China, have a narrow range of δ^7Li values from +1.7 to +7.5‰, with an average of +4 ± 1.4‰ (1σ), which is indistinguishable from the upper mantle.
2. The 44 granulite-facies xenoliths from East China (Hannuoba suite) and Queensland, Australia (Chudleigh and McBride suites) display a much larger range in δ^7Li, from –17.9‰ to +15.7 with average values decreasing in the order: Hannuoba (–0.7 ± 4.9‰), Chudleigh (-2.5 ± 5.5‰) and McBride (–3.8 ± 7.6‰).
3. The difference in δ^7Li between xenoliths and terranes reflect the processes affecting Li in metamorphic rocks: retrograde fluid homogenization in the terrane vs. metamorphic dehydration in the xenoliths.

4. Overall, the deep continental crust is heterogeneous, with an average Li isotopic composition of +1 ± 6‰ (1s). This value is similar to that of the upper continental crust and is slightly lighter than the mantle, and reflects Li isotopic fractionation during secondary processes.
5. Based on the average Li concentration in granulite xenoliths, the average lower continental crust Li content is revised to 8 ppm, which is similar to previous estimates.

Chapter 4: Lithium isotopic fractionation during granite differentiation

Abstract

Lithium isotopic compositions and concentrations have been measured for the S-type Harney Peak Granite, the spatially associated Tin Mountain pegmatite and possible metasedimentary source rocks. The Harney Peak Granite is isotopically heterogeneous with δ^7Li varying from -3.1 to +6.6‰. The δ^7Li values of Proterozoic metasedimentary rocks that are possible sources of the Harney Peak Granite range from -3.1 to +2.5‰ and overlap with post-Archean shales and the Harney Peak Granite. For the granite suite, there is no correlation between δ^7Li and elements indicative of degrees of granite differentiation (SiO_2, Li, Rb, etc.). The Li isotopic composition of the Harney Peak Granite, therefore, appears to be a function of source composition.

Minerals from the zoned Tin Mountain pegmatite have extremely high Li contents and heavier Li isotopic compositions than the granite or surrounding Black Hills metasedimentary rocks. The heavier compositions may reflect Li isotopic fractionation resulting from extensive crystal-melt fractionation and fluid exsolution. Lithium concentrations decrease in the order: spodumene (~3.7 wt %), muscovite (0.2 to 2.0 wt.%), plagioclase (100-1100 ppm), quartz (30-140 ppm). Plagioclase, muscovite, and spodumene in all zones display a relatively narrow range in δ^7Li of +7.9 to +11.4‰. In contrast, quartz is isotopically heavier and more variable (+14.7 to +21.3‰), with δ^7Li showing an inverse correlation with Li concentration. This correlation may reflect mixing between heavy Li in quartz and lighter Li in fluid inclusions. Extrapolation of this trend to an estimated intrinsic Li concentration in quartz of <30 ppm, yields an inferred δ^7Li for

fluid inclusion-free quartz of >+21‰. The large difference in δ^7Li between quartz and other minerals may reflect ^{7}Li preference for less highly coordinated sites, which have higher bond-energies (i.e., the two- or four-fold site in quartz vs. higher coordination number sites in other minerals).

1. Introduction

Recent studies have significantly increased our knowledge of Li isotope geochemistry by documenting the Li isotopic variations in different geological reservoirs, and understanding the processes that may produce these variations (see recent reviews by Chan, 2004; Elliott et al., 2004; Tomascak, 2004). These studies have shown that Li isotopes in the outer layers of the Earth (hydrosphere, crust and lithospheric mantle) can be strongly fractionated, with the observed extent of Li isotope fractionation in the near–surface environment of > 60‰ (Tomascak, 2004).

Lithium isotopic fractionation has been documented in a variety of geological processes, such as weathering (Huh et al., 2004; Kisakurek et al., 2004; Pistiner and Henderson, 2003; Rudnick et al., 2004), seafloor alteration (Bouman et al., 2004; Chan et al., 1992; 2002a; Foustoukos et al., 2004; James et al., 2003; Seyfried Jr. et al., 1998), metamorphic dehydration (Benton et al., 2004; Teng et al., 2004b; Williams and Hervig, 2005; Zack et al., 2003) and high temperature diffusive exchange during magma-rock interaction (Lundstrom et al., 2005). In contrast, little isotopic fractionation is inferred to occur during high temperature igneous differentiation, be it in basaltic (Tomascak et al., 1999b) or granitic (Bryant et al., 2004b; Teng et al., 2004a; Tomascak et al., 1995) systems. However, large Li isotopic fractionations between minerals and hydrothermal

fluids may occur in aqueous fluid-rich granitic pegmatite systems at relatively low temperatures (Lynton et al., 2005).

In order to further examine Li isotope fractionation in evolved granitic systems, including relatively wet, low temperature pegmatite, we examined well-characterized samples of the Harney Peak Granite, the spatially associated, Li-rich Tin Mountain pegmatite, and metasedimentary country rocks all from the Black Hills, South Dakota. The goals of this study are to (1) study Li isotopic fractionation during granite differentiation and late stage pegmatite evolution; (2) use Li isotopes to provide additional insight into the origin and evolution of Harney Peak Granite and Tin Mountain pegmatite.

2. Geological background and samples

The Black Hills Precambrian terrane consists of two Late Archean granites (Little Elk and Bear Mountain), early Proterozoic metasedimentary and metavolcanic rocks, and the Proterozoic (ca. 1700 Ma) Harney Peak Granite, which is surrounded by thousands of simple and zoned pegmatites (Duke et al., 1990; Norton and Redden, 1990; Redden et al., 1985; Shearer et al., 1987a; Walker et al., 1986b). We discuss each of these units in turn.

2.1. Country rocks

The dominant rock types in this region are early Proterozoic micaceous and quartzose schists, derived from shales and graywackes, with the highest metamorphic grade reaching sillimanite zone. The schist is composed of quartz, biotite, plagioclase and occasional minor muscovite, and has considerable variation in modal mineralogy. In order to characterize the compositional variations within the metamorphic terrane, four quartz mica schists sampled from throughout the southern Black Hills were measured for

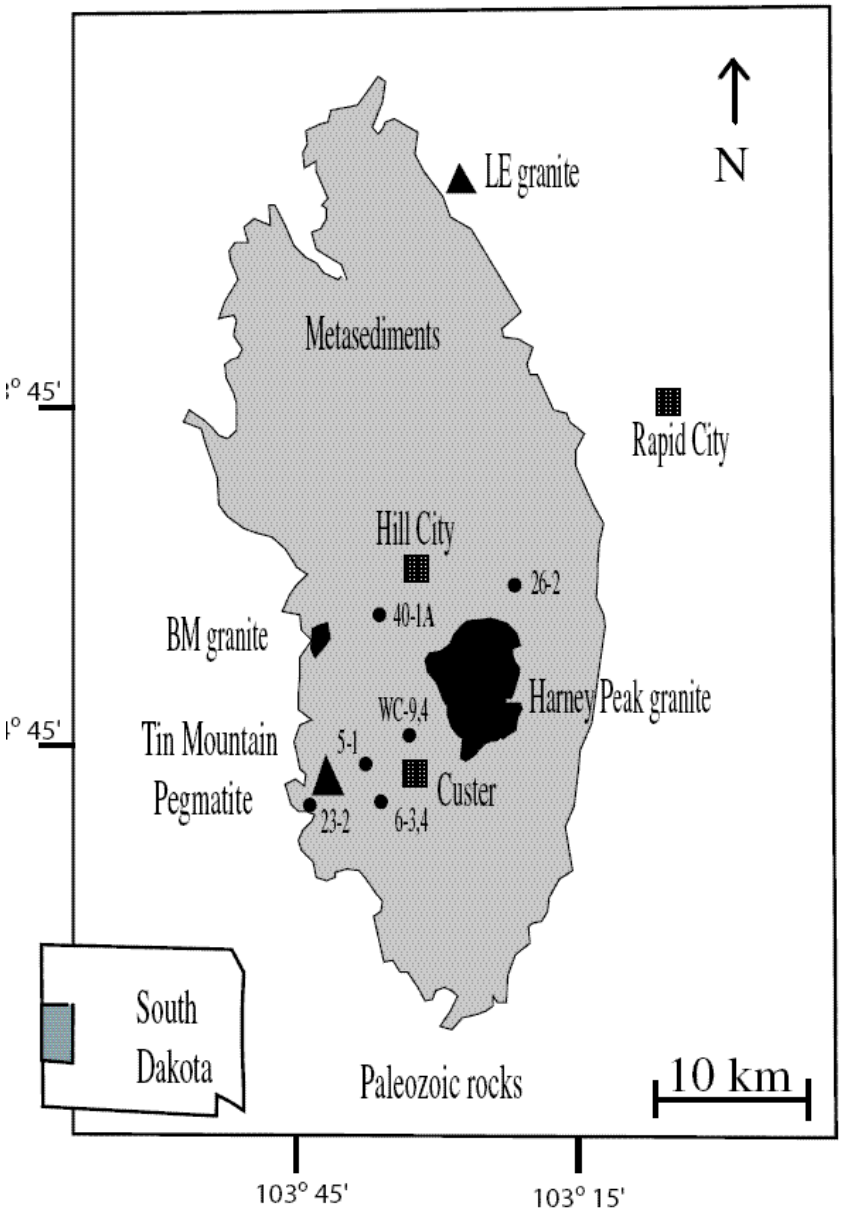

Figure 4-1. Map of the Black Hills, South Dakota.

Locations of Proterozoic Harney Peak Granite, Tin Mountain pegmatite, two Archean granites (Little Elk granite and Bear Mountain granite), four simple pegmatite and Proterozoic metasediments are shown (modified from Walker et al., 1986a).

both Li concentration and isotopic composition (Fig.1). Samples 23-2 and 40-1A were collected near the first sillimanite isograd. Samples WC-4 and 26-2 were collected near the second sillimanite isograd. These samples were taken from regions well away from most granitic outcrops and are not believed to have been affected by interactions with pegmatites, granites or fluids derived therefrom, and are therefore presumed to be representative of their original compositions.

Two late Archean granites, the Little Elk granite and the Bear Mountain granite, crop out in the region. The little Elk granite, with a U-Pb zircon age of ~2560 Ma (Zartman and Stern, 1967), is medium-grained, gneissic, and comprised primarily of plagioclase, microcline, quartz, biotite and muscovite (Walker et al., 1986a). The Bear Mountain granite, with a Rb-Sr whole-rock age of ~2450 Ma (Ratte and Zartman, 1975), is medium-grained to pegmatitic, consisting predominantly of plagioclase, quartz, microcline, muscovite, biotite and trace apatite (Walker et al., 1986a). Samples from these two Archean granites have been measured to characterize the δ^7Li of the late Archean crust (Fig. 1). No other Archean rock types are known to crop out in this region.

2.2. Harney Peak Granite

The Proterozoic Harney Peak Granite is the dominant exposed granitic rock. It does not form a single plutonic body but instead consists of hundreds of individual dikes and sills. The Harney Peak Granite is both texturally and compositionally diverse. It has a peraluminous composition, with low Ca and high water content, and with $\delta^{18}O > 10‰$, consistent with derivation from partial melting of metasedimentary rocks (Nabelek and Bartlett, 1998; Walker et al., 1986a). Nabelek et al (1992b) divided the Harney Peak Granite into two groups with different sources: biotite granite in the core of the complex,

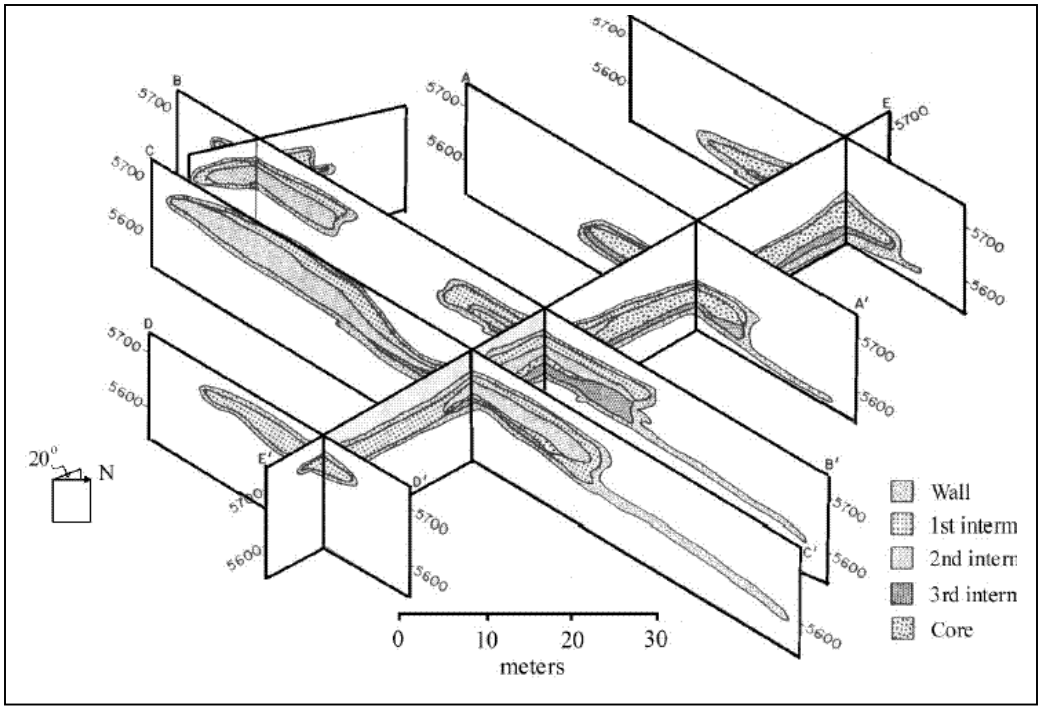

Figure 4-2. Fence diagram of the Tin Mountain pegmatite.

The vertical scale is reduced by a factor of five relative to horizontal scale (from Walker et al., 1986b).

with low $\delta^{18}O$ (+11.5 ±0.6 ‰), and tourmaline granite in the periphery of the complex, with high $\delta^{18}O$ (+13.2 ±0.8 ‰). Lead isotopes indicate that the biotite granite was derived from melting of late Archean crust, while the tourmaline granite was derived from melting of Proterozoic crust (Krogstad et al., 1993). Two potential sources for the Harney Peak Granite are sediments derived from Archean granites and the surrounding Proterozoic country rocks (Nabelek and Bartlett, 1998; Walker et al., 1989).

Twenty five samples, covering the compositional spectrum of the Harney Peak Granite, were measured in order to obtain a clear picture of $\delta^{7}Li$ variations in this heterogeneous granite. In addition, four samples of simple pegmatites from the surrounding region were also measured (Fig. 1). One of these, a pegmatitic vein (WC-9), was likely produced *in situ* from partial melting of the enclosing metasedimentary rock (WC-4), probably due to heating resulting from the intrusion of the Harney Peak Granite (Shearer et al., 1987b). This sample pair thus allows evaluation of the amount of Li isotopic fractionation attending partial melting. All samples are fresh, with H and O isotope data showing no evidence for interaction with meteoric water (Nabelek et al., 1992b).

2.3. Tin Mountain pegmatite

The Li-rich Tin Mountain pegmatite is a zoned pegmatite that discordantly intrudes both metasedimentary rocks and amphibolites, and crops out ~12 km to the southwest of the main body of the Harney Peak Granite. Walker et al (1986b) showed that this pegmatite consists of five major zones, with the wall zone forming a shell that encloses four inner zones (Fig. 2). Quartz, plagioclase and muscovite occur in all five zones; potassium feldspar dominates the 1st and 2nd intermediate zones while spodumene

mainly occurs in the 3rd intermediate zone and core. Crystallization of the wall zone occurred first, followed then by the first intermediate zone. The remaining intermediate zones and the core then crystallized simultaneously. The fracture fillings crystallized last (Walker et al., 1986b). The estimated crystallization temperature varies from >600 ^{o}C in the wall zone to 500 ^{o}C in the core, based on oxygen isotopic thermometry (Walker et al., 1986b). More recent temperature estimates based on fluid and melt inclusions yield even lower crystallization temperatures, down to 340^{o}C (Sirbescu and Nabelek, 2003a; 2003b).

Walker et al. (1989) utilized trace element and isotope (O, Nd, Sr) data to suggest two possible origins for the parental melts of this pegmatite: (1) Low degree partial melts of metasedimentary rocks that experienced moderate extents of fractional or equilibrium crystallization or (2) derivation from the Harney Peak Granite via a complex, multi-stage crystal-liquid fractional crystallization process, such as progressive equilibrium crystallization. The different zones of the Tin Mountain pegmatite resulted from crystal-melt-fluid fractionation and fluid-assisted compositional stratification (Walker et al., 1986b).

Quartz, plagioclase, muscovite, and spodumene from all major zones and fracture fillings of the Tin Mountain Pegmatite were studied. In addition, in order to characterize the Li isotopic composition of the bulk pegmatite, three whole rock composites from the wall zone were also measured. Two (9-2 and 10-3) were powdered from 5kg of rock and one (43-1) was produced from 100 kg of rock.

3. Analytical methods

All sample powders are the same as those used in previous studies (Krogstad and Walker, 1996; Nabelek et al., 1992a; 1992b; Walker et al., 1986a; 1986b; 1989) except

three of the pegmatite minerals, which were drilled directly from rock slabs, since previous powders were exhausted (see Table 2 for details).

Sample powders were dissolved in a ~ 3:1 mixture of concentrated HF-HNO_3 in Savillex screw-top beakers overnight on a hot plate (T< 120 ^{o}C), followed by replenishment of the dried residua with concentrated HNO_3 overnight and dried again, then picked up in concentrated HCl until solutions are clear. The solutions were then dried down and re-dissolved in 4 M HCl, in preparation for chromatographic separation. Around 100 ng Li in 1 ml 4 M HCl is loaded on the first column. Lithium is eluted though three sets of columns, each containing 1 ml of cation exchange resin (BioRad AG50W-x12) following the first three column procedures described by Moriguti and Nakamura (1998b). Columns were calibrated using samples with different matrix (e.g., peridotite, basalt, granite and pure Li solution). In order to check Li yields, before/after cuts for each sample were collected and analyzed by single collector ICP-MS (Thermo Finnigan Element 2). With ~100 ng sample Li loaded (corresponding to 1 to10 mg of sample), the column procedure separates Li from other matrix elements with >98% yield.

The MC-ICP-MS analysis protocol is similar to that reported in Teng et al. (2004a). In brief, prior to Li isotopic analyses, the Na/Li voltage ratio of each solution is evaluated semi-quantitatively with the mass spectrometer. Solutions with a Na/Li voltage ratio $\geq$ 5 are reprocessed through the 3rd column. Purified Li solutions (~100 ppb Li in 2% HNO_3 solutions) are introduced to the Ar plasma using an auto-sampler (ASX-100® Cetac Technologies) through a desolvating nebulizer (Aridus® Cetac Technologies) fitted with a PFA spray chamber and micro-nebulizer (Elemental Scientific Inc.). Samples are analyzed using a Nu-Plasma MC-ICP-MS (Belshaw et al., 1998), with ^{7}Li and ^{6}Li

measured simultaneously in separate Faraday cups. Each sample analysis is bracketed by measurements of the L-SVEC standard (Flesch et al., 1973) having a similar solution concentration and acid strength (although tests reveal that standard/sample concentration ratios can vary by up to an order of magnitude without detriment to the measurement). Two other Li standards (e.g., the in-house Li-UMD1, a purified Li solution from Alfa Aesar®, and IRMM-016 (Qi et al., 1997)) are routinely analyzed during the course of each analytical session. A rock standard (AO-12, a Post Archean Australian shale (PAAS), Teng et al., 2004a), is also routinely analyzed for quality control purposes. International rock standard BCR-1 was also measured during the course of this study. The in-run precision on $^{7}Li/^{6}Li$ measurements is $\leq \pm 0.2‰$ for two blocks of 20 ratios each, with no apparent instrumental fractionation. The external precision, based on 2 σ of repeat runs of both pure Li standard solutions and natural rocks, is $< \pm 1.0‰$. For example, pure Li standard solutions (IRMM-016 and UMD-1) always have values falling within previous established ranges ($-0.1 \pm 0.2‰$ and $+54.7 \pm 1‰$, Teng et al., 2004a); AO-12 gives $\delta^{7}Li = +3.5 \pm 0.6$ ‰ (2 σ, n = 36 runs with 4 replicate sample preparations); and BCR-1 gives $\delta^{7}Li = +2.0 \pm 0.7$ ‰ (2 σ, n = 10 runs).

Lithium concentrations were determined by voltage comparison with that measured for the L-SVEC standard of known concentration and then adjusting for sample weight. The precision is better than ± 10% except for spodumene. Lithium concentration in spodumene is too high, which makes it difficult to precisely constrain the sample weight loaded onto the column. The Li concentration in spodumene reported here is calculated from its standard molecular formula.

4. Results

The Li concentrations and isotopic compositions for all samples are plotted in Fig. 3. Table 1 reports data for simple pegmatites and the Harney Peak Granite, Table 2 for mineral separates and whole rock samples from Tin Mountain pegmatite and Table 3 for the quartz-mica schists and Archean granites. Major, trace element and isotopic data (Sr, Nd, Pb and O) of these samples were reported in Walker et al. (1986a; 1986b; 1989), Krogstad et al (1993) and Nabelek et al. (1992a; 1992b).

4.1. Lithium concentration and isotopic composition of granites and schists

The δ^7Li values for 25 Harney Peak Granite range from –3.1 to +6.6‰, with Li concentration ranging from 10 to 205 ppm. These concentrations are similar to values previously reported (8 to 171 ppm, Shearer et al, 1987a). In contrast to the distinct oxygen isotopic difference observed between biotite granites and tourmaline granites (Nabelek et al., 1992b), Li isotopic compositions are indistinguishable between these two types of granites (Fig. 4a) and show no correlation with Nd. Archean granite samples (Little Elk granite and Bear Mountain granite) have δ^7Li values within the range of the Harney Peak Granite, but with lower Li concentrations (4.9 and 7.7 ppm). Four simple pegmatites have the lowest Li concentrations of the granitic rocks (3 to 7.5 ppm), with δ^7Li ranging from +1.4 to +7.3‰. Four quartz mica schists have δ^7Li values that range from –3.1 to +2.5‰, overlapping with the values of Harney Peak Granite. The Li contents in these schists are ~ 70 ppm except for one that is a factor of two higher (150 ppm).

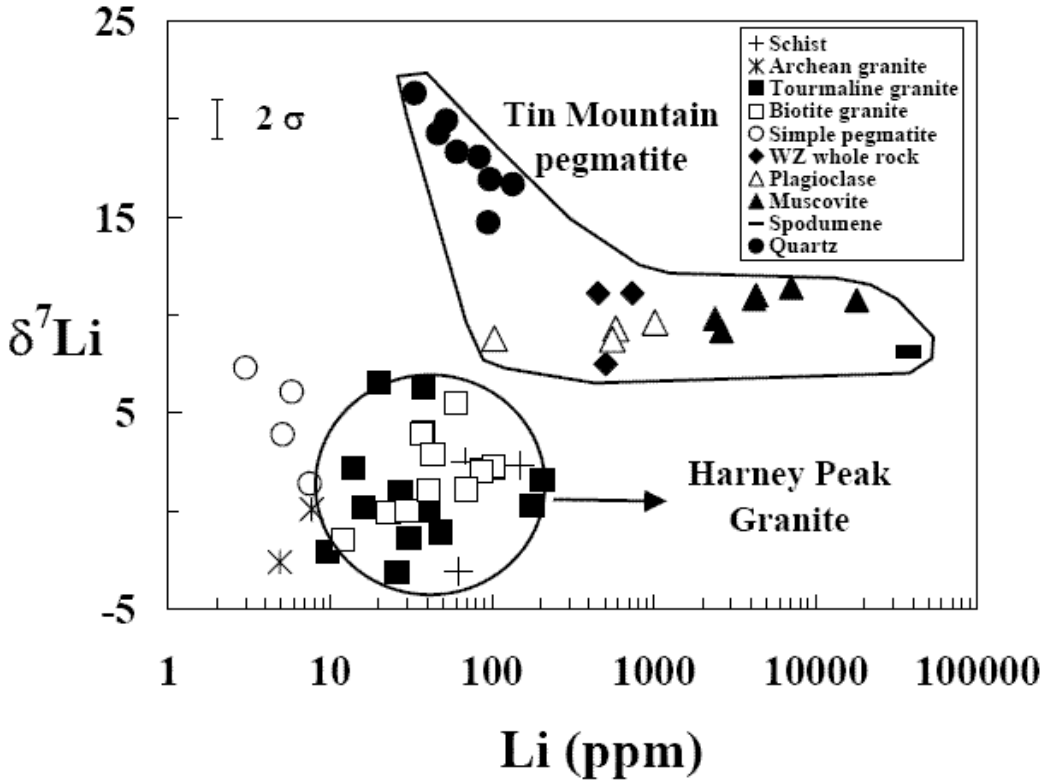

Figure 4-3. Plots of δ^7Li versus Li for all samples.
Data from Tables 4-1, 4-2, 4-3.

Table 4-1. Lithium isotopic composition and concentration of Harney Peak Granite and simple pegmatites from Black Hills, South Dakota

Location[1]	Sample ID	δ^7Li[2]	Li[3] (ppm)	$\delta^{18}O$[4]
HP	3-1B	+4.0	38	13.41
	3-1B replicate[5]	+3.9		
HP	4-1	+6.6	38	13.84
	4-1 replicate	+6.2		
HP	1-1	+2.1	86	12.88
HP	2-1	+0.2	16	13.23
HP	HP-3B	+1.6	205	13.69
HP	HP-8 4L	+1.1	69	11.92
HP	HP-8 8L	+0.0	30	11.78
HP	HP-20	+2.9	43	10.94
HP	HP-1	-3.1	26	14.08
HP	HP-2	-2.1	9.7	13.34
HP	HP-6	-1.5	12	12.41
HP	HP-14	-1.4	31	12.76
HP	HP2A	+2.2	14	13
HP	HP10B	+0.3	178	12.9
HP	HP13A	+2.2	103	11.9
HP	HP13C	+2.3	103	12
HP	HP14A	+2.0	86	10.8
HP	HP17	-1.1	48	13
HP	HP22	-0.1	23	11.9
HP	HP24B	+3.9	37	12.7
HP	HP30A	+5.5	60	12.3
HP	HP39A	+6.6	20	13
HP	HP43A	0	41	13
HP	HP44A	+1.1	41	11.3
HP	HP45B	+1.0	27	12.5
SP	WC-9	+1.4	7.5	13.83
SP	5-1	+3.9	5.1	13.36
SP	6-3	+6.1	5.7	12.68
SP	6-4	+7.3	3.0	11.59

1. HP- Harney Peak Granite, SP-simple pegmatite.
2. Analytical uncertainty is $< \pm 1‰$ (2σ), based on both pure Li solutions and natural rock standard (see text for details).

3. Lithium concentration measured by voltage comparison with standard of known concentration (see text for details).
4. Data from Walker et al (1986a; 1989) and (Nabelek et al., 1992a).
5. Replicate: repeat column chemistry from the same sample solution.

Table 4-2. Lithium isotopic composition and concentration of mineral and whole rock samples from Tin Mountain pegmatite, Black Hills, South Dakota

Sample ID[1]	Zone	δ^7Li[2]	Li (ppm)[3]	$\delta^{18}O$[4]
		Quartz		
11-3A	Wall zone	+18.3	61	12.4
17-1C	2nd zone	+16.9	97	12.5
16-2C	3rd zone	+17.0	141	12.9
16-2C replicate[5]		+16.3	129	
16-10A	3rd zone	+14.7	92	12.5
16-10A replicate		+14.7	98	
18-2A	Core zone	+18.4	87	12.7
18-2A replicate		+17.7	79	
19-1A	Core zone	+19.3	47	12.5
19-1A replicate		+19.2	46	
15-1A	Fracture filling	+19.9	52	12.6
15-3A	Fracture filling	+21.3	33	12.8
		Plagioclase		
11-3C	Wall zone	+8.8	104	11
16-2D	3rd zone	+9.7	578	11.4
16-2D replicate		+8.9	587	
16-10B	3rd zone	+9.2	564	11.2
16-10Breplicate		+8.3	543	
19-1C	Core zone	+9.9	1098	11.3
19-1C replicate		+9.3	940	
		Muscovite		
11-3B	Wall zone	+9.8	2399	10
16-8	2nd zone	+11.0	4305	10.5
16-2B	3rd zone	+11.4	7072	9.8
16-10C	3rd zone	+11.1	20119	9.9
16-10C replicate		+10.4	15808	
18-2D	Core zone	+11.0	4194	9.9
18-2D replicate		+10.6	4138	
19-1B	Core zone	+9.8	2625	10
19-1B replicate		+8.5		
		Spodumene		
18-1C	Core zone	+8.3	37300	10.4
16-6	Core zone	+7.9	37300	10.5
15-1C	Fracture filling	+8.0	37300	11.8
15-3B	Fracture filling	+8.1	37300	10.4
		Wall zone whole rock		
WZ	10-3	+11.1	453.2	11.4
WZ	9-2	+7.5	504.3	12.1
WZ	43-1	+11.1	735.4	11.7

1. All mineral separates are the same as those used in Walker et al.(1986b) except 16-2B, 11-3A and 11-3C, which were drilled from rock sample during this study. The amount of drilled sample is <1 mg and dissolved in $HF+HNO_3$ without any cleaning.
2. Analytical uncertainty is $<\pm$ 1‰ (2σ), based on both pure Li solutions and natural rocks (see text for details).
3. Lithium concentration measured by voltage comparison with standard of known concentration, except for spodumene, which is calculated from its standard molecular formula (see text for details).
4. $\delta^{18}O$ from Walker et al (1986b).
5. Replicate: repeat column chemistry from the same sample solution.

Table 4-3. Lithium isotopic composition and concentration of quartz mica schists and Archean granites

Sample ID	δ^7Li[1]	Li (ppm)[2]	$\delta^{18}O$[3]
Proterozoic schists			
23-2	+2.5	68	11.8
40-1A	-3.1	62	12.5
WC-4	+1.6	79	13.7
26-2	+2.3	150	12.3
Archean granites			
39-1 (Bear Mountain)	+0.1	7.7	11
41-1 (Little Elk)	-2.6	4.9	7.3

1. Analytical uncertainty is <± 1‰ (2σ), based on both pure Li solutions and natural rocks (see text for details).
2. Lithium concentration measured by voltage comparison with standard of known concentration. See text for details.
3. Data from Walker et al (1986a).

4.2. Lithium concentration and isotopic composition of Tin Mountain pegmatite

Three wall-zone whole-rock samples of the Tin Mountain pegmatite have Li concentrations ranging from 450 ppm to 735 ppm, two to 100 times higher than Harney Peak Granite (4.9 to 205 ppm). Compared with same minerals from granites (Bea et al., 1994; Neves, 1997; Pereira and Shaw, 1996), Li concentrations in minerals from all zones of Tin Mountain pegmatite are also extremely high. Quartz has Li concentration ranging from 33 ppm to 135 ppm, while spodumene, muscovite and plagioclase have higher Li concentrations, decreasing in the order: spodumene (~3.7 wt%), muscovite (0.2 to 2.0 wt.%), plagioclase (100-1100 ppm) (Fig. 5a). The Li isotopic composition of these pegmatite samples is quite heavy. The three composite "whole-rock" samples from the wall zone have δ^7Li values ranging from +7.5 to +11.1‰, consistently heavier than Harney Peak Granite (Fig. 3). From the wall zone to the core, plagioclase, muscovite and spodumene display a narrow range in δ^7Li from +7.9 to +11.4‰, with resolvable systematic differences between minerals, whereas quartz displays a much larger range, from +14.7 to +21.3‰ (Fig. 5b), has systematically heavier δ^7Li values than coexisting minerals, and Li concentration inversely correlates with δ^7Li (Fig. 3).

5. Discussion

Granites and granitic pegmatites are commonly found in spatial association and may be genetically related to each other, with pegmatites potentially representing the final differentiation products of an evolving granite magmatic system. Study of the Harney Peak Granite, Tin Mountain pegmatite and associated potential source rocks thus

provide a means with which to determine how Li isotopes fractionate during crustal melting and granite differentiation.

5.1. Lithium isotopic fractionation during granite petrogenesis

The amount by which Li isotopes fractionate during igneous differentiation is not fully understood. Tomascak et al. (1999b) measured the Li isotopic composition of the crystallizing Kilauea Iki lava lake, for which crystallization temperatures of 1050 ^{o}C to 1216^{o}C are well established. These investigators found no detectable Li isotopic fractionation within uncertainties of the measurement (±1.1‰). More recent studies of the Li isotopic composition of olivine and coexisting basalt corroborate these initial findings (Chan and Frey, 2003; Jeffcoate et al., 2004b). Collectively, these studies suggest the amount of Li isotope fractionation attending basalt differentiation at temperatures between 1050 ^{o}C and 1216^{o}C is below analytical uncertainties.

In contrast to the high temperatures and rapid crystallization and cooling experienced in dry, basaltic melts, granite is typically generated at lower temperatures (750-850 ^{o}C) by fluid-absent melting of crustal materials (Chappell et al., 2000), which is often followed by fractional crystallization, exsolution of a vapor phase and slow cooling. Each of these processes (partial melting, fractional crystallization, fluid exsolution, cooling) could, in principal, produce isotopic fractionation. Below we explore the general factors that influence Li concentration and isotopic composition in granitic systems, and then explore what new insights the data from the Harney Peak Granite and Tin Mountain pegmatite provide.

5.1.1. Lithium isotopic fractionation during crystal-melt equilibria

5.1.1.1. Theoretical considerations

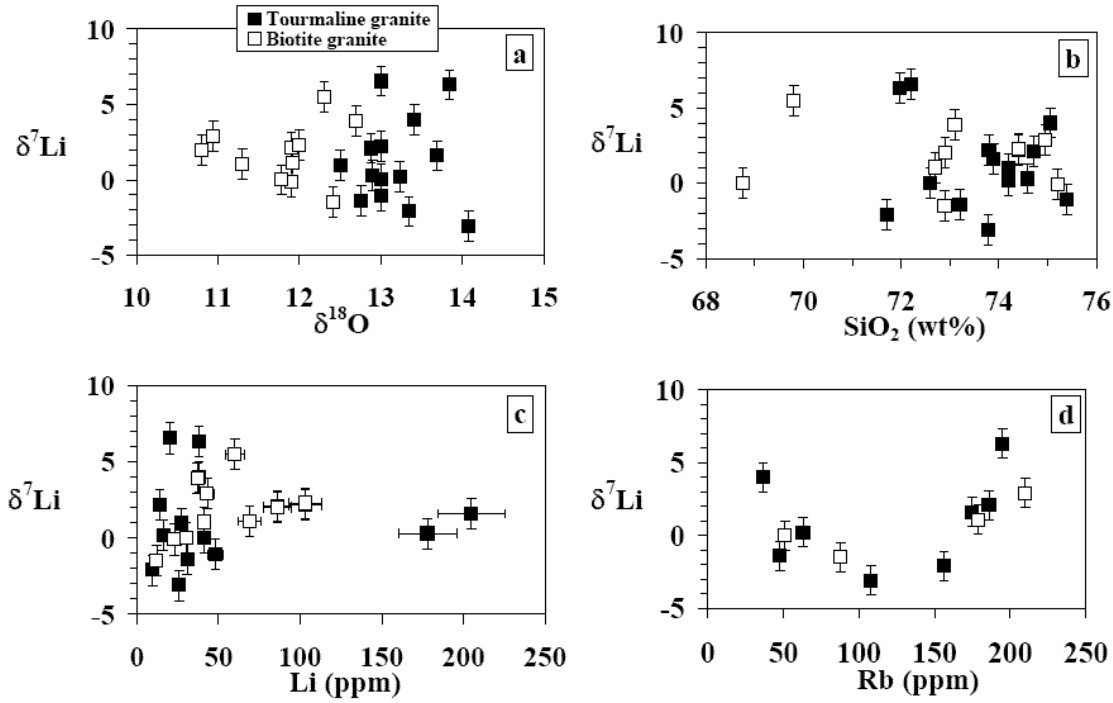

Figure 4-4. Plots of δ^7Li verses δ^{18}O, SiO_2, Li, and Rb for Harney Peak Granite Data from Table 4-1, Walker et al (1986a; 1989) and Nabelek et al (1992a).

Lithium concentrations in granites are controlled by bulk partition coefficients between melt and solid, which vary with the compositions of both minerals and melts. Lithium in S-type granites is mainly contained within micas (biotite and muscovite), with lesser amounts in cordierite (Bea et al., 1994; Neves, 1997; Pereira and Shaw, 1996). Experimental studies of Li partitioning between biotite, muscovite, cordierite and coexisting peraluminous silicic melt show that Li is slightly compatible in biotite ($D_{Li}^{Bt/melt}$ ranges from 1.0-1.7, and decreases with increasing temperature) and is incompatible in muscovite ($D_{Li}^{Ms/melt} \sim 0.8$) and cordierite ($D_{Li}^{Crd/melt}$ ranges from 0.44 to 0.12, decreasing with increasing temperature) (Evensen and London, 2003; Icenhower and London, 1995). Collectively, these studies suggest that Li behaves as a moderately incompatible element during granite differentiation, and Li concentrations are thus expected to decrease with degree of melting and increase with progressive crystal-melt fractionation.

Lithium isotope fractionation between minerals and melt is governed by the general rules of stable isotope fractionation. As discussed in Chacko et al. (2001), equilibrium isotope fractionation is due to differences in zero point energy (ΔZPE) between molecules with different isotopes. Substances with larger ΔZPE during isotope substitution favor the heavier isotope. Since substances with stronger bonds will have larger ΔZPE during isotope substitution, heavy isotopes, therefore, will favor substances with stronger bonds or higher energy sites. Lithium is monovalent (1^+) and, hence, not redox sensitive. In addition, Li, like B and other light cations, is bonded to oxygen in most silicates (Wenger and Armbruster, 1991), and isotopic fractionation in silicates is controlled strictly by the relative site energies at the same temperature. In most solids, Li

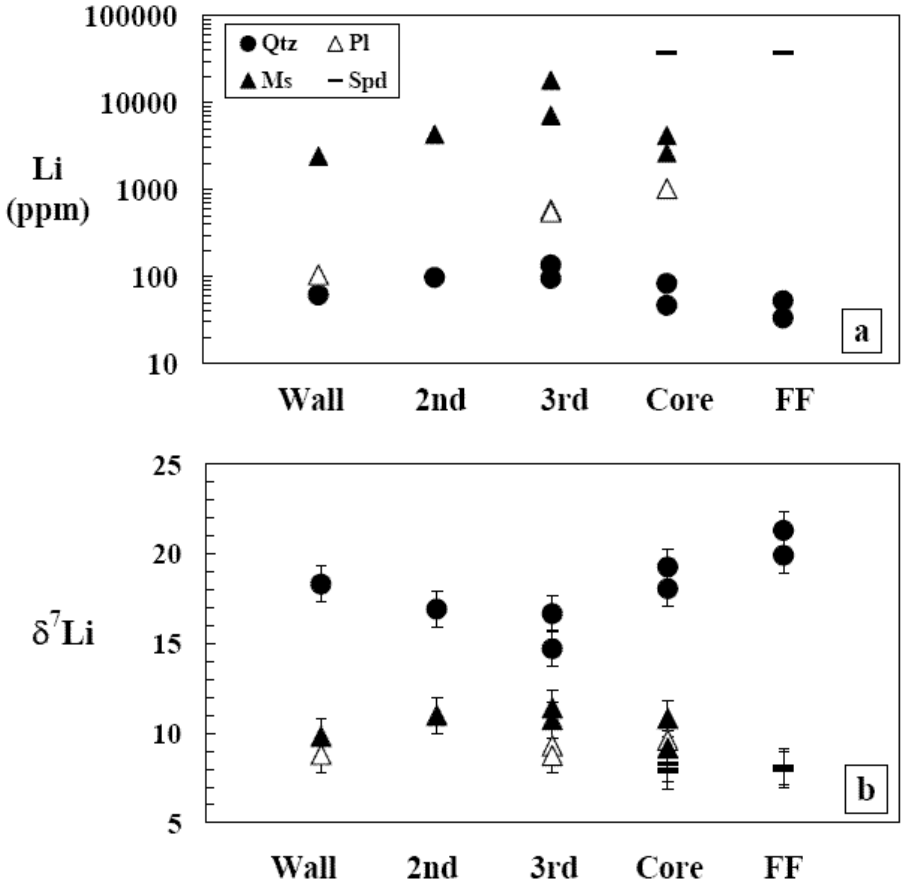

Figure 4-5. δ^7Li and Li concentration for minerals in different zones of the Tin Mountain pegmatite

Pl = plagioclase, Ms = muscovite, Spd = spodumene, Qtz = Quartz. Data from Table 4-2.

occupies either tetrahedrally- or octahedrally coordinated sites and potential energies in the polyhedra generally decrease with increasing coordination numbers (Wenger and Armbruster, 1991). Therefore, substances with tetrahedrally coordinated Li are expected to prefer heavy Li isotopes to those where Li is octahedrally coordinated. This can only be considered as a rather general guide since Li coordination polyhedra are more or less distorted in most minerals due to its small ionic radii and lower charge and hence the potential energies can be largely changed and overlapping.

Lithium enters two- and four-fold coordinated interstitial sites in quartz (Sartbaeva et al., 2004), but the concentration in quartz is typically low, so quartz is not expected to exert a major control on isotopic fractionation. In the most Li-rich minerals, Li is octahedrally coordinated (e.g., spodumene (Clarke and Spink, 1969; Li and Peacor, 1968), micas (Brigatti et al., 2000; 2003; Robert et al., 1983), and cordierite (Bertoldi et al., 2004)). In contrast, Li is tetrahedrally coordinated in granitic melts (Soltay and Henderson, 2005a; 2005b; Zhao et al., 1998). At low temperatures, these different coordination numbers for Li between melts and crystals may produce measurable Li isotopic fractionation. Based on the above considerations, the most important Li-bearing minerals (e.g., micas, spodumene) are expected to be isotopically lighter than coexisting melts. If the fractionation or differentiation is large enough, granites should evolve to isotopically heavier δ^7Li values with differentiation (Fig. 6a).

5.1.1.2. Observations from the Harney Peak Granite

The data for the Harney Peak Granite indicate that Li isotopic fractionation at the temperature of anatexis is small, granite crystallization does not significantly affect the Li isotopic composition of Harney Peak Granite, and that the δ^7Li value of the Harney Peak

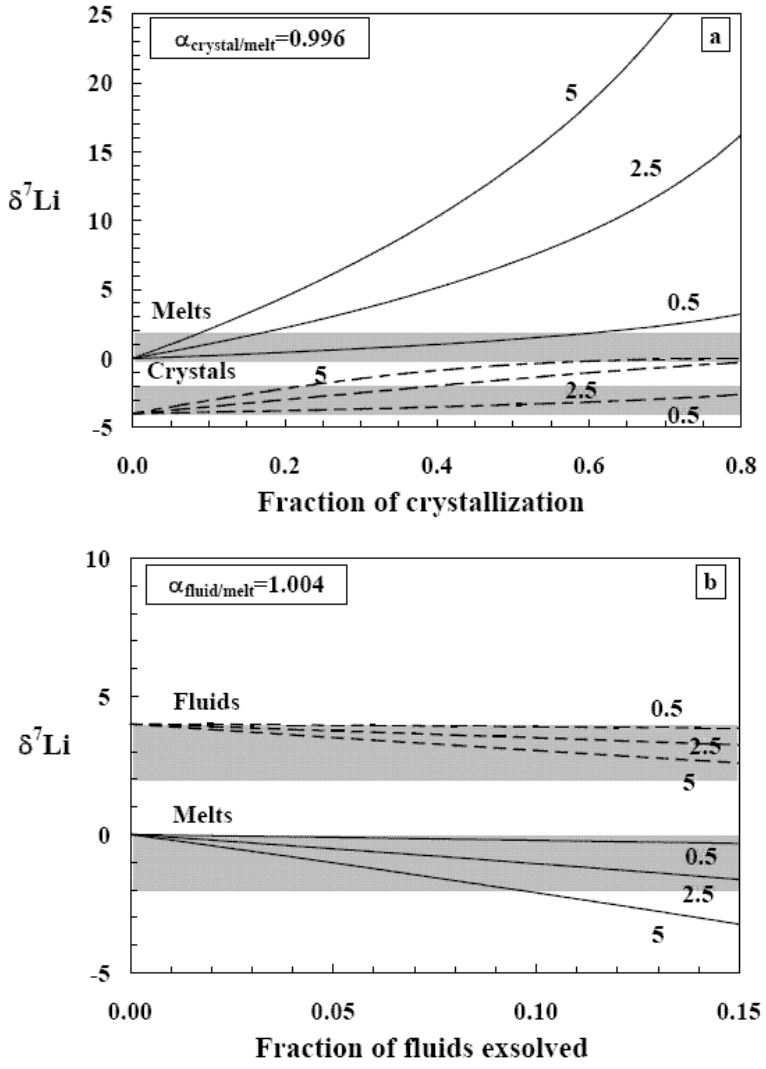

Figure 4-6. Lithium isotopic fractionation modeled by Rayleigh distillation during: a) crystal-melt fractionation; b) fluid exsolution. Numbers on lines represent Li partition coefficient (D) between crystals (a) or fluids (b) and melts. Shaded areas represent measurement uncertainty (± 1‰, 2σ). Equations and variables used: $\delta^7Li_m = (\delta^7Li_i + 1000)f^{(\alpha-1)} - 1000$; $C_m = C_i(1-F)^{D-1}$; α: Li isotopic fractionation factor defined as Li isotopic ratio between crystals or fluids and melts; D: Li partition coefficient defined as Li concentration ratio between crystals or fluids and melts; f: the fraction of Li remaining in the melts; F: fraction of crystal or fluid removed. m: remaining melt; *i*: initial melt.

Granite mainly represents that of its source rock. The primary observations that lead to these conclusions are:

1) Identical Li isotopic compositions are observed for the metasedimentary rock WC-4 and its inferred *in situ* melt (pegmatitic vein WC-9).
2) δ^7Li shows no correlation with degree of differentiation, as inferred from various compositional parameters (e.g., SiO_2, Li, Rb contents) (Fig. 4).
3) δ^7Li values of most Harney Peak Granite (-3.1 to +4.0‰) lie within the range observed in their potential source rocks (-3.1 to +2.5‰) with the exception of three samples with heavier values (+5.5 to +6.6‰).

The origin of the three isotopically heavier granite samples is uncertain. Sample HP30A has elevated δD, which may reflect interactions with isotopically heavy H_2O from metamorphic dehydration of country rocks (Nabelek et al., 1992b). Another granite sample, 4-1, has the highest Sr and Ba, high Rb and low Li content and may derive from isotopically heavy source rock that was not sampled.

The conclusion that source rocks mainly control Li isotopic composition of the Harney Peak Granite is consistent with other granite studies. Thirteen S-type granites from Australia display a very limited range of Li isotopic compositions (-1.4 to +2.8‰) over a large range of granite compositions. The δ^7Li range is similar to that observed in their presumed protoliths (Bryant et al., 2004b; Teng et al., 2004a). In contrast, I-type granites from Australia show large Li isotopic variations (+1.9 to +8.1‰), which correlate with inferred differences in source rocks (Bryant et al., 2004b). The δ^7Li values in these I-type granites does not correlate with the degree of differentiation (Bryant et al., 2004b; Teng et al., 2004a). Collectively, these studies indicate that Li isotopic

compositions of source rocks are the most important factor controlling the Li isotope compositions of the granites and that the extent of partial melting and crystal-melt fractionation does not significantly affect Li isotopic composition in the system.

5.1.2. Lithium isotopic fractionation during fluid-melt equilibria

5.1.2.1. Theoretical considerations

Compared with Li partitioning between mineral and melt, there is a considerable range in Li partition coefficients between supercritical fluids and melts (Candela and Piccoli, 1995). The most important factors controlling Li partitioning between fluid and melt are fluid composition and temperature. For example, in peraluminous granite-pegmatite systems, $D_{Li}^{fluid/melt}$ is ~ 0.4 and does not change within a temperature interval of 650-775 ^{o}C at 200 MPa (London et al., 1988). In a metaluminous system at similar temperatures and pressures (i.e., 800 ^{o}C and 200 MPa), but with a much higher Cl content, Webster et al (1989) found higher $D_{Li}^{fluid/melt}$, which increases from 1.1 to 2.5 as the Cl content of the vapor doubles. In addition, Webster et al (1989) reported that partition coefficients between fluid and melt also increase with temperature and the mole fraction of water present in the fluids.

Lithium in supercritical fluids bonds with Cl to form LiCl (Candela and Piccoli, 1995). In granitic melts, Li bonds with O (Soltay and Henderson, 2005a; 2005b; Zhao et al., 1998). These different types of bonds (ionic vs. covalent) make it impossible to use the difference of Li coordination to predict the isotopic fractionation between these two phases. To date, no experiment has measured the Li isotopic fractionation factor between supercritical fluids and melts. A recent experimental study of Li isotopic fractionation between minerals and hydrothermal fluids found that fluids are isotopically lighter than

minerals (Lynton et al., 2005), while a few empirical studies on Li isotopic compositions of hydrothermal fluids and altered basalts suggest that fluids are isotopically heavier than basalts (Chan et al., 1993; 1994; Foustoukos et al., 2004). The cause of the difference between the experimental and empirical studies remains unknown. If there is Li isotopic fractionation during the process of supercritical fluid separation from granitic melts, the minerals crystallized from the fluids would have different Li isotopic compositions than those from the melts, with the difference depending on the Li isotopic fractionation factor between fluid and melt (α). For conditions where α is between 0.996-1.004, $D_{Li}^{fluid/melt} \leq$ 2.5 (the maximum value at 800oC, 200Mpa with 6.13m Cl in fluid, Webster et al., 1989) and the fraction of fluids exsolved (F) $\leq$ 14% (the maximum concentration of H_2O at saturation in peraluminous melt, London et al., 1988), the isotopic compositions of both residual melts and exsolved fluids change little with progressive fluid exsolution (Fig. 6b).

This calculation suggests that fluid exsolution should have minimal effect on Li isotopic composition of granites that exsolve modest quantities of water. However, if a large amount of fluids exsolve (i.e., F is large), at relatively low temperature (i.e., α is large), then fluid exsolution may influence the Li isotopic compositions of granitic systems. For example, granitic pegmatites may form during the later stages of granite evolution in the presence of a fluid phase or from H_2O undersaturated granitic melts by undercooling (for more details, see recent review of London, 2005). For those that crystallize in the presence of substantial fluids present, the Li isotopic compositions are expected to be quite different from that of their precursors.

5.1.2.2. Observations from the Tin Mountain pegmatite

Previous studies have shown that the Tin Mountain pegmatite crystallized from a coexisting fluid-melt system through all internal zones. Apatites from all zones have kinked chondrite-normalized REE patterns (Walker et al., 1986b) (the tetrad effect, Peppard et al., 1969), which normally occurs during late stage granite evolution accompanied by strong hydrothermal interactions. It is produced by REE partitioning between melt and coexisting compositionally complicated fluids (see review of Jahn et al., 2001). Melt and fluid inclusions occurs in both wall and core zones of the Tin Mountain pegmatite, which further confirms this conclusion. Therefore, the Tin Mountain pegmatite is expected to be isotopically different from its presumed Harney Peak Granite precursor.

The Tin Mountain pegmatite is isotopically heavier than its precursor Harney Peak Granite, suggesting that exsolved fluids are isotopically heavier than the granitic melts. Three whole rock samples from the wall zone have δ^7Li values ranging from +7.5 to +11.1‰, with an average δ^7Li =+9.9 ± 2.1‰. The wall zone has relatively low incompatible element concentrations (Rb, Cs, and Li) and high compatible element concentrations (Ba and Sr), relative to the rest of the zones, suggesting that the wall zone was the first material to crystallize from the pegmatite melt (Walker et al., 1986b). In addition, two of the three whole rocks from the wall zone (samples 10-3 and 43-1) show the tetrad effect and these are isotopically heavier than the one without tetrad effect (sample 9-2). This may indicate that crystallization of the wall zone resulted in the creation of an isotopically heavier fluid phase, with all later zones, including part of the wall zone, crystallizing from coexisting fluid and melt. Thus, the whole rock average from the wall zone may best represent that of the melt-fluid-system.

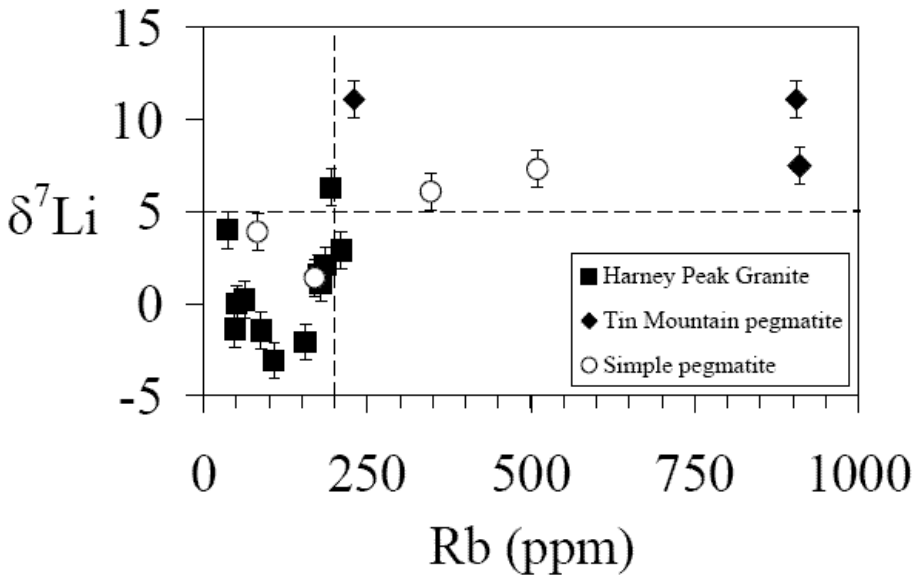

Figure 4-7. Plot of δ^7Li versus Rb for the wall zone whole rocks from the Tin Mountain pegmatite, simple pegmatites and Harney Peak Granite

Data from Tables 4-1, 4-2 and Walker et al (1986b; 1989).

Compared with the Harney Peak Granite, the Tin Mountain pegmatite experienced extensive crystal-melt fractionation, during which Li isotopes could have been significantly fractionated. As discussed previously, when the degree of crystal fractionation is low and temperatures are high, crystal-melt fractionation will not significantly affect the Li isotopic composition of granitic melts, as observed for the Harney Peak Granite. In contrast, for highly evolved granitic systems at lower temperatures, the effect of crystal-melt fractionation on Li isotopic composition of granitic melt could be large and shift the granitic melt to isotopically heavier compositions e.g., the Tin Mountain pegmatite (Fig. 6a). A plot of δ^7Li vs. Rb for Harney Peak Granite, simple pegmatites and Tin Mountain pegmatite shows that highly fractionated samples (e.g., pegmatites with Rb >200 ppm) have heavier Li isotopic compositions than the moderately fractioned granites (e.g., granites and pegmatites with Rb <200 ppm) (Fig. 7).

5.2. Lithium isotopic fractionation within the Tin Mountain pegmatite

Inter-mineral isotopic fractionation is important for understanding both Li isotopic systematics and potentially using Li isotopes for thermometry. The Li-enriched Tin Mountain pegmatite crystallized at relatively low temperatures (Sirbescu and Nabelek, 2003a; 2003b; Walker et al., 1986b), so Li isotope fractionation may be dramatic.

The Li isotope composition of quartz is distinct from that of all other minerals examined from the Tin Mountain pegmatite (Fig. 8). Quartz shows a relatively large range in δ^7Li from +14.7 to +21.3‰, and δ^7Li correlates negatively with Li concentration (Fig. 8). This quartz contains both primary and secondary fluid inclusions (Sirbescu and

Nabelek, 2003a; 2003b). The negative correlation between Li concentration and δ^7Li in quartz may reflect the mass balance of Li in quartz vs. the fluid inclusions. Based on the Li- δ^7Li correlation, the quartz is expected to have a relatively low Li concentration (≤ 30 ppm) and heavy Li isotopic composition (≥ +21‰); this agrees with the only available Li isotopic data for fluid-inclusion-free quartz (from a Li-rich granitic pegmatite), which has δ^7Li = +27±2.1‰ and 17.2 ppm Li (Lynton et al., 2005). This suggests that the fluid inclusions should be Li-rich (≥140 ppm) and isotopically lighter (≤+15 ‰). The Li isotopic composition of the coexisting fluid can be constrained from other minerals. Plagioclase, muscovite and spodumene from all zones that crystallized from a coexisting fluid-melt phase and show relatively constant Li isotopic composition (δ^7Li = +9.4 ± 1.2‰). Their δ^7Li values should partially reflect that of the fluids, assuming no, or small, isotopic fractionation during crystallization. Therefore, the δ^7Li of the fluids should be similar to or slightly heavier than these minerals.

The δ^7Li difference between quartz and other minerals may result from equilibrium isotopic fractionation during crystallization and reflect the preference of quartz for heavy Li, where Li is in two- or four-fold sites, whereas for other minerals Li is octahedrally coordinated. The data collected here are, however, different from those recently reported by Lynton et al (2005) in several important ways. They found that at 500 ^{o}C, muscovite is 9‰ heavier than quartz, which, in turn, is 10‰ heavier than fluids. Moreover, they observed that Li isotopic fractionation between minerals (muscovite/quartz) and fluids depends on the Li concentration in the fluids and reduces to ~10‰ when Li concentration in fluids increases. Finally, they found that Li isotopic fractionation between quartz and fluids decreases from 10‰ to 5‰ when the temperature

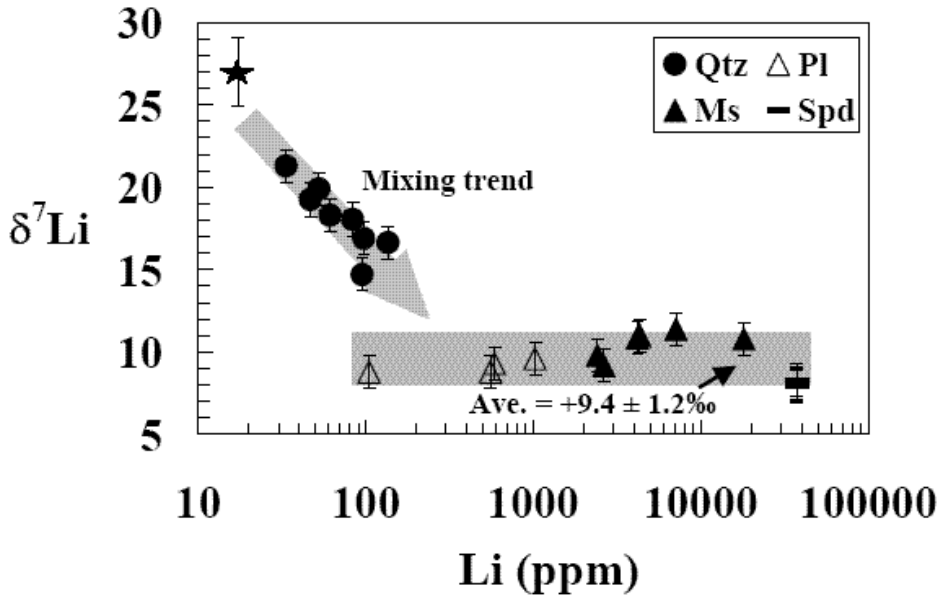

Figure 4-8. Plot of δ^7Li versus Li for minerals from Tin Mountain pegmatite
Shaded rectangle represents the average δ^7Li value of all minerals except quartz (+9.4 ± 1.2‰, 1σ). Star represents quartz from Lynton et al (2005).

of the experiment decreases from 500 to 400 ^{o}C. These observations contradict the general theory of isotope fractionation, e.g., isotopic fractionation factor should decrease with increasing temperature and be independent of element concentration in phases (i.e., Li in solutions here) (Chacko et al., 2001). Clearly more studies are needed to fully understand the cause of these differences.

6. Conclusions

1. The Harney Peak Granite has δ^7Li ranging from -3.1 to +6.6‰, with most falling within the range defined by their potential metasedimentary sources (-3.1 to +2.5‰), from both Archean and Proterozoic crust. There is no correlation between δ^7Li and geochemical indicators of granitic differentiation, suggesting that the Li isotopic compositions of the granite mainly reflect those of their sources.
2. Three bulk rocks from the wall zone provide the best estimate of the bulk composition of the Tin Mountain pegmatite. Their average of +9.9‰ is much heavier than that of the Harney Peak Granite. This isotopically heavy signature results from extensive crystal-melt fractionation and fluid exsolution. The pegmatite data, compared with the data from the Harney Peak Granite, suggest that both crystal-melt and fluid-melt fractionation during granite differentiation can affect the Li isotopic compositions of highly fractionated granites, but does not play an important role in low to moderately fractionated granites.
3. All minerals from the Tin Mountain pegmatite have high Li concentrations and similar δ^7Li values of ~+9.4‰, except quartz. Quartz is less enriched in Li, is ~ 6-11‰ heavier than all other minerals, and displays a negative correlation between

δ^7Li and Li concentration. This correlation reflects a mass balance between heavy Li bounded in quartz (> +21‰) and lighter, Li-rich fluid inclusions (+9‰). The large difference in isotopic composition between quartz and other minerals reflects equilibrium Li isotopic fractionation, with heavy Li preferring low-coordination sites (quartz) to more highly coordinated ones.

Chapter 5: Lithium isotopic fractionation during diffusion

Abstract

Lithium concentrations and isotopic compositions in the country rocks (amphibolites and schists) of the Tin Mountain pegmatite show systematic changes with distance to the contact. Both Li and δ^7Li decrease dramatically along a ~10 m traverse from the pegmatite into amphibolite, with Li concentration decreasing from 471 to 68 ppm and δ^7Li decreasing from +7.6 to –19.9‰. Rubidium and Cs also decrease from the pegmatite contact into the country rock, but only within the first two meters of the contact, after which their concentrations remain constant. Neither mixing between pegmatite fluids and amphibolite, nor Li isotope fractionation by Rayleigh distillation during fluid infiltration are likely explanations of these observations due to the extremely light isotopic composition required for the amphibolite end-member in the mixing model (–20‰) and the similarly extreme isotopic fractionation required in a Rayleigh distillation model. Rather, these variations are likely due to isotopic fractionation accompanying Li diffusion from the Li-rich pegmatite (Li = 450 to 730 ppm) into amphibolites (Li = 20 ppm). The fact that other alkali element concentrations vary only within two meters of the contact reflects the orders of magnitude faster diffusion of Li relative to heavier elements.

Quartz mica schists in contact with the pegmatite also show large variations in both Li and δ^7Li as a function of distance from contact (~1 wt.% to ~70 ppm and +10.8 to –18.6 ‰ respectively), but over a longer distance of ~300 m. Lithium concentrations of the schist decrease from ~1 wt.% adjacent to the contact to ~70 ppm 300 m from the contact; the latter is a typical concentration in metapelites. The nature of the δ^7Li

variations in the schists is different than in the amphibolites. Schists within the first two meters of the contact have nearly identical δ^7Li of +10‰, which mimics that of the estimated bulk pegmatite (+8 to +11‰). At a distance of 30 m the δ^7Li reaches the lowest value in the schists of –18.6‰ (similar to the lowest amphibolite measured). At a distance of 300 m the δ^7Li climbs back to +2.5‰, which is within the range of δ^7Li of other schists in the region and metapelites worldwide. The behavior of Li in the schists can also be modeled by Li diffusion, with the effective diffusion coefficient in the schist being ~ 10 times greater than that in the amphibolite. The effective diffusion coefficients of Li in the amphibolite and schist are >2 orders of greater that those in minerals, which implicates the importance of fluid-assisted grain-boundary diffusion over solid-state diffusion in transporting Li through these rocks.

1. Introduction

Lithium is a fluid-mobile, moderately incompatible element having two stable isotopes with ~17% relative mass difference. This large mass difference gives rise to significant isotopic fractionations in different geological environments, especially those involving fluid-rock interactions (see review of Tomascak, 2004). Lithium isotope fractionation, like other stable isotope systems (Chacko et al., 2001), is due to differences in bond energies between different phases for the two isotopes (e.g., mineral and fluid), with heavy Li (^{7}Li) preferring the higher-energy bond. Bond energy is, in turn, related to coordination number, with lower coordination number sites having higher bond energy (Wenger and Armbruster, 1991). Thus Li substituting for Mg in octahedral mineral sites (e.g., pyroxenes) will be isotopically lighter than Li found in fluids, which is believed to be in tetrahedral coordination (Wenger and Armbruster, 1991; Yamaji et al., 2001).

These characteristics result in distinct Li concentration and isotopic composition in the hydrosphere, continental crust and mantle. In general, the hydrosphere is isotopically heavy (seawater = +32‰), the mantle is intermediate at +4‰, whereas the weathered, upper continental crust is isotopically light (~0‰) (Teng et al., 2004a; Tomascak, 2004) .

Recent studies using both laboratory experiments and natural rocks have demonstrated the existence of another type of Li isotopic fractionation, produced by the different diffusivities of ^{6}Li and ^{7}Li in silicate melts and solids. Diffusion couple experiments have reported ~40‰ Li isotopic fractionation between juxtaposed molten rhyolite and basalt, with an initial Li concentration ratio of ~ 15 (Richter et al., 2003). Large Li isotopic variation (~20‰) was also observed along a ~2 m Li concentration gradient in peridotite adjacent to discordant dunites (former melt channels), and explained by diffusion-driven Li isotopic fractionation (Lundstrom et al., 2005). Compared with the isotopic fractionation produced by bond-energy differences, diffusion-driven isotopic fractionation is controlled by the concentration gradient and the relative mobility of isotopes. Thus, it can occur at high temperatures where equilibrium fractionation diminishes (Richter et al., 1999).

In this paper we report Li concentrations and isotopic compositions of country rocks adjacent to the Li-rich Tin Mountain pegmatite, Black Hills, South Dakota. Emplacement and crystallization of this pegmatite produced a large Li concentration gradient between the pegmatite and country rocks and led to Li diffusion into the country rocks. Our results demonstrate that up to 30‰ fractionation of Li isotopes was produced in this manner.

2. Geological background and samples

Samples studied here are from the country rocks of the ca. 1.7 Ga Tin Mountain pegmatite, Black Hills, South Dakota, which crops out ~ 12 km to the southwest of the main body of the Harney Peak Granite (Redden et al., 1985). The Li-rich, Tin Mountain pegmatite discordantly intruded both schists and a tabular amphibolite unit, which are the focus of this paper. The pegmatite consists of five major structural/mineralogical zones, with the wall zone forming a shell that encloses inner zones. Fracture fillings are compositionally similar to the core and traceable from the core into the surrounding zones (Walker et al., 1986b). The estimated formation pressure is ~0.3 GPa (Redden et al., 1985) with crystallization temperature varying from ~ 600 °C down to 340 °C (2003a; Sirbescu and Nabelek, 2003b; Walker et al., 1986b). Lithium isotopic compositions of minerals and whole rocks from the different zones of the Tin Mountain pegmatite, as well as the Harney Peak Granite, associated simple pegmatites and representative country rocks are reported elsewhere (Teng et al., 2005a). All samples measured here have been characterized in previous investigations (Laul et al., 1984; Walker, 1984) and previously published chemical data are provided in the electronic supplement.

2.1. Amphibolites

The amphibolite is similar in composition to tholeiitic basalt. It overlies much of the wall zone of the pegmatite, and reached amphibolite facies prior to the intrusion of the pegmatite (Redden et al., 1985). The Li isotopic variation within the amphibolite was determined for eight samples collected along a 10 m vertical traverse above the pegmatite body, where the outcrop ends at the cliff top. An additional sample, collected from a different amphibolite body 300 m away from the pegmatite, was also analyzed.

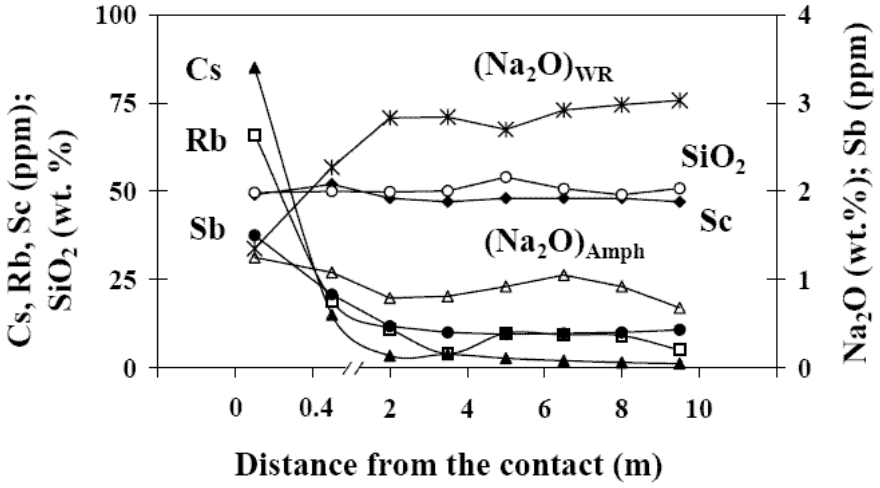

Figure 5-1. Concentration profiles of SiO_2, Sc, Cs, Rb, Sb, Na_2O in the amphibolite and Na_2O in the amphibole vs. distance from the contact with the Tin Mountain pegmatite Data from Walker (1984) and Laul et al (1984).

The amphibolite is a medium-grained rock composed predominantly of hornblende and plagioclase with minor amounts of quartz and biotite. Significant amounts of calcite (2-7%) are present in two samples (samples 12-2 and 12-3). The amphibolite is layered, with segregations of oriented hornblende alternating with layers of crystalloblastic plagioclase (Walker, 1984). Most major and trace elements have relatively constant concentration along the traverse (Fig. 1), which suggests that modal variations are insignificant. Some fluid-mobile elements, however, show large variations in amphibolites near the contact (Fig.1). Relative to the mean of the other samples, the sample taken from the contact (sample 12-8) is significantly enriched in K_2O, Rb, Cs, Sb, $\delta^{18}O$ and depleted in Na_2O (Laul et al., 1984; Walker, 1984). By comparison, sample 12-7, taken 0.5 m from the contact, shows considerably less enrichment/depletion of these elements.

Feldspars show little compositional variation along the traverse, and range from An_{30-40}, except for the sample at the contact, which is more anorthite-rich ($\sim An_{50}$). Amphibole compositions vary on the scale of a thin section, but no systematic change is observed along the traverse (Walker, 1984). FeO contents range from 12.3 to 19.9 wt% and MgO contents range from 7.6 to 12.4 wt.%. Amphibole at the contact contains more Na than amphiboles elsewhere along the traverse, a trend that is different from that observed from whole rock samples (Walker, 1984).

2.2. Quartz-mica schists

Schists are the dominant country rocks in this area. Their protolith was shale that was metamorphosed to the sillimanite zone during regional metamorphism prior to the intrusion of Tin Mountain pegmatite (Redden et al., 1985). Compared with the

amphibolites, fresh outcrops of the schists are limited and it thus proved difficult to collect systematically along a traverse away from the pegmatite. Consequently, a variety of schists were sampled in and around the pegmatite in order to determine the extent of a metasomatic halo on a lateral scale. These samples include an inlier of schist enclosed by the wall and third intermediate zones of the pegmatite (13-1), three samples collected near the lower contact of the pegmatite (9-3, 9-1 and 9-4), and two samples taken from scattered outcrops to the northwest and southwest ends of the pegmatite at distances of 30 m (23-4) and 300 m (23-2). In order to characterize any compositional variation within the Black Hills terrane, three more schist samples were taken in this region far away (e.g., > 8 km) from known granitic outcrops.

The schists are composed of quartz, biotite, plagioclase and minor muscovite. Both modal mineralogy and major element composition vary considerably. The variations are probably due to the original sedimentary layering of the protolith (Walker, 1984). Trace element concentrations do not generally correlate with modal biotite + muscovite abundances. Relative to regional schists, the inlier sample (13-1) is extremely enriched in Rb, Cs, and Zn and depleted in $\delta^{18}O$. Lesser amounts of alkali enrichment are found in two samples taken within 0.5 m of the pegmatite (i.e., 9-1 and 9-3) and no discernable enrichments are seen in samples taken from over a meter from the contact (9-4, 23-4 and 23-2) (Walker, 1984).

3. Analytical methods

Sample powders were the same as those used in previous studies (Laul et al., 1984; Walker, 1984; Walker et al., 1986a; 1989). Procedures for sample dissolution and column

chemistry are described in Rudnick et al (2004) and the method of instrumental analysis is found in Teng et al (2004a).

The external precision of Li isotopic analyses, based on 2 σ of repeat runs of pure Li standard solutions and rock solutions, is < ± 1.0‰. For example, pure Li standard solutions (IRMM-016 and UMD-1) always have values falling within previous established ranges (-0.1 ± 0.2‰ and +54.7 ± 1‰, Teng et al., 2004a); in-house rock standard AO-12, a shale from the Amadeus Basin, gives δ^7Li = +3.5 ± 0.6 ‰ (2 σ, n = 36 runs with 4 replicate sample preparations); and BCR-1 gives δ^7Li = +2.0 ± 0.7 ‰ (2 σ, n = 10 runs). The uncertainty of Li concentration measurement, determined by the comparison of signal intensities with that measured for the 100 or 50 ppb L-SVEC standard and then adjusting for sample weight, is < ± 10%. The accuracy of this method has been established in Teng et al. (2004a) to be < ± 5% as based on isotope dilution methods.

4. Results

Lithium concentration and isotopic composition for both schists and amphibolites are reported in Table 1 and plotted in Fig. 2 as a function of distance from the contact. The Li concentration and isotopic composition of the Tin Mountain pegmatite and related igneous rocks have been reported in Teng et al. (2005a). Data for three wall zone whole rock samples that represent the average composition of the Tin Mountain pegmatite are presented for comparison in Table 1.

4.1. Amphibolite

Both Li and δ^7Li decrease with distance from the contact (Fig. 2a). The amphibolite near the pegmatite contact is isotopically heavy (+7.6‰), similar to wall

Table 5-1. Lithium isotopic composition and concentration of samples from the Tin Mountain pegmatite

Sample ID	δ^7Li[1]	Li (ppm)[2]	Distance (m)
	Amphibolites		
14-1	+0.9	20	300
12-1	-19.5	72	9.5
12-1replicate[3]	-19.9		
12-2	-14.2	68	8
12-3	-13.7	98	6.5
12-4	-8.3	140	5
12-4 replicate	-7.5		
12-5	-0.9	209	3.5
12-6	+6.5	260	2
12-7	+7.5	438	0.5
12-8	+7.6	471	0.03
12-8 replicate	+7.3		
	Quartz Mica Schists		
13-1	+10.8	~10000	0
9-3	+9	1179	0.1
9-1	+8.9	1607	0.3
9-4	+10	960	1.5
23-4	-18	124	30
23-4 replicate	-18.6		
23-2	+2.5	68	300
40-1A	-3.1	62	>8000
WC-4	+1.6	79	>8000
26-2	+2.3	150	>8000
Wall zone whole rock of Tin Mountain pegmatite			
10-3	+11.1	453	
9-2	+7.5	504	
43-1	+11.1	735	

1. Analytical uncertainty is <± 1‰ (2σ), based on both pure Li solutions and natural rocks (see text for details).
2. Li measured by comparison of signal intensities with 50 or 100 ppb LSVEC.
3. Replicate: repeat column chemistry from the same sample solution.

zone samples of the pegmatite (+7.5 to +11.1‰), and it has the highest Li concentration (471 ppm). The sample at the end of the traverse, 10 m away from the contact, has the lowest Li concentration (70 ppm) and the lightest isotopic composition (-19.9‰). The regional amphibolite, taken 300 m from the Tin Mountain pegmatite, has a Li concentration (20 ppm) and isotopic composition (+0.9‰) comparable to typical upper crustal lithologies (Teng et al., 2004a).

4.2. Quartz-mica schist

Lithium concentrations and isotopic compositions of schists are also highly variable (Fig. 2b). The schist enclosed by the pegmatite (13-1) is extremely rich in Li (~1 wt.%) with pegmatite-like δ^7Li (+10.8‰). Three samples within 1.5 m of the pegmatite also show pegmatite-like Li isotopic compositions and high Li concentrations, with the furthest one (9-4, 1.5 m from the contact) showing no discernable enrichments in other fluid mobile elements. A sample collected 30 m from the pegmatite has an extremely light Li isotopic composition (-18.6‰) and a Li concentration of 124 ppm. Samples collected much further from the contact show typical shale-like Li concentrations (~ 70 ppm) and isotopic compositions (–3 to +2.5‰) (Teng et al., 2004a).

5. Discussion

The Tin Mountain pegmatite is extremely enriched in isotopically heavy Li (Teng et al., 2005a) relative to typical amphibolites and schists (Bottomley et al., 2003; Teng et al., 2004b; 2005c). Thus the compositional variations, observed within the country rocks as a function of distance from the pegmatite, must have resulted from mass transfer of elements enriched in the pegmatite into the country rocks. This transfer may have occurred by fluid infiltration and/or solid-state diffusion.

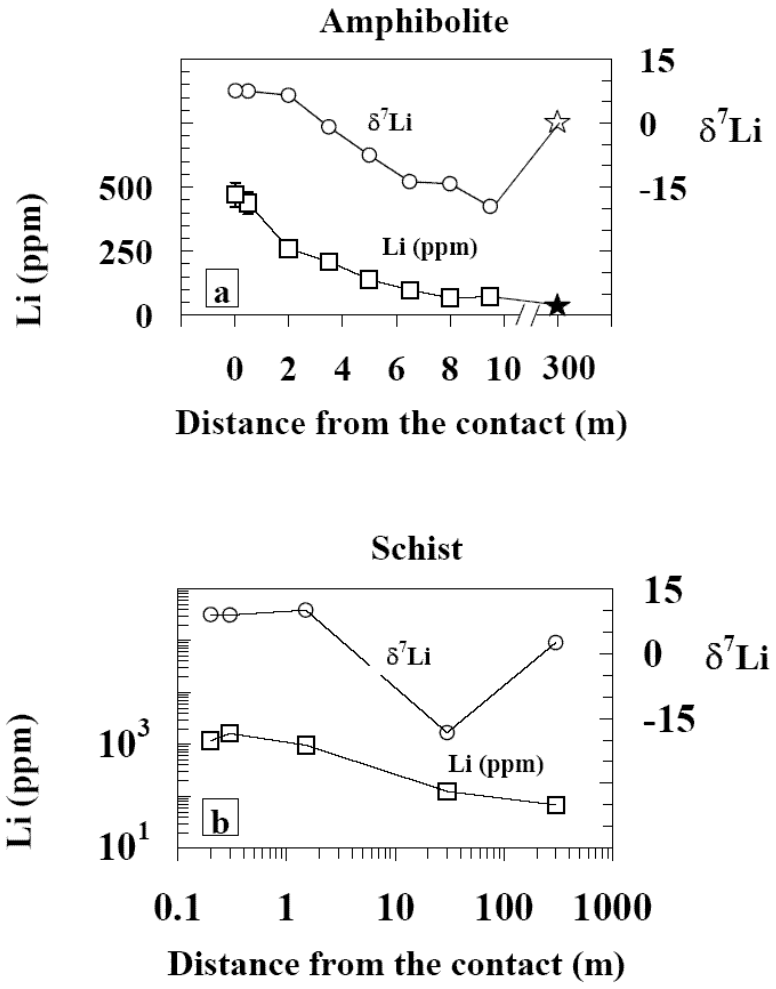

Figure 5-2. Plots of Li and δ^7Li verses distance from the contact for a) amphibolite samples taken along a vertical profile and b) schist samples taken at different distances to the contact, but not along a single profile. Stars in Fig. 5-2a represent Li (filled) and δ^7Li (open) of the regional amphibolite taken from another unit, 300 m from the contact. Data from Table 5-1.

Crystallization of the Tin Mountain pegmatite exsolved a large amount of fluids (Walker, 1984; 1986b). Since Li is fluid-mobile (Brenan et al., 1998b), infiltration of these fluids into the country rocks would have carried Li, which could then equilibrate with the country rocks. This process can be considered as simple mixing between pegmatite fluids and country rocks if no isotopic fractionation occurred, or modeled as Rayleigh Distillation if Li isotopic fractionation occurred during fluid infiltration. Alternatively, the large compositional contrast between pegmatite and country rocks could have led to diffusion of Li from the pegmatite into country rocks (Jost, 1960). Such diffusion can lead to large Li isotopic fractionations, as demonstrated by previous studies (Lundstrom et al., 2005; Richter et al., 2003). All of these processes could have modified the Li concentrations and isotopic compositions of country rocks. Below we model each process and evaluate their potentials for explaining the Tin Mountain data.

5.1. Modeling the Li profile in amphibolite country rocks

Amphibolites show a ten-fold decrease in Li concentration and a ~30‰ drop in Li isotopic composition along the 10 m traverse. Variations in both Li and δ^7Li values do not correlate with either modal amphibole and plagioclase abundances or amphibole compositions. They therefore likely reflect interactions between the amphibolites and the Tin Mountain pegmatite.

5.1.1. Mixing model

If no Li isotopic fractionation during fluid-rock interactions occurred, then fluid infiltration can be modeled as two-end member mixing between isotopically heavy Li

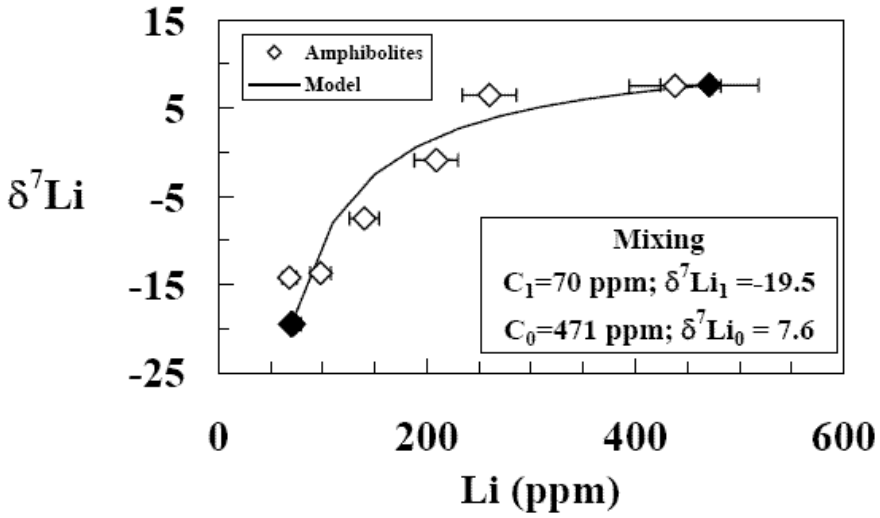

Figure 5-3. Plots of Li and δ^7Li for amphibolites and two end-member mixing model Mixing equation used: $\delta^7Li=(\delta^7Li)_1 \times f_1 +(\delta^7Li)_0 \times (1-f_1)$, f_1= faction of Li in end member 1. End members are shown as solid symbols and represent the measured values of amphibolites at either end of the transect (Table 5-1).

from the pegmatite and lighter Li in the original amphibolite. Using amphibolites at either end of the transect as end-members, the mixing model fits the data well (Fig.3).

The high Li concentration and δ^7Li of the amphibolite at the contact is similar to the Tin Mountain pegmatite, and suggests that Li in this sample is dominated by the pegmatite. The other amphibolite end member, however, is richer in Li (70 ppm) and isotopically lighter (-19.9‰) than regional amphibolite (sample 14-1) or amphibolites from other regions (Bottomley et al., 2003; Teng et al., 2004b). The regional amphibolite was likely not affected by the intrusion of this pegmatite or other plutons, and can be considered as representative of unaltered amphibolites in this area. The large difference in Li and δ^7Li between the amphibolite end member used in these mixing calculations and typical amphibolites suggests that the end-member has been substantially affected by Li infiltration from the pegmatite, and thus this simple mixing model cannot explain the data.

5.1.2. Rayleigh distillation model

Previous studies have shown that Li isotopes can be strongly fractionated during low-T fluid-rock interactions, with isotopically heavy Li partitioning into fluids relative to rocks (e.g., Chan et al., 1992; Huh et al., 1998; Rudnick et al., 2004). Although fluid infiltration of amphibolite country rocks occurred at relatively high temperature (T > 340^{o}C) (2003a; Sirbescu and Nabelek, 2003b; Walker et al., 1986b), Li isotopes may still be fractionated (the isotopic exchange between minerals and fluids has not yet been fully quantified as a function of temperature). Therefore, we explore fluid infiltration accompanied by isotopic fractionation using a Rayleigh fractionation law.

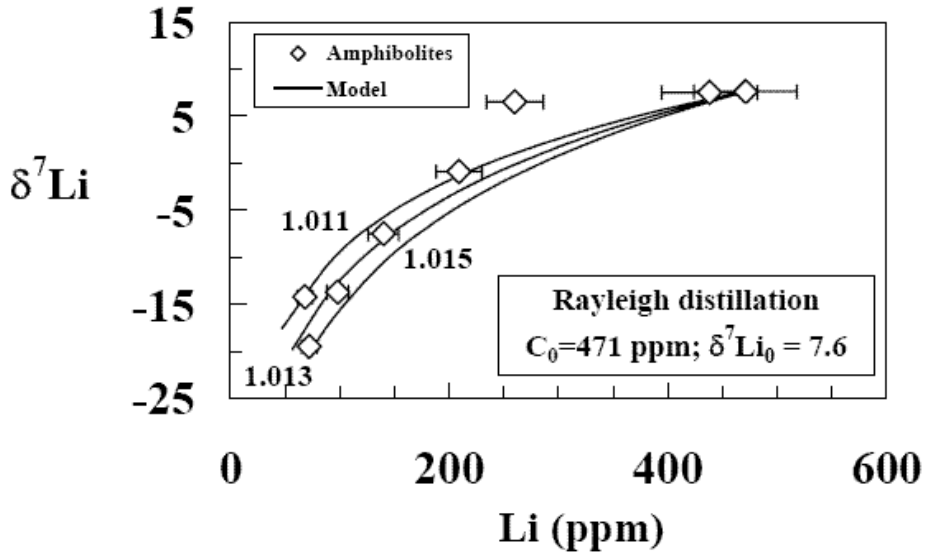

Figure 5-4. Plots of Li and δ^7Li for amphibolites and Rayleigh distillation model Numbers on lines represent Li isotopic fractionation factor between fluids and amphibolites. Rayleigh distillation equation: $\delta^7Li_{amph} = (\delta^7Li_0 + 1000)f^{(\alpha-1)} - 1000$; α: Li isotopic fractionation factor defined as $^7Li/^6Li$ isotopic ratio between fluids and amphibolites; f: the fraction of Li remaining in the rock, calculated from Li_{amph}/Li_0; 0: amphibolite at the contact.

A series of Rayleigh distillation curves can be calculated to fit most of the data (Fig. 4), assuming that the Li isotopic fractionation factor between fluids and minerals (α) is ~ 1.013 ± 0.002, i.e., there is ~13‰ difference between fluids and amphibolites. Since, in reality, fluid infiltration may not obey perfectly a Rayleigh distillation process, which is the most effective process at fractionating isotopes, these estimated α values are considered to be minimum values. Although experimentally measured fractionation factors between hydrothermal fluids and amphibolites are not currently available, data for α determined for seafloor alteration can be used as a comparison. At ~ 2^{o}C, the Li isotopic fractionation factor between seawater and clays produced by alteration of basalts (α) is inferred to be 1.019 (Chan et al., 1992); while at 350 ^{o}C, α between hydrothermal fluids and basalts decreases to 1.003-1.007 (Chan et al., 1993; 1994). Given a minimum crystallization temperature for this system of ~340 °C (2003a; Sirbescu and Nabelek, 2003b; Walker et al., 1986b), the fractionation factor required to fit the data (1.013) is significantly greater than those observed at comparable temperatures in the oceanic environments. Therefore, this process is unlikely to explain the data.

5.1.3. Diffusion model

The above discussions suggest that fluid infiltration, with or without isotopic fractionation, is unlikely to produce the Li profile observed in the amphibolite country rocks. Instead, we explore the likelihood that diffusion of Li played an important role in producing the extreme isotopic fractionation observed. The importance of diffusion in producing the Li variations is consistent with the differences in scales observed in chemical modification of the country rocks for Li versus other elements. All other elements that change systematically within the amphibolite transect show concentration

variations only within 2 m of the contact (Fig.1). The much larger scale of Li variation (≥ 10 m) may reflect greater Li diffusivity relative to the other elements examined. Although Li diffusivity in amphibole is unknown, studies of other silicate minerals and melts demonstrate that Li diffusion is orders of magnitude faster than other elements (Coogan et al., 2005; Giletti and Shanahan, 1997; Lundstrom, 2003; Richter et al., 2003). For example, Li diffuses more than four orders of magnitude faster than other alkali elements in plagioclase feldspar (Giletti and Shanahan, 1997) and 100 times faster than most trace elements in a liquid basalt (Richter et al., 2003).

To model the data, the pegmatite is considered as an infinite Li reservoir relative to the country rocks; therefore, the diffusion model used to fit the data is a one-dimensional diffusion model (Crank, 1975):

$$[(C_x-C_1)/(C_0-C_1)] = \mathrm{erfc}[x/2(Dt)^{1/2}]$$

Where here, x = distance from the contact; C_x = element concentration at distance x from the contact; C_0 = element concentration at the contact at x=0; C_1 = element concentration in unaffected country rocks; D = diffusion coefficient; t = duration of the diffusion process; erfc = complementary error function.

^{6}Li and ^{7}Li are treated as two different elements and each diffusion curve is modeled separately. The ^{7}Li/^{6}Li ratio or δ^7Li is calculated by combining concentrations at different distances. By using the regional amphibolite to represent the unaltered amphibolite country rock, and the pegmatite as the concentration at the contact, the following parameters are derived: C_1=20 ppm and δ^7Li = +0.9. This, with C_0 =471 ppm and δ^7Li =7.6, will allow $C_{1,6}$ (or $C_{1,7}$) and $C_{0,6}$ (or $C_{0,7}$) to be calculated. Since neither ^{7}Li and ^{6}Li diffusion coefficients, nor the duration of diffusion are known, the value of

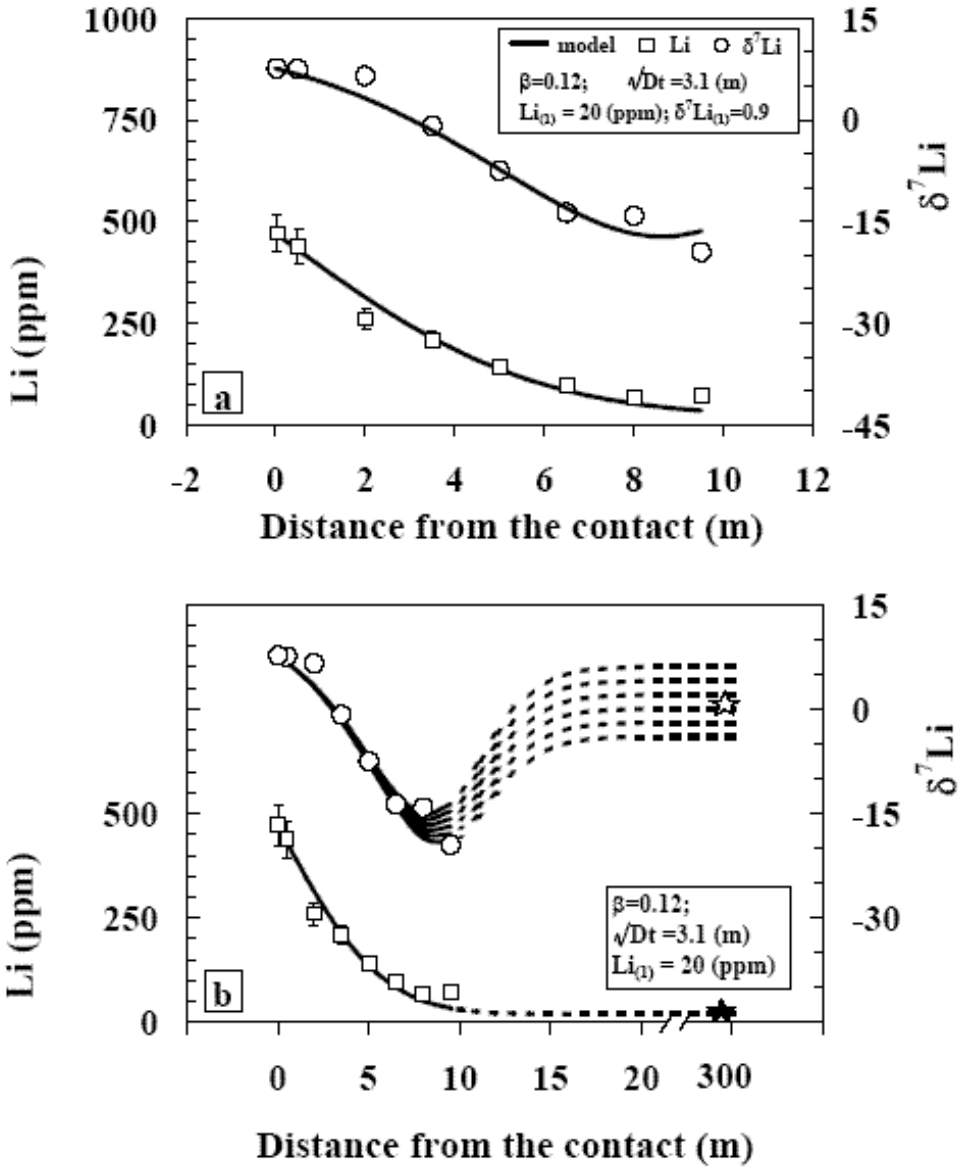

Figure 5-5. Curves modeled by diffusion for Li and δ^7Li of amphibolites vs. distance from the contact

a) shows the model for the amphibolite profile and b) shows how varying the initial Li isotopic composition of the unaltered amphibolite has little effect on outcome. Star in b) represents the Li (filled) and δ^7Li (open) of the regional amphibolite, which is used as the initial Li and δ^7Li values in the modeling in a); see text for details.

$\sqrt{Dt}$ is calculated to best fit the Li concentration profile (Fig.5a). The best value of $\sqrt{Dt}$ = 3.12 (m) was determined by using the Microsoft Excel® solver function. The diffusion coefficient derived here is the average D of both ^{7}Li and ^{6}Li, but since > 90% of Li is ^{7}Li, this diffusion coefficient is considered to represent D_7 and thus the Li diffusion curve can be considered to be that of ^{7}Li.

In order to model the $\delta^{7}Li$ curve, the diffusion curve for ^{6}Li is needed. If the relationship between D_7 and D_6 can be found, then the ^{6}Li diffusion curve can be modeled, followed by the $\delta^{7}Li$ curve. Here the assumption of Richter et al. (1999) is used: the ratio of the effective diffusion coefficients of the isotopes 1 (light) and 2 (heavy) of element i are related to their mass by the following equation: $D_{i,1}/D_{i,2} = (m_{i,2}/m_{i,1})^{\beta}$, where β is an empirical parameter determined from the experimental data. For ideal gases, β is equal to 0.5, while in condensed matter it is < 0.5. For example, a β value of ~ 0.2 was determined experimentally for Li diffusion in silicate melts (Richter et al., 2003).

The effective diffusion coefficients depend on temperature, pressure and matrix (composition, mineralogy, fluid, etc., see recent review of Cole and Chakraborty, 2001). The estimated crystallization temperature of the Tin Mountain pegmatite varied from ~ 600 °C to 340 °C (2003a; Sirbescu and Nabelek, 2003b; Walker et al., 1986b) at an intrusion depth of ~ 10 km (Redden et al., 1985). At a normal geothermal gradient of ~ 35 ^{o}C/km (Brown and Mussett, 1993), the country rocks at this depth should have had a temperature of ~ 350 °C, similar to the end stages of pegmatite crystallization. Therefore, the temperature gradient in the country rocks produced by the intrusion should be small. Moreover, both the major element composition and the mineralogy of the amphibolites along the traverse change little, so the diffusion coefficients of both ^{6}Li and ^{7}Li in the

amphibolite are assumed to have remained constant, i.e., $D_6/D_7 = (m_7/m_6)^{\beta}$ = constant, which means β is constant. The β value yielding the best fit to the data is 0.118 (Fig.5a) and the corresponding ratio of $D_6/D_7 = 1.018$. Furthermore, it is important to note that the initial Li isotopic composition of unaltered amphibolite is not important for this modeling (Fig.5 b). The calculated curves still fit the data well even if the δ^7Li values were varied from –4 to +6.

In summary, the Li profile observed in the amphibolite country rocks cannot be explained by mixing between pegmatite fluids and amphibolite due to the extremely light δ^7Li required for the amphibolite end-member (≤ -20‰). Nor can Li isotope fractionation by Rayleigh distillation during fluid infiltration explain the trend due to the extreme fractionation factors required (≥1.013). Instead, these variations can be explained by isotopic fractionation accompanying Li diffusion from the pegmatite into amphibolites with employing reasonable diffusion coefficients, β values and δ^7Li value for the unaltered amphibolite.

5.2. Modeling the Li profile in schist country rocks

The Li concentrations and isotopic compositions of schists taken from the inlier within the pegmatite and from near the contact with the pegmatite are dominated by Li from the Tin Mountain pegmatite. Samples taken far from the pegmatite (> 300 m) have Li similar to schists and shales worldwide (Moriguti and Nakamura, 1998a; Teng et al., 2004a; 2005c). These distal schists may, therefore, represent samples that have not been affected by interactions with any pluton. The sample taken 30 m from the pegmatite, however, has extremely light Li isotopic composition and was likely influenced by the interaction.

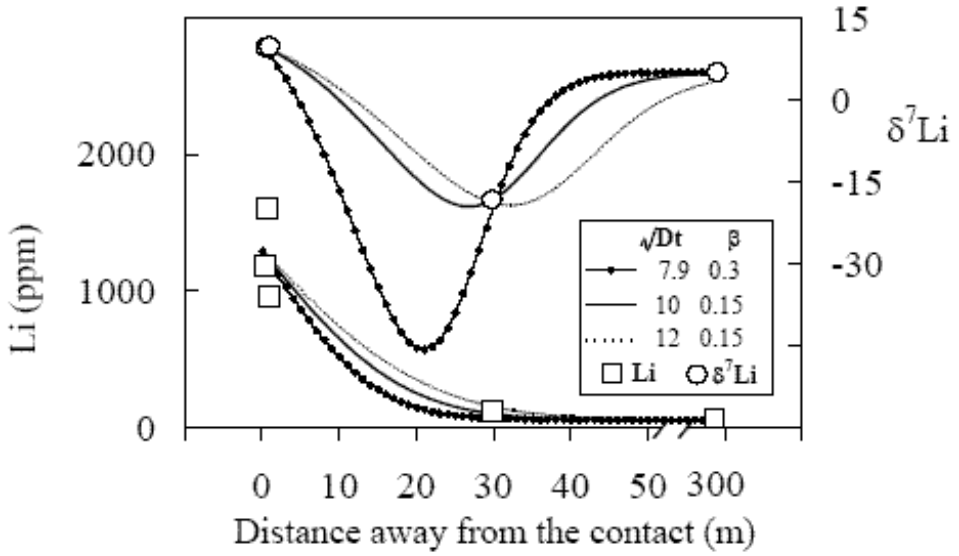

Figure 5-6. Model curves by diffusion for Li and δ^7Li of schists vs. distance from the contact
Due to few samples, this modeling is not unique.

This isotopically light schist, like the isotopically light amphibolite, may also result from Li isotopic fractionation through diffusion-related process. Applying the approach outlined above to the schist data provides a best-fit $\sqrt{Dt}$ = 10 (m) and β = 0.151 (Fig. 6). The schist's relatively large $\sqrt{Dt}$ value compared with that in amphibolite is consistent with earlier findings that demonstrated that Li can migrate to a greater distance in schist country rocks (the Etta pegmatite near the Harney Peak Granite) than amphibolite country rocks of the Tin Mountain pegmatite (Laul et al., 1984).

5.3. Implications for the nature of diffusion

Data from the country rocks of the Tin Mountain pegmatite demonstrate that Li isotopes can be strongly fractionated by diffusion at moderate temperature (down to 340 ^{o}C). This implies that isotopic heterogeneity may exist in zoned minerals or minerals that interacted with fluids. Moreover, results of this modeling can be used to constrain the effective diffusion coefficients in the country rocks and to constrain the type of diffusion: grain-boundary diffusion vs. volume diffusion.

Based on the best fits to the Li concentration profiles, the value for $\sqrt{Dt}$ differs between the amphibolite and schist with $D_{schist}/D_{amphibolite}$ = ~ 10. Although neither the diffusion coefficient (D) nor the duration of the diffusion process (t) is known, the minimum D can be calculated by assuming that the maximum time of diffusion is equal to the age of the Tin Mountain pegmatite (1.7 Ga). As a result, the minimum $D_{amphibolite}$ for Li is calculated to be 2 x 10^{-12} cm^2/s and the D_{schist} is ~ 10 times higher accordingly (Fig. 7). These estimated minimum D values are >2 orders of magnitude higher than those measured in silicate minerals (e.g., feldspar and pyroxene) (Coogan et al., 2005; Giletti and Shanahan, 1997), which suggests that Li diffusion in both country rocks was

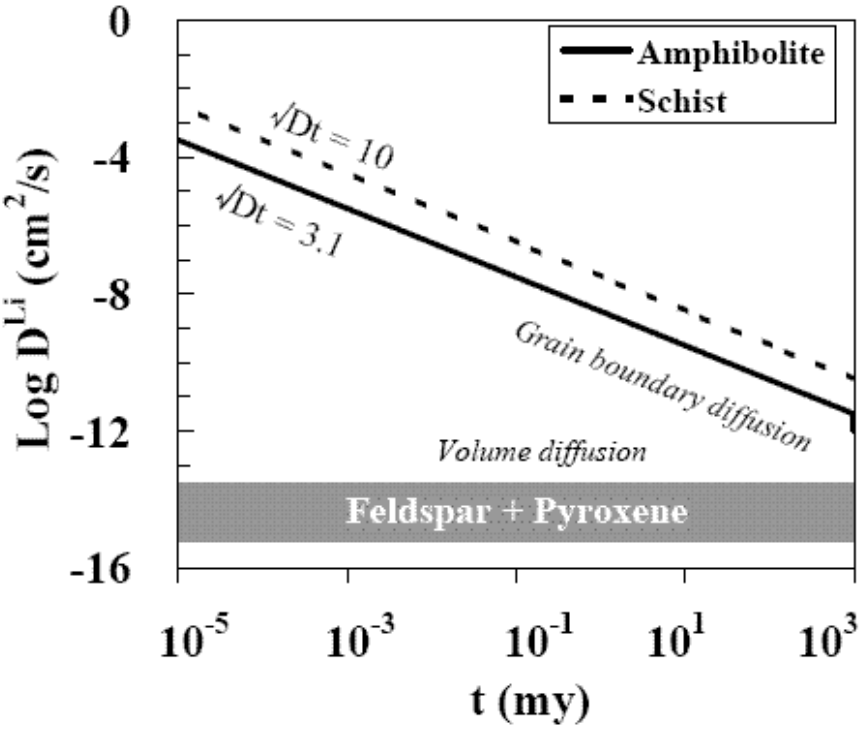

Figure 5-7. Plot of D vs. t
Assuming √Dt = 3.12 and 10 in amphibolites and schists separately; D values for Li in plagioclase and pyroxene from Giletti and Shanahan (1997) and Coogan et al. (2005).

not constrained to volume diffusion, but rather occurred in a fluid phase that wetted the grain boundaries. As discussed in Ferry et al. (2001), the effective diffusion coefficient is directly controlled by both the diffusion coefficient in fluids and effective interconnected porosity of the rock. Assuming the diffusion coefficients of fluids are the same in amphibolites and schists, the effective interconnected porosity in schists is ~ 10 times larger than in amphibolite. This reflects the different permeability of country rocks. Amphibolites are dense and impervious whereas schists are more permeable to the late-stage pegmatite fluids.

6. Conclusions

The country rocks of the Tin Mountain pegmatite exhibit ~ 30‰ Li isotopic change over a ~10 m traverse in the amphibolites and ~300 m in the schist. These observations are unlikely to be due to either mixing between pegmatite and country rocks or Li isotope fractionation by Rayleigh distillation during fluid infiltration. Instead, they reflect extreme Li isotopic fractionation accompanying Li diffusion from the Li-rich pegmatite into country rocks. These extreme fractionations are due to the large differences in diffusion coefficients between ^{6}Li and ^{7}Li, and in Li concentrations between the pegmatite and country rocks.

Lithium diffusion in the schists is inferred to be ~10 times faster than in the amphibolites. However, in both types of rocks, Li diffuses much faster than other alkali elements, as concentrations of these elements vary only within two meters of the contact. The effective diffusion coefficient of Li in both rocks are >2 orders of magnitude greater than in minerals, which indicates Li diffusion in country rocks was dominated by fluid-assisted grain-boundary diffusion over solid-state diffusion.

Chapter 6: Lithium isotopic fractionation during metamorphic dehydration

Abstract

The major, trace element, Li concentration and isotopic composition of metapelite and a granodiorite from the Onawa pluton and surrounding contact aureole have been measured in order to document the behavior of Li and Li isotopes during metamorphic dehydration. Major and trace element concentrations in the contact aureole vary little while loss on ignition (LOI) decreases with increasing metamorphic grade. Lithium concentration correlates with LOI and decreases by a factor of two while Li isotopic compositions remain relatively constant, within the range observed in schists and typical post Archean shales. The granodiorite has 45 ppm Li and δ^7Li = -0.2, within the range of typical granites.

These observations are consistent with the removal of Li via Rayleigh distillation during progressive metamorphism. The fractionation factors between fluids and rocks are estimated to be ~ 1.002 with Li partition coefficients ~ 15, suggesting no isotopic fractionation through this range of metamorphic temperatures. These results indicate that except metamorphic temperature, protolith and mineralogy of metamorphic rocks are two important factors controlling Li concentration and isotopic compositions of metamorphic rocks. The comparison of this study with results from a study of another contact halo around the Tin Mountain pegmatite suggests that intrusions can play crucial roles in controlling the behavior of Li in contact rocks.

1. Introduction

In order to fully utilize Li isotopes as geochemical tracers, it will be necessary to both characterize the Li isotopic compositions of different geological reservoirs, and quantify the magnitude of isotopic fractionations for various conditions. The continental crust appears to have lighter Li isotopic composition than the upper mantle, from which it was derived (Teng et al., 2004a; 2004b). Given that Li isotopes do not fractionate during high-T magmatism (Tomascak et al., 1999b), juvenile crust and the mantle should have identical Li isotopic compositions. The isotopically light continental crust, therefore, is likely a result of secondary processes, e.g., weathering, low-T intracrustal melting and metamorphism. Recent studies have demonstrated large Li isotopic fractionation during surface weathering (Huh et al., 2004; Kisakurek et al., 2004; Pistiner and Henderson, 2003; Rudnick et al., 2004), seafloor alteration (Bouman et al., 2004; Chan et al., 1992; 2002a; Foustoukos et al., 2004; James et al., 2003; Seyfried Jr. et al., 1998) and small Li isotopic fractionation during granite differentiation (Bryant et al., 2004b; Teng et al., 2004a; 2005a). The nature of Li isotopic fractionation during progressive metamorphism, however, is not well established.

Studying Li isotopic fractionation during metamorphism could help us understand not only the Li isotopic composition and evolution of the crust, but also Li behavior during subduction processes. Some eclogites and granulites are extremely light in Li isotopic compositions (Teng et al., 2004b; Zack et al., 2003), while forearc serpentinites, which are interpreted to have interacted with slab-derived fluids, have both light and heavy Li isotopic compositions (Benton et al., 2004; Decitre et al., 2002). All these observations have been explained by Li isotopic fractionation associated with

dehydration, with isotopically heavy Li preferring fluids to rocks. Recent experimental study supports this conclusion and shows that Li isotopes are largely fractionated from +6 to –13‰ during the reaction of smectite to illite at 300 ^{o}C and 1kbar (Williams and Hervig, 2005). However, to date, no comprehensive analysis on a suite of progressively metamorphosed rocks has been carried out.

Here we present Li isotopic data for a suite of metapelite from the well-characterized Onawa contact aureole, Maine, USA. These metapelite were metamorphosed at 3.0 ± 0.8 kbar and 480 ^{o}C to 650 ^{o}C, with the metamorphic grade ranging from lower greenschist facies to the start of melting. Our results demonstrate that although a large amount of Li was released into fluids during metamorphic dehydration, the δ^{7}Li remains relatively constant, suggesting that Li isotopic fractionation at this range of temperature is very small and reflecting the importance of protolith and mineralogy of metamorphic rocks on controlling Li concentration and isotopic compositions of metamorphic rocks.

2. Geological background and samples

The Onawa pluton is a 2 x 5 km composite intrusion composed of quartz diorite and granodiorite. The intrusion of this pluton into chlorite-zone regional metasedimentary rocks of the Carrabassett Formation during the late stages of the Acadian orogeny produced a ~1.5 km wide contact aureole (Philbrick, 1936; Symmes and Ferry, 1995). Based on mineral assemblages, five metamorphic zones have been delineated (Fig. 1): chlorite zone (chl, >1500m from the pluton), andalusite-cordierite zone (a-c, 800-1500m), alkali feldspar zone (ksp, 500-800m), sillimanite zone (sil, 300-500m) and leucocratic-vein zone (l-v, <300m). The a-c zone can be further divided into two subzones: the

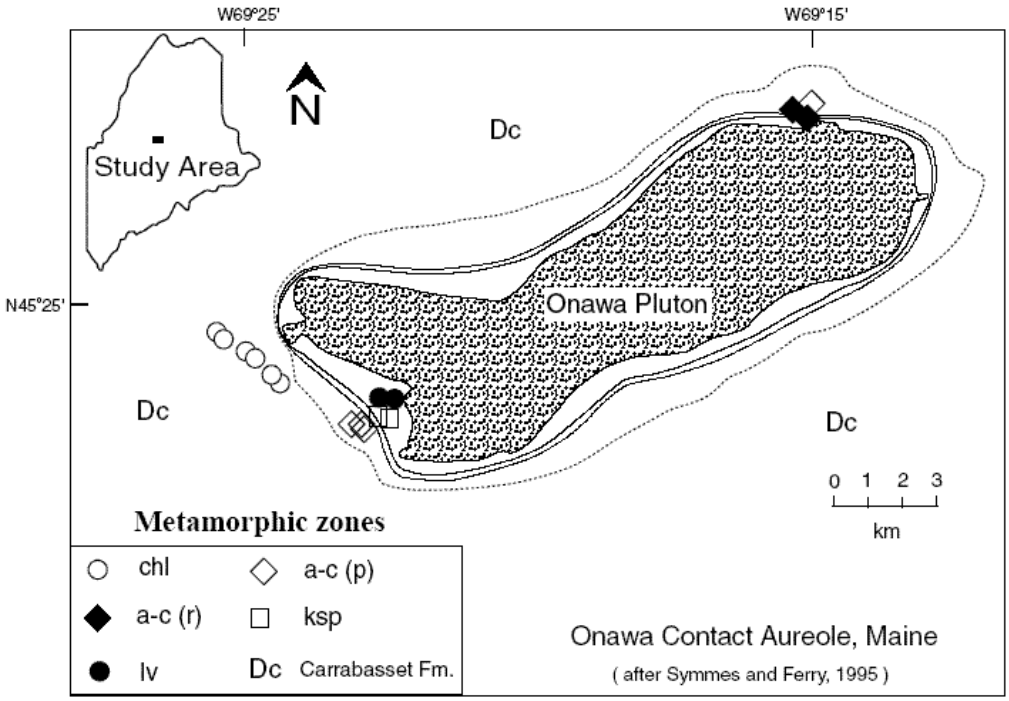

Figure 6-1. Metamorphic map of study area with sample locations.

Inset at upper left shows location of field area in central Maine. Modified from Symmes and Ferry (1995).

prograde zone (a-c (p)) with fresh cordierite and/or no chlorite; and the retrograde zone (a-c (r)) with no fresh cordierite. The P-T conditions at the peak of metamorphism were estimated from the mineral equilibria. The pressure of the contact metamorphism was ~3 kbar, with the metamorphic temperature ranging from 480 ^{o}C - 540 ^{o}C in the andalusite-cordierite zone to 640 ^{o}C - 650 ^{o}C in the leucocratic-vein zone with uncertainties of ~ 10 ^{o}C - 20 ^{o}C (Symmes and Ferry, 1995).

All metapelitic rocks contain muscovite, quartz, plagioclase and ilmenite, with minor quantities of tourmaline and zircon. Chlorite and graphite are mainly concentrated in the outer zones (chl, a-c) while biotite, cordierite and andalusite appear in all zones except the chl zone. Alkali feldspar and sillimanite occur in the inner zones (ksp, sil and l-v). Due to the small scale of the aureole (~1.5 km), metapelitic rocks can be sampled from the same lithologic units at different grades. Samples from the igneous intrusion and all zones except the sillimanite zone have been measured. All these samples are the same as those used in Wing and Ferry (2003), Marchildon and Brown (2001), and taken from the same spots as those in Symmes and Ferry (1995).

3. Analytical methods

Major and minor elements were determined by using XRF at the Geoanalytical Laboratory of Washington State University (Johnson et al., 1999). Lithium analyses were performed at the Geochemical Laboratory of University of Maryland, College Park. Procedures for sample dissolution, column chemistry, and instrumental analysis are similar to those reported in Teng et al. (2005a).

The external precision of Li isotopic analyses, based on 2 σ of repeat runs of pure Li standard solutions and rock solutions, is < ± 1.0‰. For example, pure Li standard

solutions (IRMM-016 and UMD-1) always have values falling within previous established ranges (-0.1 ± 0.2‰ and +54.7 ± 1‰, Teng et al., 2004a); AO-12 gives δ^7Li = +3.5 ± 0.6 ‰ (2 σ, n = 50 runs with 4 replicate sample preparations over a two-year period) (Fig. 2). The uncertainty of Li concentration measurement, determined by voltage comparison between sample solution and that measured for 50 ppb L-SVEC standard solution and then adjusting for sample weight, is < ± 10%.

4. Results

Lithium concentrations and isotopic compositions of all samples are reported in Table 1, along with the major, trace element data, metamorphic grade and chemical index of alteration (CIA).

Major and trace element concentrations in all metapelite are similar to values previously reported (Symmes and Ferry, 1995) and vary little (Fig.3). Loss on ignition (LOI) decreases with increasing metamorphic grade with samples from a-c (r) zones significantly higher than those from a-c (p) zones (Table 1). The homogeneous chemical compositions result in a small range in CIA values from 72 to 78 with an average of 75 ± 2. Lithium concentrations correlate with LOI and decrease with progressive metamorphism towards the pluton, while samples from the a-c (r) and l-v zones have higher Li concentrations than their prograde count parts (Fig. 4). Lithium isotopic compositions remain relatively constant from –3.5 to –1.0 for samples in prograde metamorphic zones and –1.7 to +0.9 for samples from a-c (r) and l-v zones (Fig. 4). Overall, the Li concentrations and isotopic compositions of metapelite fall within the range observed in typical post Archean shales and schists (Teng et al., 2004a; 2005a).

Table 6-1. Major, trace element and Li concentration and isotopic composition of samples from the Onawa contact aureole, Maine

Sample	Zone	Li[1] (ppm)	δ^7Li[2]	SiO_2	TiO_2	Al_2O_3	FeO[3]	MnO	MgO	CaO	Na_2O	K_2O	P_2O_5	LOI[4] (%)	Total	CIA[5]
BMW1b	chl	106	-1.0	67.4	1.0	15.4	6.3	0.1	2.1	0.3	1.3	2.9	0.1	3.0	99.9	73
SL15a	chl	97	-2.2	64.5	1.0	17.4	5.8	0.1	2.1	0.4	1.2	3.9	0.1	3.4	99.9	72
SL14b	chl	87	-1.9	71.9	0.9	15.0	5.5	0.1	1.3	0.1	0.9	2.5	0.1	2.6	100.9	78
BMW2b	chl	131	-1.4	59.5	1.0	19.7	7.5	0.1	2.3	0.6	1.4	3.6	0.2	3.9	99.8	74
BMW3a	chl	93	-1.4	65.4	1.0	17.3	6.4	0.1	1.7	0.3	1.1	3.3	0.1	3.2	99.9	75
SL6b	chl	108	-2.0	58.3	1.2	21.0	7.5	0.1	2.1	0.4	1.0	4.3	0.2	4.0	100.1	76
ME2a	a-c (p)	91	-1.8	66.4	1.1	17.8	6.7	0.1	1.8	0.4	1.3	3.2	0.2	1.1	100.1	75
ME2b	a-c (p)	82	-2.4	67.0	1.0	17.5	6.1	0.1	1.8	0.5	1.4	3.3	0.1	1.2	100.0	73
ME2d	a-c (p)	82	-2.6	63.0	1.1	19.4	6.9	0.1	2.1	0.9	2.0	2.5	0.2	1.8	100.0	73
BME3a	a-c (p)	73	-1.8	66.3	0.9	14.9	7.0	0.2	2.9	1.9	2.1	2.6	0.2	1.1	100.1	62
BME1a	a-c (r)	124	0.9	62.0	1.1	19.6	7.0	0.1	1.8	0.3	1.1	3.7	0.2	3.2	100.1	77
BME5a	a-c (r)	117	-1.6	64.6	1.1	18.6	6.8	0.1	1.6	0.2	0.9	3.5	0.1	2.6	100.1	78
ONA-2	ksp	65	-2.1	60.2	1.2	20.6	7.6	0.1	2.5	0.6	1.6	4.1	0.1	1.4	100.0	72
ONA-5	ksp	64	-3.5	63.7	1.1	19.3	6.7	0.1	2.0	0.3	1.3	4.2	0.1	1.1	99.9	73
BMW5a	lv	94	-0.5	61.7	1.1	20.5	6.7	0.1	1.7	0.3	1.7	4.3	0.2	1.8	100.1	73
BMW6a	lv	82	-1.7	62.3	1.1	20.3	7.5	0.1	2.1	0.4	1.2	3.7	0.2	1.1	100.0	77
ONA-11	pluton	45	-0.2	58.8	1.4	18.0	7.2	0.1	2.4	5.6	3.0	3.0	0.2	0.3	100.0	50

Sample	Zone	Ni	Cr	Sc	V	Ba	Rb	Sr	Zr	Y	Nb	Ga	Cu	Zn	Pb	La	Ce	Th	Nd
BMW1b	chl	58	112	15	121	445	134	114	435	42	16.7	19	14	97	15	44	90	13	40
SL15a	chl	66	122	21	164	519	190	160	213	35	17.7	25	13	116	23	57	111	15	49
SL14b	chl	55	97	17	142	474	152	137	257	37	18.0	22	13	98	19	55	101	13	47
BMW2b	chl	58	112	20	162	683	173	166	260	42	19.6	26	1	105	31	54	110	16	48
BMW3a	chl	60	119	19	172	560	165	157	252	39	19.3	27	8	114	25	54	110	15	47
SL6b	chl	65	121	21	173	623	201	133	287	47	20.9	28	13	112	32	60	119	16	52
ME2a	a-c (p)	42	82	14	109	378	119	99	331	34	15.8	18	24	76	17	40	81	12	36
ME2b	a-c (p)	64	115	17	140	597	173	114	304	40	18.5	23	34	117	18	52	96	14	43
ME2d	a-c (p)	51	102	18	139	483	140	132	267	39	19.1	23	28	101	25	48	91	13	41
BME3a	a-c (p)	58	103	17	136	484	135	136	301	38	18.4	22	22	98	24	46	91	13	41
BME1a	a-c (r)	81	123	17	126	403	126	153	226	37	13.8	20	5	97	21	42	77	11	37
BME5a	a-c (r)	48	102	18	142	522	168	144	275	39	18.3	24	25	78	26	49	96	15	43
ONA-2	ksp	24	60	22	127	388	123	199	403	44	12.7	24	17	87	18	40	82	11	39
ONA-5	ksp	69	133	21	179	589	191	153	256	43	20.9	25	2	119	27	64	119	16	56
BMW5a	lv	59	136	19	154	423	133	206	282	35	20.4	25	3	110	24	51	103	15	46
BMW6a	lv	56	110	19	161	553	180	148	224	38	18.3	26	7	94	25	54	100	14	43
ONA-11	pluton	58	112	19	154	603	180	138	253	40	19.3	27	14	103	24	49	99	14	44

Analytical uncertainty is <1% for the major elements and < 10% for the minor elements (Johnson et al., 1999)

1. Li measured by comparison of signal intensities with 50 or 100 ppb LSVEC.
2. Analytical uncertainty is $\leq \pm$ 1‰ (2σ), based on both pure Li solutions and natural rocks (see text for details).
3. FeO: total Fe as FeO.
4. LOI: loss on ignition at 900^{o}C.

5. CIA is the molar $Al_2O_3/(Al_2O_3+K_2O+Na_2O+CaO^*) \times 100$, where CaO^* refers to Ca in silicate only and not contained in carbonate and phosphate (Nesbitt and Young, 1982). McLennan ‘s (1993) correction to the measured CaO content for the presence of Ca in carbonates and phosphates is used here. CIA value increases with the degree of weathering. Unweathered igneous rocks have CIA ~ 50 while shales have higher values between 60 and 80 (Nesbitt and Young, 1982).

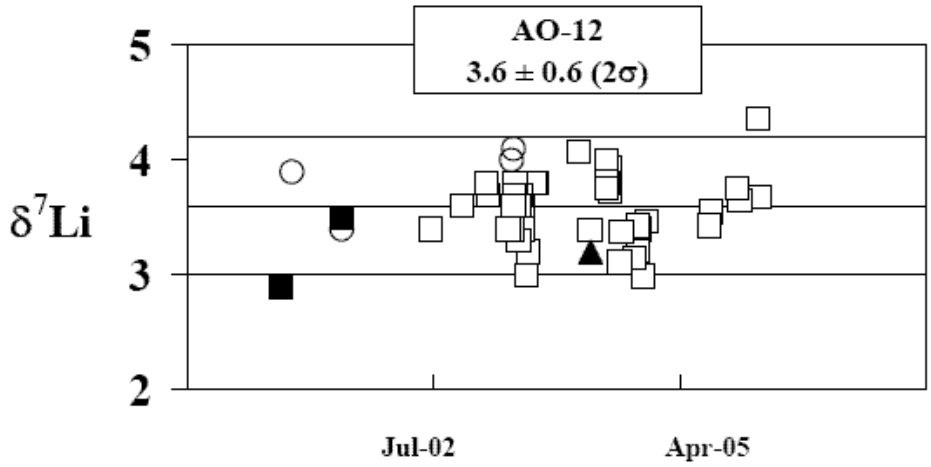

Figure 6-2. Compilation of analyses of four preparations of shale standard AO-12, from the Amadeus Basin.

Different symbols denote analyses of separate digestion and preparation with Li concentration ranging from 50 ppb to 150 ppb. Filled-squares represent samples taken through column chemistry procedure described in Teng et al (2004a) and all other samples were taken through column chemistry procedure described in Rudnick et al (2004). The overall mean $\delta^7Li = 3.6 \pm 0.6$ (2σ).

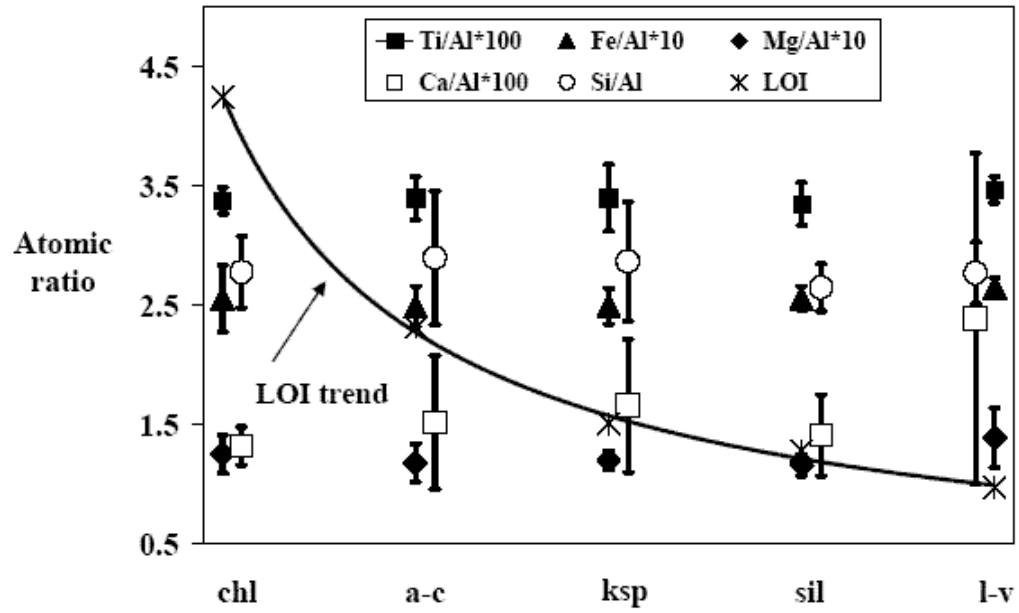

Figure 6-3. Plots of mean whole-rock atomic i/Al for all metapelite samples in all zones Data from Table 6-1 and Symmes and Ferry (1995).

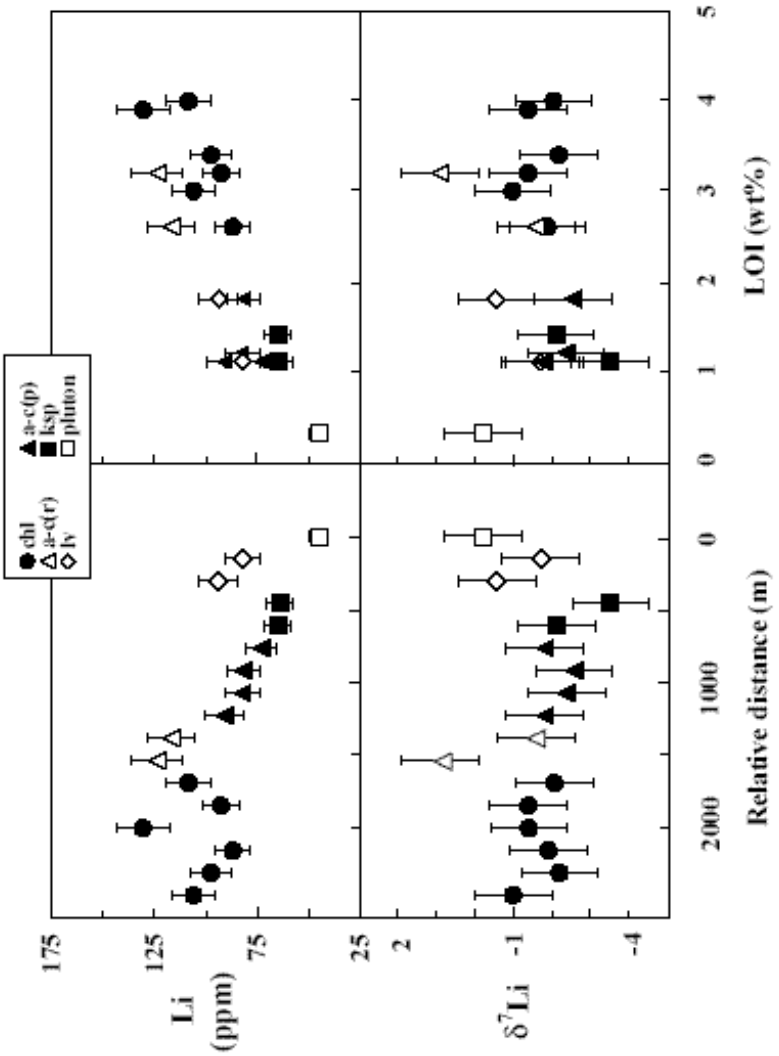

Figure 6-4. Plots of Li, δ^7Li versus LOI and the distance to the intrusion
Filled symbols represent metapelite from progressive metamorphism while open symbols represent pluton (granodiorite) and samples reacted with fluids; data from Table 6-1.

The granodiorite sample, taken from the Onawa pluton, has 45 ppm Li and δ^7Li = -0.2, falling in the range of typical granites (Bryant et al., 2004b; Teng et al., 2004a; 2005a).

5. Discussion

The Li and δ^7Li values of these metapelite, which are similar to schists and typical post Archean shales (Teng et al., 2004a; 2005a), may reflect their protolith Li and δ^7Li values. Alternatively, they may derive from processes that can affect Li e.g., metamorphic dehydration during the regional and contact metamorphism, fluid infiltration from the intrusion and surface weathering. In this section, we first discuss the general factors controlling Li in metamorphic rocks and then use these factors to constrain the origin of Li variation in these metapelites and other grade of metamorphic rocks. Finally we compare this study with a similar Li study to illustrate how the character of the igneous intrusion affects Li in contact metamorphic rocks differently.

5.1. Factors controlling Li in metamorphic rocks

Because of the large relative mass difference, moderate incompatibility and fluid mobility, the Li concentration and isotopic composition in terrestrial rocks vary significantly (Tomascak, 2004). This indicates that the Li content and isotopic composition of metamorphic rocks is influenced strongly by the natural of the protolith. Regardless of protoliths, most prograde metamorphic reactions experience the release of H_2O with Li partitioning and Li isotopes fractionating between fluids and minerals. Lithium concentrations and isotopic compositions of metamorphic rocks therefore depend on the fraction of fluids released (F), Li partition coefficient (D, defined as Li

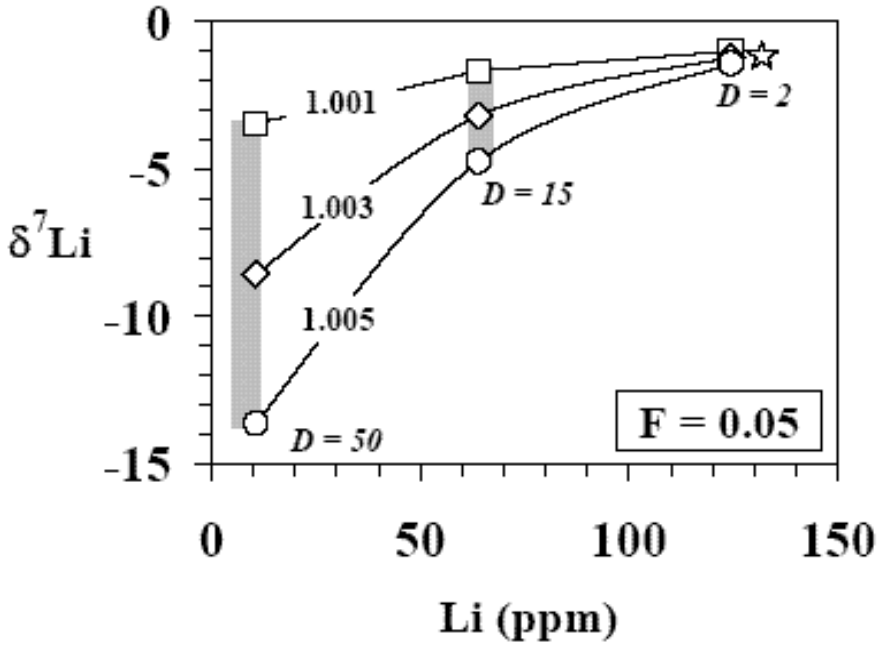

Figure 6-5. Li and δ^7Li variations with α and *D* at given F, by Rayleigh distillation $\alpha = {}^7Li/{}^6Li$ ratio between fluid and mineral; *D* = Li concentration ratio between fluid and mineral; F = fraction of fluids removed, the maximum F value in the metapelite is given at 0.05. Star represents the protolith. Shaded rectangles represent estimated δ^7Li values for metapelite from the ksp zones and granulite xenolith, at given Li concentrations at ~ 65 ppm and ~8 ppm respectively.

concentration ratio between fluid and mineral), and isotopic fractionation factor (α, defined as ^{7}Li /^{6}Li ratio between fluid and mineral). All these factors are directly controlled by metamorphic temperature, mineralogy and composition of metamorphic rocks.

Lithium partitions into common pelitic metamorphic minerals in the following order: staurolite >cordierite > biotite > muscovite > garnet (Dutrow et al., 1986). Experimental studies show that the Li partition coefficient between fluids and rocks (D) increases with temperature (Berger et al., 1988; Brenan et al., 1998b; 1984; Seyfried Jr. et al., 1998). While the isotopic fractionation factor (α) decreases with increasing temperature, as predicted by stable isotopic fractionation theory (Chacko et al., 2001). Collectively, the above discussion indicates that Li content and isotopic composition of metamorphic rocks will decrease with metamorphic dehydration. If the process of metamorphic dehydration follows Rayleigh distillation law, then at given amount of fluids removed i.e., F is fixed, the larger the D or α value, the larger the isotopic fractionation and Li depletion in a given metamorphic rock (Fig. 5). Since D increases while α decreases with increasing temperature, Li concentration in a metamorphic rock will change more dramatically with temperatures relative to Li isotopic composition (Fig. 5).

5.2. Lithium in metapelites of the Onawa contact aureole

As in many contact aureoles, the Onawa contact aureole has a relatively simple geological setting and metamorphic history; therefore, many processes that potentially can affect Li isotopes can be ruled out. First, the small scale of the aureole (~1.5 km) allows metapelite to be sampled from the same lithologic unit with similar compositions

at different grades, which rules out significant source heterogeneity. Second, pluton emplacement and contact metamorphism occurred during the late stages of the Acadian orogeny; the regional metamorphism, therefore, has little effect on this contact aureole (Symmes and Ferry, 1995). Third, all metapelite protoliths show similar degrees of weathering, as reflected by the constant CIA values (75 ± 2). Finally, although in general the magmas are the sources of heat, mass and mechanical energy that yield contact metamorphism and associated deformation (Bergantz, 1991; Labotka, 1991), the Onawa pluton has a lower Li concentration and heavier Li isotopic composition than all metapelite except one from the retrograde a-c zone. Even if a fluid phase were exsolved from the crystallization of the pluton, it should have a similar or slightly heavier Li isotopic composition than the pluton (Teng et al., 2005a). Thus fluid infiltration is expected to shift metapelite towards higher Li concentration and isotopically heavier composition, which is the opposite from that is observed in the aureole (Fig. 4). Moreover, the constant major and most trace element compositions within the contact aureole further indicate that the effect of the Onawa pluton on the chemical composition of the aureole is small.

The variation in Li concentration and isotopic composition of these metapelite, however, may result from progressive metamorphic dehydration reactions driven by the heat from the Onawa pluton. Data from the metapelite clearly show that substantial amounts (up to 50% of total) of Li were removed during progressive metamorphism as indicated by the decrease of Li concentration towards the pluton and the positive correlation between Li and LOI. Compared with the large variation in Li concentration, δ^7Li shows small variation (Fig. 4). This progressive removal of Li can be modeled by

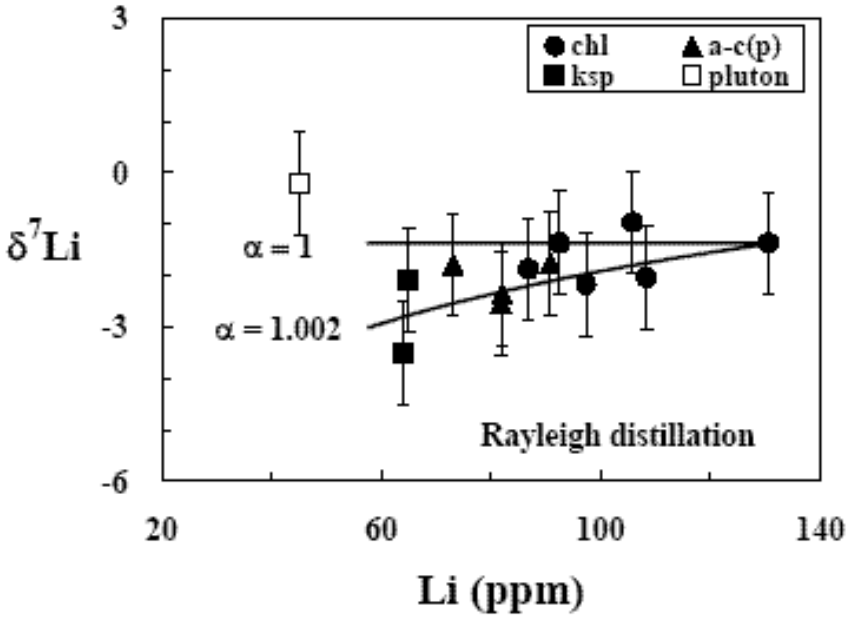

Figure 6-6. Rayleigh distillation model for Li and δ^7Li in prograde metapelite
α is defined as ^{7}Li /^{6}Li ratio between fluid and mineral.

Rayleigh distillation with $\alpha \sim 1.002$, suggesting no Li isotopic fractionation over this range of temperatures (Fig. 6). The lack of Li isotopic fractionation is also supported by data from the metapelite reacted with retrograde fluids. Although metapelite from a-c (r) zones is enriched in Li, their Li isotopic compositions are similar or slighter heavier than those from a-c (p) zones, suggesting that the difference in δ^7Li between retrograde fluids and metamorphic rocks is small and Li isotopic fractionation during metamorphic dehydration is insignificant.

5.3. Implications for the Li isotopic composition of metamorphic rocks

Metapelite from the Onawa contact aureole experienced a large range of temperature, lost a large amount of fluids and up to 50% of Li but have relatively constant δ^7Li. This result can be interpreted in two ways:

1) These metapelite were regionally metamorphosed to low greenschist grade before the intrusion of the Onawa pluton. Therefore, Li isotopic fractionation associated with metamorphism of these metapelite may occur at grades lower than those exposed here. However, the high Li concentration, shale-like Li isotopic composition and high LOI indicate that the low-grade regional metamorphism did not significantly affect Li in these metapelite, mainly due to the small D and F values, even if the α value is expected to be larger at the relatively lower temperatures.

2) Alternatively, this may indicate that isotopic fractionation at these temperatures will only be manifest at greater degrees of Li loss i.e., larger D or F value. For example, the average Li concentrations in metapelite from ksp zone and granulite xenolith are ~ 65 ppm and ~ 8 ppm respectively (Teng et

al., 2004b). The δ^7Li of granulite xenolith thus is expected to be more variable and lighter than that of ksp zone metapelite (Fig. 5). This is supported by the fact that most granulite xenoliths are isotopically lighter than their potential protoliths (Teng et al., 2004b). Furthermore, if F is fixed, at given Li and δ^7Li, both D and α can be constrained (Fig. 5), e.g., the D is estimated to be ~15 and α = ~ 1.002 for ksp zone metapelites.

Based on the definition, α, D and F are directly controlled by metamorphic temperature, mineralogy and composition of metamorphic rocks. However, very few data are available for these variables at different T and in different metamorphic rocks, which makes precise modeling impossible.

5.4. Roles of the igneous pluton on contact rocks

Data from this study illustrate the importance of prograde metamorphism and retrograde reactions in controlling Li in contact metamorphic rocks while the igneous intrusion plays a minor role. These results are in sharp contrast with those obtained for contact halos around the Tin Mountain pegmatite, South Dakota. This Li-rich pegmatite intruded both amphibolite and schist country rocks. The large Li concentration gradient between pluton and country rock, coupled with the large amounts of fluids exsolved from the pegmatite led to Li diffusion from the pegmatite into country rocks and produced a large isotopic fractionation with both Li and δ^7Li values decreasing away from the contact into country rocks (Teng et al., 2005b). Lithium from the igneous intrusion, therefore, dominated the Li concentration and isotopic composition in these country rocks, while the effect of contact metamorphism is not dramatic (Teng et al., 2005b). The different role played by the igneous intrusion in these two studies may reflect the

different types of igneous plutons and the environment of pluton emplacement. Considering that Li isotopic fractionation accompanying the contact metamorphic dehydration is relatively small compared to diffusion-induced Li isotopic fractionation, Li could potentially be a useful means of evaluating the roles the igneous pluton played during the contact metamorphism.

6. Conclusions

Results for the Li concentration and isotopic composition of metapelite from the Onawa contact aureole demonstrate that metapelite become more Li depleted with increasing metamorphic grade and correlate positively with LOI while δ^7Li remains relatively constant. Samples reacted with retrograde fluids are enriched in Li and have similar δ^7Li to their prograde counterparts. These metapelite experienced contact metamorphism over a large range of temperatures from 480 ^{o}C to 650 ^{o}C, released large amount of fluids (e.g., LOI decreasing from 4.0% to 1.1%) and showed two-fold variation in Li concentration while δ^7Li shows small variations. A Rayleigh distillation model suggests that the fractionation factors between fluids and rocks (α) were ~ 1.002, with Li partition coefficients between fluids and rocks (D) ~ 15, suggesting that metamorphic dehydration didn't significantly fractionate Li isotopes. However, large isotopic fractionation may happen at relatively higher grade with greater degrees of Li loss due to the larger D and F values.

Chapter 7: Summary and future work

Over the past 20 years, studies on Li isotopes have largely concentrated on subduction zones. This is based on the following philosophy: surface materials have different Li isotopic compositions relative to the mantle due to the significant mass-dependent isotopic fractionation at low temperature fluid-rock interactions. Thus, subducted surface materials should be sampled in oceanic basalts or arc lavas. Lithium isotopes therefore can be used to trace crust-mantle interactions. This is why arc lavas and basalts have been the focus of Li isotope geochemistry while as little is known about continental rocks, or about processes by which Li isotopes are fractionated. Both of them are important for understanding the signature of crustal recycling in the mantle, as well as understanding the processes that have modified the continental crust composition. It is the purpose of this dissertation to characterize the Li isotopic composition of the continental crust and the magnitude of isotopic fractionations for various conditions. The main conclusions drawn from this dissertation are:

1. The Li isotopic composition of the upper continental crust, characterized by studies of loess, shale, granite, and upper crustal composites, is ~0 ± 2‰ (1σ) and is isotopically lighter than the average upper mantle (+4 ± 2‰).
2. The Li isotopic composition of the deep continental crust has been characterized by analyses of samples from high-grade metamorphic rocks and granulite xenoliths. Thirty composite samples with different lithologies from eight Archean terranes in East China, have a mantle-

like Li isotopic compositions from +1.7 to +7.5‰ with an average of +4 ± 1.4‰ (1σ). In contrast, 44 granulite xenoliths from three locations display a much larger Li isotopic range from –17.9‰ to +15.7 with an average of -1± 7‰ (1σ), isotopically lighter than the mantle. Overall, the deep crust is also isotopically lighter than the mantle and the difference in Li isotopic composition between high-grade terranes and granulite xenoliths reflect the different roles retrograde fluids and metamorphic dehydration play.

3. The continental crust therefore has lighter Li isotopic composition than the upper mantle, from which it was derived. Given that Li isotopes do not fractionate during high-T magmatism, juvenile crust and the mantle should have identical Li isotopic compositions. The isotopically light continental crust, therefore, is considered as a result of secondary processes, e.g., weathering, metamorphism and low-T intracrustal melting.

4. Studies of Harney Peak granites, the spatially associated Tin Mountain pegmatite and possible metasedimentary source rocks indicate that main-stage granite differentiation doesn't significantly fractionate Li isotopes. In contrast, significant isotopic fractionation occurs in system involving extensive melt-aqueous fluid fractionation with ^{7}Li enriched in the fluids.

5. Lithium isotopic fractionation by diffusion has been clearly documented by studying samples from country rocks of the Tin Mountain pegmatite.

Both Li and δ^7Li vary greatly within amphibolite (~10 m traverse) and schist country rocks (~300 m traverse). These large variations can be modeled by Li diffusion and diffusion-induced isotopic fractionation. Simple two end-member mixing or Li isotopic fractionation during fluid infiltration cannot produce this large range of δ^7Li.

6. Study of a suite of prograde metamorphic rocks from the Onawa contact aureole surrounding the Onawa pluton, Maine, indicate that Li isotopic fractionation is not significant during progressive metamorphism even if a lot of Li and water have been lost.

The work done in this dissertation provides a basis for understanding Li isotopic systematics of the continental crust. However, compared with other stable isotopic systematics, many fundamental problems concerning Li isotopes are still not resolved including:

1. Lithium isotopic systematics of meteorites are not well understood. Characterizing Li in meteorites can help us not only constrain the Li isotopic composition of the bulk silicate Earth but also understand any secondary processes that occurred on meteorites since Li is fluid mobile during both weathering and metamorphism.
2. Lithium isotopic composition of the mantle is not well characterized. Only a few studies have been published on peridotites and oceanic basalts. Further studies on well-characterized peridotites and oceanic basalts are needed.
3. Lithium isotopic composition of the Archean crust is still unknown. Considering the large Li isotopic fractionation during weathering and the different nature of

Archean atmosphere and crust, Li isotopic composition of the Archean crust may be different from post Archean one and can be used to trace chemical weathering, as well as the evolution of crust.

4. Although lots of studies have been done on arc lavas, very few data are available for adakites. If adakite is produced by partial melting of subducted slabs at hot subduction zones with less interaction with overlying mantle, then they should be isotopically light relative to other arc lavas produced at cold convergent boundaries. Therefore, studies of adakite may provide us with different views about Li isotopic geochemistry and crust-mantle recycling.
5. Little is known about Li isotopic fractionation factors in different phases or minerals while only a few Li partition coefficient data are available. Both of these are important for understanding Li behavior during different processes e.g., metamorphic dehydration and granite differentiation.
6. Lithium isotopes can be greatly fractionated by diffusion. This type of Li isotopic fractionation may cause heterogeneous Li isotopic composition in zoned minerals or between minerals with different Li concentrations at high temperature. This type of isotopic heterogeneity can only be investigated by in-situ isotopic analysis. New techniques for in-situ Li isotopic analysis are strongly needed.

References

Barth M. G., McDonough W. F., and Rudnick R. L. (2000) Tracking the budget of Nb and Ta in the continental crust. *Chemical Geology* 165(3-4), 197-213.

Bea F., Pereira M. D., and Stroh A. (1994) Mineral leucosome trace-element partitioning in a peraluminous migmatite (a Laser Ablation-ICP-MS Study). *Chemical Geology* 117(1-4), 291-312.

Belshaw N. S., Freedman P. A., O'Nions R. K., Frank M., and Guo Y. (1998) A new variable dispersion double-focusing plasma mass spectrometer with performance illustrated for Pb isotopes. *International Journal of Mass Spectrometry* 181, 51-58.

Benton L. D., Ryan J. G., and Savov I. P. (2004) Lithium abundance and isotope systematics of forearc serpentinites, Conical Seamount, Mariana forearc: Insights into the mechanics of slab-mantle exchange during subduction. *Geochemistry Geophysics Geosystems* 5.

Bergantz G. W. (1991) Physical and chemical characterization of plutons. In *Contact metamorphism*, Vol. 26 (ed. D. M. Kerrick), pp. 13-42. Mineralogical Society of America.

Berger G., Schott J., and Guy C. (1988) Behavior of Li, Rb and Cs during basalt glass and olivine dissolution and chlorite, smectite and zeolite precipitation from Seawater - experimental investigations and modelization between 50 C and 300 C. *Chemical Geology* 71(4), 297-312.

Bertoldi C., Proyer A., Garbe-Schonberg D., Behrens H., and Dachs E. (2004) Comprehensive chemical analyses of natural cordierites: implications for exchange mechanisms. *Lithos* 78(4), 389-409.

Bottomley D. J., Chan L. H., Katz A., Starinsky A., and Clark I. D. (2003) Lithium isotope geochemistry and origin of Canadian Shield brines. *Ground Water* 41(6), 847-856.

Bouman C., Elliott T., and Vroon P. Z. (2004) Lithium inputs to subduction zones. *Chemical Geology* 212(1-2), 59-79.

Brenan J. M., Neroda E., Lundstrom C. C., Shaw H. F., Ryerson F. J., and Phinney D. L. (1998a) Behaviour of boron, beryllium, and lithium during melting and crystallization: constraints from mineral-melt partitioning experiments. *Geochimica et Cosmochimica Acta* 62(12), 2129-2141.

Brenan J. M., Ryerson F. J., and Shaw H. F. (1998b) The role of aqueous fluids in the slab-to-mantle transfer of boron, beryllium, and lithium during subduction: Experiments and models. *Geochimica Et Cosmochimica Acta* 62(19-20), 3337-3347.

Brigatti M. F., Lugli C., Poppi L., Foord E. E., and Kile D. E. (2000) Crystal chemical variations in Li- and Fe-rich micas from Pikes Peak batholith (central Colorado). *American Mineralogist* 85(9), 1275-1286.

Brigatti M. F., Kile D. E., and Poppi L. (2003) Crystal structure and chemistry of lithium-bearing trioctahedral micas-3T. *European Journal of Mineralogy* 15(2), 349-355.

Brown G. C. and Mussett A. E. (1993) *The inaccessible Earth: An integrated view of its structure and composition*. Chapman &Hall.

Bryant C. J., Chappell B. W., Bennett V. C., and McCulloch M. T. (2003a) Li isotopic variations in Eastern Australian granites. *Geochimica et Cosmochimica Acta* 67(18), A47-A47.

Bryant C. J., McCulloch M. T., and Bennett V. C. (2003b) Impact of matrix effects on the accurate measurement of Li isotope ratios by inductively coupled plasma mass spectrometry (MC-ICP-MS) under "cold" plasma conditions. *J. Anal. At. Spectrom* 18, 734-737.

Bryant C. J., Bennett V. C., Chappell B. W., and Mcculloch M. T. (2004a) Lithium isotopes in crustal rocks: a case study of the New England Batholith, southeastern Australia. *Submitted to Geochimica Cosmica et Acta*.

Bryant C. J., Chappell B. W., Bennett V. C., and McCulloch M. T. (2004b) Lithium isotopic composition of the New England Batholith: correlations with inferred source rock compositions. *Transactions of the Royal Society of Edinburgh-Earth Sciences* 95, 199-214.

Candela P. A. and Piccoli P. M. (1995) Model ore-metal partitioning from melts into vapor and vapor/brine mixtures. In *Granites, Fluids, and Ore Deposits*, Vol. 23 (ed. J. F. H. Thompson), pp. 101-128. Mineralogical Association of Canada.

Chacko T., Cole D. R., and Horita J. (2001) Equilibrium oxygen, hydrogen and carbon isotope fractionation factors applicable to geological systems. In *Stable isotope geochemistry*, Vol. 43 (ed. J. W. Valley and D. R. Cole), pp. 1-82. Mineralogical Society of America, Washington, DC.

Chan L. H. (1987) Lithium Isotope Analysis by Thermal Ionization Mass- Spectrometry of Lithium Tetraborate. *Analytical Chemistry* 59(22), 2662-2665.

Chan L. H. and Edmond J. M. (1988) Variation of lithium isotope composition in the marine-environment - a preliminary-report. *Geochimica et Cosmochimica Acta* 52(6), 1711-1717.

Chan L. H., Edmond J. M., Thompson G., and Gillis K. (1992) Lithium isotopic composition of submarine basalts: implications for the lithium cycle in the oceans. *Earth and Planetary Science Letters* 108(1-3), 151-160.

Chan L. H., Edmond J. M., and Thompson G. (1993) A lithium isotope study of hot-springs and metabasalts from Mid-Ocean ridge hydrothermal systems. *Journal of Geophysical Research-Solid Earth* 98(B6), 9653-9659.

Chan L. H., Gieskes J. M., You C. F., and Edmond J. M. (1994) Lithium isotope geochemistry of sediments and hydrothermal fluids of the Guaymas Basin, Gulf of California. *Geochimica et Cosmochimica Acta* 58(20), 4443-4454.

Chan L. H., Alt J. C., and Teagle D. A. H. (2002a) Lithium and lithium isotope profiles through the upper oceanic crust: a study of seawater-basalt exchange at ODP Sites 504B and 896A. *Earth and Planetary Science Letters* 201(1), 187-201.

Chan L. H., Leeman W. P., and You C. F. (2002b) Lithium isotopic composition of Central American volcanic arc lavas: implications for modification of subarc mantle by slab- derived fluids: correction. *Chemical Geology* 182(2-4), 293-300.

Chan L. H. and Frey F. A. (2003) Lithium isotope geochemistry of the Hawaiian plume: Results from the Hawaii Scientific Drilling Project and Koolau volcano. *Geochemistry Geophysics Geosystems* 4, art. no.-8707.

Chan L. H. (2004) Mass spectrometric techniques for the determination of lithium isotopic composition in geological material. In *Handbook of Stable Isotope Analytical Techniques*, Vol. 1 (ed. P. A. De Groot), pp. 122-141. Elsevier.

Chan L.-H. and Kastner M. (2000) Lithium isotopic compositions of pore fluids and sediments in the Costa Rica subduction zone: implications for fluid processes and

sediment contribution to the arc volcanoes. *Earth and Planetary Science Letters* 183(1-2), 275-290.

Chappell B. W. and White A. J. R. (1974) Two contrasting granite types. *Pacific Geology* 8, 173-174.

Chappell B. W. (1984) Source rocks of I-type and S-type granites in the Lachlan Fold Belt, southeastern Australia. *Philosophical Transactions of the Royal Society of London Series a-Mathematical Physical and Engineering Sciences* 310(1514), 693-707.

Chappell B. W. and White A. J. R. (1992) I-type and S-type granites in the Lachlan Fold Belt. *Transactions of the Royal Society of Edinburgh-Earth Sciences* 83, 1-26.

Chappell B. W., White A. J. R., Williams I. S., Wyborn D., and Wyborn L. A. I. (2000) Lachlan Fold Belt granites revisited: high- and low-temperature granites and their implications. *Australian Journal of Earth Sciences* 47(1), 123-138.

Chaussidon M. and Robert F. (1998) 7Li/6Li and 11B/10B variations in chondrules from the Semarkona unequilibrated chondrite. *Earth and Planetary Science Letters* 164(3-4), 577-589.

Clarke F. W. (1889) The relative abundance of chemical elements. *Philosophical Society of Washington Bulletin* X1, 131-142.

Clarke F. W. and Washington H. S. (1924) The composition of the Earth's crust. *U.S.G.S. Prof. Paper*, 127.

Clarke P. T. and Spink J. M. (1969) Crystal structure of Beta spodumene, LiAlSi2O6-Li. *Zeitschrift Fur Kristallographie Kristallgeometrie Kristallphysik Kristallchemie* 130(4-6), 420-&.

Cole D. R. and Chakraborty S. (2001) Rates and mechanisms of isotopic exchange. In *Stable isotope geochemistry*, Vol. 43 (ed. J. W. Valley and D. R. Cole), pp. 83-224. The Mineralogical Society of America.

Coogan L. A., Kasemann S. A., and Chakraborty S. (2005) Rates of hydrothermal cooling of new oceanic upper crust derived from lithium-geospeedometry. *Earth and Planetary Science Letters* in press.

Crank J. (1975) *The mathematics of diffusion*. Clarendon Press.

Datta B. P., Khodade P. S., Parab A. R., Goyal A. H., Chitambar S. A., and Jain H. C. (1992) Thermal Ionization Mass-Spectrometry of Li2bo2+ Ions - Determination of the Isotopic Abundance Ratio of Lithium (Int J Mass Spectrom Ion Proc, Vol 116, Pg 87, 1992). *International Journal of Mass Spectrometry and Ion Processes* 121(3), 247-247.

Decitre S., Deloule E., Reisberg L., James R., Agrinier P., and Mevel C. (2002) Behavior of Li and its isotopes during serpentinization of oceanic peridotites. *Geochemistry Geophysics Geosystems* 3.

Dostal J., Dupuy C., and Leyreloup A. (1980) Geochemistry and Petrology of Meta-Igneous Granulitic Xenoliths in Neogene Volcanic-Rocks of the Massif Central, France - Implications for the Lower Crust. *Earth and Planetary Science Letters* 50(1), 31-40.

Downes H., Bodinier J. L., Dupuy C., Leyreloup A., and Dostal J. (1989) Isotope and Trace-Element Heterogeneities in High-Grade Basic Metamorphic Rocks of Marvejols - Tectonic Implications for the Hercynian Suture Zone of the French Massif Central. *Lithos* 24(1), 37-54.

Duke E. F., Shearer C. K., Redden J. A., and Papike J. J. (1990) Proterozoic granite-pegmatite magmatism, Black Hills, South Dakota: Structure and geochemical zonation. In *Tthe Trans-Hudson Orogen* (ed. J. F. Lewry and M. R. Stauffer), pp. 253-269. Geol. Assoc. Canda Spec. Paper 37.

Dutrow B. L., Holdaway M. J., and Hinton R. W. (1986) Lithium in staurolite and its petrologic significance. *Contributions to Mineralogy and Petrology* 94, 496-506.

Edmond J. M., Measures C., McDuff R. E., Chan L. H., Collier R., Grant B., Gordon L. I., and Corliss J. B. (1979) Ridge Crest Hydrothermal Activity and the Balances of the Major and Minor Elements in the Ocean - Galapagos Data. *Earth and Planetary Science Letters* 46(1), 1-18.

Eiler J. M. (2001) Oxygen isotope variation of basaltic lavas and upper mantle rocks. In *Stable isotope geochemistry*, Vol. 43 (ed. J. W. Valley and D. R. Cole), pp. 319-364. Mineralogical Society of America.

Elliott T., Jeffcoate A. B., and Bouman C. (2004) The terrestrial Li isotope cycle: light-weight constrains on mantle convection. *Earth and Planetary Science Letters* 220, 231-245.

Evensen J. M. and London D. (2003) Experimental partitioning of Be, Cs, and other trace elements between cordierite and felsic melt, and the chemical signature of S-type granite. *Contributions to Mineralogy and Petrology* 144(6), 739-757.

Ferry J. M., Wing B. A., and Rumble III D. (2001) Formation of wollastonite by chemically reactive fluid flow during contact metamorphism, Mt. Morrison Pendant, Sierra Nevada, California, USA. *Journal of Petrology* 42(9), 1705-1728.

Flesch G. D., Anderson A. R. J., and Svec H. J. (1973) A secondary isotopic standard for 6Li/7Li determinations. *Int. J. Mass Spectrom. Ion Proc.* 12(265-272).

Flint R. F. (1947) *Glacial geology and the Pleistocene epoch.* John Wiley and Sons. Inc.

Foustoukos D. I., James R. H., Berndt M. E., and Seyfried J., W.E. (2004) Lithium isotopic systematics of hydrothermal vent fluids at the Main Endeavour Field, Northern Juan de Fuca Ridge. *Chemical Geology* 212(1-2), 17-26.

Gallet S., Jahn B. M., Lanoe B. V., Dia A., and Rossello E. (1998) Loess geochemistry and its implications for particle origin and composition of the upper continental crust. *Earth and Planetary Science Letters* 156(3-4), 157-172.

Gao S., Zhang B. R., Xie Q. L., Gu X. M., Ouyang J. P., Wang D. P., and Gao C. G. (1991) Average chemical-compositions of Post-Archean sedimentary and volcanic-rocks from the Qinling Orogenic Belt and its adjacent North China and Yangtze Cratons. *Chemical Geology* 92(4), 261-282.

Gao S., Zhang B. R., Luo T. C., Li Z. J., Xie Q. L., Gu X. M., Zhang H. F., Ouyang J. P., Wang D. P., and Gao C. L. (1992) Chemical-composition of the continental-crust in the Qinling Orogenic Belt and its adjacent North China and Yangtze Cratons. *Geochimica et Cosmochimica Acta* 56(11), 3933-3950.

Gao S., Zhang B. R., Wang D. P., Ouyang J. P., and Xie Q. L. (1996) Geochemical evidence for the Proterozoic tectonic evolution of the Qinling orogenic belt and its adjacent margins of the north China and Yangtze cratons. *Precambrian Research* 80(1-2), 23-48.

Gao S., Luo T. C., Zhang B. R., Zhang H. F., Han Y. W., Zhao Z. D., and Hu Y. K. (1998) Chemical composition of the continental crust as revealed by studies in East China. *Geochimica et Cosmochimica Acta* 62(11), 1959-1975.

Giletti B. J. and Shanahan T. M. (1997) Alkali diffusion in plagioclase feldspar. *Chemical Geology* 139(1-4), 3-20.

Green L. W., Leppinen J. J., and Elliot N. L. (1988) Isotopic Analysis of Lithium as Thermal Dilithium Fluoride Ions. *Analytical Chemistry* 60(1), 34-37.

Gregoire D. C., Acheson B. M., and Taylor R. P. (1996) Measurement of lithium isotope ratios by inductively coupled plasma mass spectrometry: Application to geological materials. *Journal of Analytical Atomic Spectrometry* 11(9), 765-772.

Gurenko A. A., Trumbull R. B., Thomas R., and Lindsay J. M. (2005) A melt inclusion record of volatiles, trace elements and Li-B isotope variations in a single magma system from the Plat Pays Volcanic Complex, Dominica, Lesser Antilles. *Journal of Petrology* 46(12), 2495-2526.

Hall J. M. (2005) Foraminiferal lithium as a paleoceanographic proxy. *Geochimica Et Cosmochimica Acta* 69(10), A128-A128.

Heier K. S. and Adams J. A. S. (1964) The geochemistry of the alkali metals. *Physics and Chemistry of the Earth* V, 253-381.

Hervig R. L., Bell D. R., Moore G., Williams L. B., Yamamoto J., and Buseck P. R. (2004) SIMS analysis for Li isotopic ratios: From olivine to clay minerals. *ESO 85 (47), Abstr. V51C-0593*.

Hoefs J. and Sywall M. (1997) Lithium isotope composition of Quaternary and Tertiary biogene carbonates and a global lithium isotope balance. *Geochimica et Cosmochimica Acta* 61(13), 2679-2690.

Hogan J. F. and Blum J. D. (2003) Boron and lithium isotopes as groundwater tracers: a study at the Fresh Kills Landfill, Staten Island, New York, USA. *Applied Geochemistry* 18(4), 615-627.

Holland H. D. (1984) *The chemical Evolution of the Atmosphere and Oceans.* Princeton University Press.

Huh Y., Chan L.-H., Zhang L., and Edmond J. M. (1998) Lithium and its isotopes in major world rivers: implications for weathering and the oceanic budget. *Geochimica et Cosmochimica Acta* 62(12), 2039-2051.

Huh Y., Chan L.-H., and Edmond J. M. (2001) Lithium isotopes as a probe of weathering processes: Orinoco River. *Earth and Planetary Science Letters* 194(1-2), 189-199.

Huh Y., Chan L. H., and Chadwick O. A. (2004) Behavior of lithium and its isotopes during weathering of Hawaiian basalt. *Geochemistry Geophysics Geosystems* 5(9).

Icenhower J. and London D. (1995) An experimental study of element partitioning among biotite, muscovite, and coexisting peraluminous silicic melt at 200 MPa (H_2O). *American Mineralogist* 80(11-12), 1229-1251.

Jagoutz E., Palmer H., Baddenhausen H., Blum K., Cendales M., Dreibus G., Spettel B., Lorenz V., and Wanke H. (1979) The abundances of major, minor and trace elements in the earth's mantle as derived from primitive ultramafic nodules. *Proc. 10th Lunar Planet. Sci. Conf.*, 2031-2050.

Jahn B. M., Wu F. Y., Capdevila R., Martineau F., Zhao Z. H., and Wang Y. X. (2001) Highly evolved juvenile granites with tetrad REE patterns: the Woduhe and Baerzhe granites from the Great Xing'an Mountains in NE China. *Lithos* 59(4), 171-198.

James R. H., Rudnicki M. D., and Palmer M. R. (1999) The alkali element and boron geochemistry of the Escanaba Trough sediment-hosted hydrothermal system. *Earth and Planetary Science Letters* 171(1), 157-169.

James R. H. and Palmer M. R. (2000) The lithium isotope composition of international rock standards. *Chemical Geology* 166(3-4), 319-326.

James R. H., Allen D. E., and Seyfried W. E., Jr. (2003) An experimental study of alteration of oceanic crust and terrigenous sediments at moderate temperatures (51 to 350 ^{o}C): Insights as to chemical processes in near-shore ridge-flank hydrothermal systems. *Geochimica et Cosmochimica Acta* 67(4), 681-691.

Jeffcoate A. B., Elliott T., Thomas A., and Bouman C. (2004a) Precise, small sample size determinations of lithium isotopic compositions of geological reference materials and modern seawater by MC-ICP-MS. *Geostandards and Geoanalytical Research* 28(1), 161-172.

Jeffcoate A. B., Kasemann S. A., and Elliott T. (2004b) High-spatial resolution lithium isotope variation in mantle minerals. *Geochimica et Cosmochimica Acta* 68(11), A52-A52.

Johnson D. D., Hooper P. R., and Conrey R. M. (1999) XRF analysis of rocks and minerals for major and trace elements on a single low dilution Li-tetraborate fused bead. *Advances in X-ray analysis* 41, 843-867.

Jost W. (1960) *Diffusion in Solids, Liquids, and Gases*. Academic Press.

Kasemann S. A., Jeffcoate A. B., and Elliott T. (2005) Lithium isotope composition of basalt glass reference material. *Analytical Chemistry* 77(16), 5251-5257.

Kempton P. D. and Harmon R. S. (1992) Oxygen Isotope Evidence for Large-Scale Hybridization of the Lower Crust During Magmatic Underplating. *Geochimica Et Cosmochimica Acta* 56(3), 971-986.

Kisakurek B., Widdowson M., and James R. H. (2004) Behaviour of Li isotopes during continental weathering: The Bidar laterite profile, India. *Chemical Geology* 212(1-2), 27-44.

Klossa B., Pierre A., and Minster J.-F. (1981) Mesures de la composition isotopique du lithium dans les inclusions refractaires d'Allende. *Earth and Planetary Science Letters* 52(1), 25-30.

Kobayashi K., Tanaka R., Moriguti T., Shimizu K., and Nakamura E. (2004) Lithium, boron, and lead isotope systematics of glass inclusions in olivines from Hawaiian lavas: evidence for recycled components in the Hawaiian plume. *Chemical Geology* 212(1-2), 143-161.

Kogiso T., Tatsumi Y., and Nakano S. (1997) Trace element transport during dehydration processes in the subducted oceanic crust .1. Experiments and implications for the origin of ocean island basalts. *Earth and Planetary Science Letters* 148(1-2), 193-205.

Koirtyohann S. R. (1994) Precise Determination of Isotopic-Ratios for Some Biologically Significant Elements by Inductively-Coupled Plasma-Mass Spectroscopy. *Spectrochimica Acta Part B-Atomic Spectroscopy* 49(12-14), 1305-1311.

Kosler J., Kucera M., and Sylvester P. (2001) Precise measurement of Li isotopes in planktonic foraminiferal tests by quadrupole ICPMS. *Chemical Geology* 181(1-4), 169-179.

Krankowsky D. and Muller O. (1967) Isotopic composition and abundance of lithium in meteoritic matter. *Geochimica et Cosmochimica Acta* 31(10), 1833-1842.

Krogstad E. J., Walker R. J., Nabelek P. I., and Russnabelek C. (1993) Lead isotopic evidence for mixed sources of Proterozoic granites and pegmatites, Black-Hills, South-Dakota, USA. *Geochimica et Cosmochimica Acta* 57(19), 4677-4685.

Krogstad E. J. and Walker R. J. (1996) Evidence of heterogeneous crustal sources: The Harney peak granite, South Dakota, USA. *Transactions of the Royal Society of Edinburgh-Earth Sciences* 87, 331-337.

Labotka T. C. (1991) Chemical and physical properties of fluids. In *Contact metamorphism*, Vol. 26 (ed. D. M. Kerrick), pp. 43-104. Mineralogical Society of America.

Laul J. C., Walker R. J., Shearer C. K., Papike J. J., and Simon S. B. (1984) Chemical migration by contact metamorphism between pegmatite and country rocks: Natural analogs for radionuclide migration. *Material Research Society Symposium Proceedings* 26, 951-958.

Leeman W. P., Sisson V. B., and Reid M. R. (1992) Boron Geochemistry of the Lower Crust - Evidence from Granulite Terranes and Deep Crustal Xenoliths. *Geochimica Et Cosmochimica Acta* 56(2), 775-788.

Leeman W. P., Tonarini S., Chan L. H., and Borg L. E. (2004) Boron and lithium isotopic variations in a hot subduction zone - the southern Washington Cascades. *Chemical Geology* 212(1-2), 101-124.

Leyreloup A., Dupuy C., and Andriambololona R. (1977) Catazonal Xenoliths in French Neogene Volcanic-Rocks - Constitution of Lower Crust .2. Chemical Composition and Consequences of Evolution of French Massif Central Precambrian Crust. *Contributions to Mineralogy and Petrology* 62(3), 283-300.

Li C. T. and Peacor D. R. (1968) Crystal structure of $LiAlSi_2O_6$-2 (β Spodumene). *Zeitschrift Fur Kristallographie Kristallgeometrie Kristallphysik Kristallchemie* 126(1-3), 46-&.

Liu Y. S., Gao S., Jin S. Y., Hu S. H., Sun M., Zhao Z. B., and Feng J. L. (2001) Geochemistry of lower crustal xenoliths from Neogene Hannuoba Basalt, North China Craton: Implications for petrogenesis and lower crustal composition. *Geochimica et Cosmochimica Acta* 65(15), 2589-2604.

Liu Y. S., Gao S., Yuan H. L., Zhou L., Liu X. M., Wang X. C., Hu Z. C., and Wang L. S. (2004) U-Pb zircon ages and Nd, Sr, and Pb isotopes of lower crustal xenoliths from North China Craton: insights on evolution of lower continental crust. *Chemical Geology* 211(1-2), 87-109.

London D., Hervig R. L., and Morgan G. B. (1988) Melt-vapor solubilities and elemental partitioning in peraluminous granite-pegmatite systems - experimental results with Macusani Glass at 200 MPa. *Contributions to Mineralogy and Petrology* 99(3), 360-373.

London D. (2005) Granitic pegmatites: an assessment of current concepts and directions for the future. *Lithos* 80(1-4), 281-303.

Lundstrom C. C. (2003) An experimental investigation of the diffusive infiltration of alkalis into partially molten peridotite: Implications for mantle melting processes. *Geochemistry Geophysics Geosystems* 4(9).

Lundstrom C. C., Chaussidon M., Hsui A. T., Kelemen P., and Zimmerman M. (2005) Observations of Li isotopic variations in the Trinity Ophiolite: Evidence for isotopic fractionation by diffusion during mantle melting. *Geochimica et Cosmochimica Acta* 69(3), 735-751.

Lynton S. J., Walker R. J., and Candela P. A. (2005) Lithium isotopes in the system Qz-Ms-fluid:An experimental study. *Geochimica et Cosmochimica Acta* 69(13), 3337-3347.

Magna T., Wiechert U. H., and Halliday A. N. (2004) Low-blank isotope ratio measurement of small samples of lithium using multiple-collector ICPMS. *International Journal of Mass Spectrometry* 239(1), 67-76.

Marchildon N. and Brown M. (2001) Melt segregation in late syn-tectonic anatectic migmatites: An example from the Onawa contact aureole, Maine, USA. *Physics and Chemistry of the Earth Part a-Solid Earth and Geodesy* 26(4-5), 225-229.

McDonough W. F. and Sun S. S. (1995) The Composition of the Earth. *Chemical Geology* 120(3-4), 223-253.

McLennan S. M. (1993) Weathering and global denudation. *Journal of Geology* 101(2), 295-303.

McLennan S. M. (2001) Relationships between the trace element composition of sedimentary rocks and upper continental crust. *Geochemistry Geophysics Geosystems* 2, art. no.-2000GC000109.

Mengel K. (1990) Crustal Xenoliths from Tertiary Volcanics of the Northern Hessian Depression - Petrological and Chemical Evolution. *Contributions to Mineralogy and Petrology* 104(1), 8-26.

Mengel K. and Hoefs J. (1990) Li-Delta-O-18-Sio2 Systematics in Volcanic-Rocks and Mafic Lower Crustal Granulite Xenoliths. *Earth and Planetary Science Letters* 101(1), 42-53.

Michiels E. and Debievre P. (1983) Absolute Isotopic Composition and the Atomic Weight of a Natural Sample of Lithium. *International Journal of Mass Spectrometry and Ion Processes* 49(2), 265-274.

Moriguti T. and Nakamura E. (1993) Precise Lithium Isotopic Analysis by Thermal Ionization Mass-Spectrometry Using Lithium Phosphate as an Ion-Source Material. *Proceedings of the Japan Academy Series B-Physical and Biological Sciences* 69(6), 123-128.

Moriguti T. and Nakamura E. (1998a) Across-arc variation of Li isotopes in lavas and implications for crust/mantle recycling at subduction zones. *Earth and Planetary Science Letters* 163(1-4), 167-174.

Moriguti T. and Nakamura E. (1998b) High-yield lithium separation and the precise isotopic analysis for natural rock and aqueous samples. *Chemical Geology* 145(1-2), 91-104.

Moriguti T., Shibata T., and Nakamura E. (2004) Lithium, boron and lead isotope and trace element systematics of Quaternary basaltic volcanic rocks in northeastern Japan: mineralogical controls on slab-derived fluid composition. *Chemical Geology* 212(1-2), 81-100.

Nabelek P. I., Rusnabelek C., and Denison J. R. (1992a) The generation and crystallization conditions of the Proterozoic Harney Peak leukogranite, Black Hills, South-Dakota, USA - petrologic and geochemical constraints. *Contributions to Mineralogy and Petrology* 110(2-3), 173-191.

Nabelek P. I., Russnabelek C., and Haeussler G. T. (1992b) Stable isotope evidence for the petrogenesis and fluid evolution in the Proterozoic Harney Peak leukogranite, Black-Hills, South-Dakota. *Geochimica et Cosmochimica Acta* 56(1), 403-417.

Nabelek P. I. and Bartlett C. D. (1998) Petrologic and geochemical links between the post-collisional Proterozoic Harney Peak leucogranite, South Dakota, USA, and its source rocks. *Lithos* 45(1-4), 71-85.

Nance W. B. and Taylor S. R. (1976) Rare-earth element patterns and crustal evolution .1. Australian Post-Archean sedimentary-rocks. *Geochimica et Cosmochimica Acta* 40(12), 1539-1551.

Nesbitt H. W. and Young G. M. (1982) Early Proterozoic climates and plate Motions inferred from major element chemistry of lutites. *Nature* 299(5885), 715-717.

Neves L. (1997) Trace element content and partitioning between biotite and muscovite of granitic rocks: a study in the Viseu region (Central Portugal). *European Journal of Mineralogy* 9(4), 849-857.

Nishio Y. and Nakai S. (2002) Accurate and precise lithium isotopic determinations of igneous rock samples using multi-collector inductively coupled plasma mass spectrometry. *Analytica Chimica Acta* 456(2), 271-281.

Njo H. B., Rudnick R. L., and Tomascak P. B. (2003) Lithium isotopic fractionation during continental weathering. *13th V. M. Goldschmidt Conference. Kurashiki, Japan.*

Norton J. J. and Redden J. A. (1990) Relations of zoned pegmatites to other pegmatites, granite, and metamorphic rocks in the southern Black Hills, South Dakota. *American Mineralogist* 75, 631-655.

Oi T., Odagiri T., and Nomura M. (1997) Extraction of lithium from GSJ rock reference samples and determination of their lithium isotopic compositions. *Analytica Chimica Acta* 340(1-3), 221-225.

Olive K. A. and Schramm D. N. (1992) Astrophysical Li-7 as a Product of Big-Bang Nucleosynthesis and Galactic Cosmic-Ray Spallation. *Nature* 360(6403), 439-442.

O'Neil J. R. and Chappell B. W. (1977) Oxygen and hydrogen isotopic relations in the Berridale batholith. *Journal of the Geological Society of London* 133, 559-571.

Peppard D. F., Mason G. W., and Lewey S. (1969) A tetrad effect in liquid-liquid extraction ordering of lanthanides(3). *Journal of Inorganic & Nuclear Chemistry* 31(7), 2271-&.

Pereira M. D. and Shaw D. M. (1996) B and Li distribution in the Pena Negra complex: An alpha-track study. *American Mineralogist* 81(1-2), 141-145.

Peucker-Ehrenbrink B. and Jahn B. M. (2001) Rhenium-osmium isotope systematics and platinum group element concentrations: Loess and the upper continental crust. *Geochemistry Geophysics Geosystems* 2.

Philbrick S. S. (1936) The contact metamorphism of the Onawa pluton, Piscatquis County, Maine. *American Journal of Science* 31, 1-40.

Pistiner J. S. and Henderson G. M. (2003) Lithium-isotope fractionation during continental weathering processes. *Earth and Planetary Science Letters* 214(1-2), 327-339.

Qi H. P., Taylor P. D. P., Berglund M., and De Bievre P. (1997) Calibrated measurements of the isotopic composition and atomic weight of the natural Li isotopic reference material IRMM-016. *International Journal of Mass Spectrometry* 171(1-3), 263-268.

Ratte J. C. and Zartman R. E. (1975) Bear Mountain gneiss dome, Black Hills, South Dakota. *Geol. Surv. Amer. Abstr. Progs.* 2(5), 345.

Redden J. A., Norton J. J., and McLaughlin R. J. (1985) Geology of the Harney Peak granite, Black Hills, South Dakota. In *Geology of the Black Hills, South Dakota and Wyoming* (ed. F. J. Rich), pp. 225-240. Amer. Geol. Inst.

Richter F. M., Liang Y., and Davis A. M. (1999) Isotope fractionation by diffusion in molten oxides. *Geochimica et Cosmochimica Acta* 63(18), 2853-2861.

Richter F. M., Davis A. M., DePaolo D. J., and Watson E. B. (2003) Isotope fractionation by chemical diffusion between molten basalt and rhyolite. *Geochimica et Cosmochimica Acta* 67(20), 3905-3923.

Robert J. L., Volfinger M., Barrandon J. N., and Basutcu M. (1983) Lithium in the interlayer space of synthetic trioctahedral micas. *Chemical Geology* 40(3-4), 337-351.

Rudnick R. L., Mcdonough W. F., Mcculloch M. T., and Taylor S. R. (1986) Lower Crustal Xenoliths from Queensland, Australia - Evidence for Deep Crustal Assimilation and Fractionation of Continental Basalts. *Geochimica et Cosmochimica Acta* 50(6), 1099-1115.

Rudnick R. L. and Taylor S. R. (1987) The Composition and Petrogenesis of the Lower Crust - a Xenolith Study. *Journal of Geophysical Research-Solid Earth and Planets* 92(B13), 13981-14005.

Rudnick R. L. and Williams I. S. (1987) Dating the Lower Crust by Ion Microprobe. *Earth and Planetary Science Letters* 85(1-3), 145-161.

Rudnick R. L. (1990) Nd and Sr Isotopic Compositions of Lower-Crustal Xenoliths from North Queensland, Australia - Implications for Nd Model Ages and Crustal Growth-Processes. *Chemical Geology* 83(3-4), 195-208.

Rudnick R. L. and Goldstein S. L. (1990) The Pb Isotopic Compositions of Lower Crustal Xenoliths and the Evolution of Lower Crustal Pb. *Earth and Planetary Science Letters* 98(2), 192-207.

Rudnick R. L. and Taylor S. R. (1991) Petrology and geochemistry of lower crustal xenoliths from northern Queensland and inferences on lower crustal composition. In *The Australian Lithosphere* (ed. B. Drummond), pp. 189-208. Spec. Publ. Geol. Soc. Aust.

Rudnick R. L. (1992) Xenoliths - Samples of the lower continental crust. In *Continental Lower Crust* (ed. D. M. Fountain, R. J. Arculus, and R. W. Kay), pp. 269-316. Elsevier Sci.

Rudnick R. L. and Fountain D. M. (1995) Nature and composition of the continental-crust - a lower crustal perspective. *Reviews of Geophysics* 33(3), 267-309.

Rudnick R. L. and Gao S. (2003) Composition of the continental crust. In *The Crust*, Vol. 3 (ed. R. L. Rudnick), pp. 1-64. Elsevier, Oxford.

Rudnick R. L., Tomascak P. B., Njo H. B., and Gardner L. R. (2004) Extreme lithium isotopic fractionation during continental weathering revealed in saprolites from South Carolina. *Chemical Geology* 212(1-2), 45-57.

Ryan J. G. and Langmuir C. H. (1987) The systematics of lithium abundances in young volcanic-rocks. *Geochimica et Cosmochimica Acta* 51(6), 1727-1741.

Ryan J. G. and Kyle P. R. (2004) Lithium abundance and lithium isotope variations in mantle sources: insights from intraplate volcanic rocks from Ross Island and Marie Byrd Land (Antarctica) and other oceanic islands. *Chemical Geology* 212(1-2), 125-142.

Saal A. E., Rudnick R. L., Ravizza G. E., and Hart S. R. (1998) Re-Os isotope evidence for the composition, formation and age of the lower continental crust. *Nature* 393(6680), 58-61.

Sahoo S. K. and Masuda A. (1998) Precise determination of lithium isotopic composition by thermal ionization mass spectrometry in natural samples such as seawater. *Analytica Chimica Acta* 370(2-3), 215-220.

Sartbaeva A., Wells S. A., and Redfern S. A. T. (2004) Li^+ ion motion in quartz and beta-eucryptite studied by dielectric spectroscopy and atomistic simulations. *Journal of Physics-Condensed Matter* 16(46), 8173-8189.

Seitz H.-M., Brey G. P., Lahaye Y., Durali S., and Weyer S. (2004) Lithium isotopic signatures of peridotite xenoliths and isotopic fractionation at high temperature between olivine and pyroxenes. *Chemical Geology* 212(1-2), 163-177.

Seyfried Jr. W. E., Janecky D. R., and Mottl M. J. (1984) Alteration of the oceanic crust: Implications for geochemical cycles of lithium and boron. *Geochimica et Cosmochimica Acta* 48(3), 557-569.

Seyfried Jr. W. E., Chen X., and Chan L.-H. (1998) Trace element mobility and lithium isotope exchange during hydrothermal alteration of seafloor weathered basalt: An experimental study at 350 ^{o}C, 500 bars. *Geochimica et Cosmochimica Acta* 62(6), 949-960.

Shaw D. M., Reilly G. A., Muysson J. R., Pattenden G. E., and Campbell F. E. (1967) The chemical composition of the Canadian Precambrian shield. *Can. J. Earth Sci.* 4, 829-854.

Shaw D. M., Dostal J., and Keays R. R. (1976) Additional estimates of continental surface Precambrian shield composition in Canadian Precambrian Shield. *Canadian Journal of Earth Sciences* 4, 829-853.

Shaw D. M., Cramer J. J., Higgins M. D., and Truscott M. G. (1986) Composition of the Canadian Precambrian Shield and the continental crust of the Earth. In The nature of the LCC (ed. J. B. Dawson et al.).

Shaw D. M., Dickin A. P., Li H., McNutt R. H., Schwarcz H. P., and Truscotte M. G. (1994) Crustal geochemistry in the Wawa-Foleyet region, Ontario. *Canadian Journal of Earth Sciences* 31(7), 1104-1121.

Shearer C. K., Papike J. J., and Laul J. C. (1987a) Mineralogical and chemical evolution of a rare-element granite-pegmatite system - Harney Peak Granite, Black Hills, South-Dakota. *Geochimica et Cosmochimica Acta* 51(3), 473-486.

Shearer C. K., Papike J. J., Redden J. A., Simon S. B., Walker R. J., and Laul J. C. (1987b) Origin of pegmatitic granite segregations, Willow Creek, Black Hills, South-Dakota. *Canadian Mineralogist* 25, 159-171.

Sirbescu M. L. C. and Nabelek P. I. (2003a) Crystallization conditions and evolution of magmatic fluids in the Harney Peak Granite and associated pegmatites, Black Hills, South Dakota - Evidence from fluid inclusions. *Geochimica et Cosmochimica Acta* 67(13), 2443-2465.

Sirbescu M. L. C. and Nabelek P. I. (2003b) Crustal melts below 400 ^{o}C. *Geology* 31(8), 685-688.

Smalley I. J. and Cabrera J. G. (1970) The shape and surface texture of loess particles. *Geol. Soc. Am. Bull.* 81, 1591-1595.

Soltay L. G. and Henderson G. S. (2005a) Structural differences between lithium silicate and lithium germanate glasses by Raman Spectroscopy. *Physics and Chemistry of Glasses*, in press.

Soltay L. G. and Henderson G. S. (2005b) The structure of lithium containing silicate and germanate glasses. *Canadian Mineralogist*, in press.

Spera F. J. (1980) Aspects of magma transport. In *Physics of magmatic processes* (ed. R. B. Hargraves), pp. 265-323. Princeton Univ. Press.

Sun X. F., Ting B. T. G., Zeisel S. H., and Janghorbani M. (1987) Accurate Measurement of Stable Isotopes of Lithium by Inductively Coupled Plasma Mass-Spectrometry. *Analyst* 112(9), 1223-1228.

Svec H. J. and Anderson A. R. J. (1965) The absolute abundance of the lithium isotopes in natural sources. *Geochimica et Cosmochimica Acta* 29(6), 633-641.

Symmes G. H. and Ferry J. M. (1995) Metamorphism, fluid-flow and partial melting in pelitic rocks from the Onawa contact aureole, Central Maine, USA. *Journal of Petrology* 36(2), 587-612.

Taylor S. R. (1964) Abundance of chemical elements in the continental crust: a new table. *Geochimica et Cosmochimica Acta* 28, 1273-1285.

Taylor S. R., McLennan S. M., and McCulloch M. T. (1983) Geochemistry of loess, continental crustal composition and crustal model ages. *Geochimica et Cosmochimica Acta* 47(11), 1897-1905.

Taylor S. R. and McLennan S. M. (1985) The continental crust: its composition and evolution. Blackwell, Oxford, 312 pp.

Taylor S. R. and McLennan S. M. (1995) The geochemical evolution of the continental-crust. *Reviews of Geophysics* 33(2), 241-265.

Teng F.-Z., McDonough W. F., Rudnick R. L., Dalpe C., Tomascak P. B., Chappell B. W., and Gao S. (2004a) Lithium isotopic composition and concentration of the upper continental crust. *Geochimica et Cosmochimica Acta* 68(20), 4181-4192.

Teng F.-Z., McDonough W. F., Rudnick R. L., and Gao S. (2004b) Lithium isotopic composition of the deep continental crust. *EOS 85 (47), Abstr. V51C-0597*.

Teng F.-Z., McDonough W. F., Rudnick R. L., and Walker R. J. (2005a) Lithium isotopic systematics of granites and pegmatites from the Black Hills, South Dakota. *American Mineralogist*, in review.

Teng F.-Z., McDonough W. F., Rudnick R. L., and Walker R. J. (2005b) Diffusion-driven extreme lithium isotopic fractionation in country rocks of the Tin Mountain pegmatite. *Earth and Planetary Science Letters*, in review.

Teng F.-Z., McDonough W. F., Rudnick R. L., and Wing B. A. (2005c) Lack of lithium isotopic fractionation during progressive metamorphic dehydration in metapelite: A case study from the Onawa contact aureole, Maine. *Chemical Geology*, in review.

Tera F., Eugster O., Burnett D. S., and G.J. W. (1970) Comparative study of Li, Na, K, Rb, Cs, Ca, Sr and Ba abundances in achondrites and in Apollo 11 lunar samples. *Proceedings of the Apollo 11 Lunar Science Conference* 2, 1637-1657.

Tomascak P. B., Lynton S. J., Walker R. J., and E.J. K. (1995) Li isotope geochemistry of the Tin Mountain pegmatite, Black Hills, South Dakota. *In: The Origin of Granites and related Rocks. Brown. M, Piccoli PM (eds) US Geol Surv Circ 1129: 151-152.*

Tomascak P. B., Carlson R. W., and Shirey S. B. (1999a) Accurate and precise determination of Li isotopic compositions by multi-collector sector ICP-MS. *Chemical Geology* 158(1-2), 145-154.

Tomascak P. B. and Langmuir C. H. (1999) Lithium isotope variability in MORB. *EOS* 80, F1086-F1087.

Tomascak P. B., Tera F., Helz R. T., and Walker R. J. (1999b) The absence of lithium isotope fractionation during basalt differentiation: New measurements by multicollector sector ICP- MS. *Geochimica et Cosmochimica Acta* 63(6), 907-910.

Tomascak P. B., Ryan J. G., and Defant M. J. (2000) Lithium isotope evidence for light element decoupling in the Panama subarc mantle. *Geology* 28(6), 507-510.

Tomascak P. B., Widom E., Benton L. D., Goldstein S. L., and Ryan J. G. (2002) The control of lithium budgets in island arcs. *Earth and Planetary Science Letters* 196(3-4), 227-238.

Tomascak P. B., Hemming N. G., and Hemming S. R. (2003) The lithium isotopic composition of waters of the Mono Basin, California. *Geochimica et Cosmochimica Acta* 67(4), 601-611.

Tomascak P. B. (2004) Developments in the understanding and application of lithium isotopes in the Earth and planetary sciences. In *Geochemistry of non-traditional stable isotopes*, Vol. 55 (ed. C. Johnson, B. Beard, and F. Albarede), pp. 153-195. Mineralogical Society of America, Washington, DC.

Walker R. J. (1984) The origin of the Tin Mountain pegmatite, Black Hills, South Dakota. PhD. dissertation, Univ. New York at Stony Brook.

Walker R. J., Hanson G. N., Papike J. J., and O'Neil J. R. (1986a) Nd, O and Sr isotopic constraints on the origin of Precambrian rocks, Southern-Black-Hills, South-Dakota. *Geochimica et Cosmochimica Acta* 50(12), 2833-2846.

Walker R. J., Hanson G. N., Papike J. J., O'Neil J. R., and Laul J. C. (1986b) Internal evolution of the Tin Mountain Pegmatite, Black Hills, South-Dakota. *American Mineralogist* 71(3-4), 440-459.

Walker R. J., Hanson G. N., and Papike J. J. (1989) Trace-element constraints on pegmatite genesis - Tin Mountain Pegmatite, Black Hills, South-Dakota. *Contributions to Mineralogy and Petrology* 101(3), 290-300.

Watson E. B. and Harrison T. M. (1983) Zircon Saturation Revisited - Temperature and Composition Effects in a Variety of Crustal Magma Types. *Earth and Planetary Science Letters* 64(2), 295-304.

Webster J. D., Holloway J. R., and Hervig R. L. (1989) Partitioning of lithophile trace-elements between H_2O and $H_2O + CO_2$ fluids and topaz rhyolite melt. *Economic Geology* 84(1), 116-134.

Wedepohl K. H. (1969) Handbook of Geochemistry. Springer-Verlag.

Wedepohl K. H. (1995) The composition of the continental-crust. *Geochimica et Cosmochimica Acta* 59(7), 1217-1232.

Wenger M. and Armbruster T. (1991) Crystal-chemistry of lithium - oxygen coordination and bonding. *European Journal of Mineralogy* 3(2), 387-399.

Williams L. B. and Hervig R. L. (2003) Lithium isotopic fractionation in subduction zones: clues from clays. *EOS. Trans. AGU, 84(46), Fall Meet. Suppl., Abstract* V52A-0417.

Williams L. B. and Hervig R. L. (2005) Lithium and boron isotopes in illite/smectite: The importance of crystal size. *Geochimica et Cosmochimica Acta* in press.

Wing B. A., Ferry J. M., and Harrison T. M. (2003) Prograde destruction and formation of monazite and allanite during contact and regional metamorphism of pelites: petrology and geochronology. *Contributions to Mineralogy and Petrology* 145(2), 228-250.

Wyborn L. A. I. and Chappell B. W. (1983) Chemistry of the Ordovician and Silurian Greywackes of the Snowy Mountains, Southeastern Australia - an Example of Chemical Evolution of Sediments with Time. *Chemical Geology* 39(1-2), 81-92.

Xiao Y. K. and Beary E. S. (1989) High-Precision Isotopic Measurement of Lithium by Thermal Ionization Mass-Spectrometry. *International Journal of Mass Spectrometry and Ion Processes* 94(1-2), 101-114.

Yamaji K., Makita Y., Watanabe H., Sonoda A., Kanoh H., Hirotsu T., and Ooi K. (2001) Theoretical estimation of lithium isotopic reduced partition function ratio for lithium ions in aqueous solution. *Journal of Physical Chemistry A* 105(3), 602-613.

Yoder C. F. (1995) Astrometric and geodetic properties of Earth and the solar system. *In AGU reference shelf series: A handbook of physical constants: Global Earth Physics (Vol.1) 380 pp.*

You C. F., Chan L. H., Spivack A. J., and Gieskes J. M. (1995) Lithium, boron, and their isotopes in sediments and pore waters of Ocean Drilling Program Site-808, Nankai Trough - implications for fluid expulsion in accretionary prisms. *Geology* 23(1), 37-40.

You C. F., Castillo P. R., Gieskes J. M., Chan L. H., and Spivack A. J. (1996) Trace element behavior in hydrothermal experiments: Implications for fluid processes at

shallow depths in subduction zones. *Earth and Planetary Science Letters* 140(1-4), 41-52.

You C. F. and Chan L. H. (1996) Precise determination of lithium isotopic composition in low concentration natural samples. *Geochimica et Cosmochimica Acta* 60(5), 909-915.

Zack T., Tomascak P. B., Rudnick R. L., Dalpe C., and McDonough W. F. (2003) Extremely light Li in orogenic eclogites: The role of isotope fractionation during dehydration in subducted oceanic crust. *Earth and Planetary Science Letters* 208(3-4), 279-290.

Zartman R. E. and Stern T. W. (1967) Isotopic age and geologic relationships of the Little Elk Granite, Northern Black Hills, South Dakota. *U.S.G.S. Prof. Paper* 575D, 157-163.

Zhai M. G. (1996) *Granulites and lower continental crust in North China Archean craton*. Seismological Press.

Zhang L., Chan L.-H., and Gieskes J. M. (1998) Lithium isotope geochemistry of pore waters from ocean drilling program Sites 918 and 919, Irminger Basin. *Geochimica et Cosmochimica Acta* 62(14), 2437-2450.

Zhao G. C., Wilde S. A., Cawood P. A., and Sun M. (2001) Archean blocks and their boundaries in the North China Craton: lithological, geochemical, structural and P-T path constraints and tectonic evolution. *Precambrian Research* 107(1-2), 45-73.

Zhao J., Gaskell P. H., Cluckie M. M., and Soper A. K. (1998) A neutron diffraction, isotopic substitution study of the structure of $Li_2O.2SiO_2$ glass. *Journal of Non-Crystalline Solids* 234, 721-727.